UNIVERSITAT POLITÈCNICA DE VALÈNCIA

DOCTORADO DE INGENIERÍA Y PRODUCCIÓN INDUSTRIAL

DOCTORAL THESIS

"Development of green composites based on epoxidized vegetable oils (EVOs) with hybrid reinforcements: natural and inorganic fibers"

Author

Ph.D. Dana Luca Motoc

Advisors

PhD Santiago Ferrándiz Bou

PhD Rafael Balart Gimeno

May 2017

BACKGROUND

The overall aim of the work is to provide comprehensive means of predicting and characterizing the properties of principal hybrid polymer based composite architectures that can simultaneously yield results of practical utility. This is accomplished by comparing, whenever possible, the theoretical predictions for the effective properties to available experimental data.

The present work is divided into two parts. Part I deals with the author's scientific achievements that enabled to characterize quantitatively the main effective properties of self-developed hybrid polymer based composite architectures and different theoretical and computer-simulation methods used for comparison. Part II identifies future directions for scientific and research evolution and development.

The introductory chapter in **Chapter I** was reserved to the state-of-the-art in the subject intended to be covered with the main body of the PhD thesis. This was done on purpose to illustrate the importance of developed subject that is under continuous evolution and that expanded after herein contributions. It is noteworthy that significant advances have been made recently in the quantitative characterization of hybrid composite materials of any type both theoretically and experimentally.

The general objectives (**Chapter II**) were underlined and concise delivered to give the reader a preview of the concepts that will be discussed specifically in the subsequent chapters. Indirectly, they point toward one of the main aims of this work, namely to provide a direction for systematically analysis of hybrid polymer based composite materials.

Chapter III was dedicated to the brief presentation of individual materials' selection, manufacturing issues, details on hybrid microstructures and finally, some practical information on experimental devices and settings considered. Practically, reproducibility issue of the experimental data processing can be potentially addressed through sharing these particular information results.

Chapter IV provides several theoretical models used deploying a multi-step homogenization scheme to apply for individual combinations and effective property under consideration. These theoretical models were selected due to their ability to describe the 'details of the microstructures' (i.e. constitutive volume fractions, orientations, sizes, shapes, spatial distributions and surface areas of interfaces, etc.) and ability to encompass particular information that can be ascertained in practice.

In the light of above, particular concerns were given to those structure/property relations that can be easily understood by apprentices, unaccustomed researchers on engineering field and finally, to materials' designers bounded by cost and time to perform measures on their mechanical applications for all possible combinations, phase properties and microstructures aimed to be developed.

Chapter V extensively approaches the effective mechanical, dynamical, thermal stability and conductivity, fire retardant and electrical conductivity of particular hybrid polymer based composites developed. These effective material properties were retrieved by subjecting the various hybrid composite specimens to various loading conditions in order to address the sustainability issue and some practical implementation considerations. **Chapter VI** gathers the main results and discussion about this research work related to cyanate ester and DGEBF epoxy composites with carbon and basalt fabrics hybridized with flax fabrics. A specific part is devoted to the evaluation of mechanical elastic properties of particle composite systems.

Over the entire sections of this chapter was followed the same formalism, including: applied standards used to run the exploratory tests, particular and representative experimental curves, details on the retrieved values, predicted over recovered data comparison relevant for the effective property vs. micro-structural dependence description and analysis.

Structural design and applications emerging from this cannot be sough strictly to comply or use solely the mechanical properties. In the mechanical engineering field, the applications are driven by a multitude of influencing factors whose cross-dependencies can be regarded to the seemingly different effective properties considered here.

Moreover, the experimental data can be effectively translated to practice and have important implications for the optimal design of composites. Space limitations and overcome the settled objectives do not enable us to treat, in any detail, the cost and error minimization topics identified as the major issues that benefit from the herein retrieved information.

General conclusions presented in **Chapter VII** provide the merits of the theoretical predictions, the main reasons behind the effective property's behavior during the conditions imposed within the experimental runs and a unified framework to study a variety of different hybrid composite architectures with their tailored effective properties.

Additionally, these can be regarded as an ex-ante foundation and conditionality for further hybrid polymer based composited architectures tailored from natural reinforcements and matrices under the so called 'green' composites material category. In the light of previous mentioned and with respect to the effective properties of hybrid polymer based composites, further directions for scientific research were identified and briefly described in **Chapter VIII**.

Specific citation to the literature used, both co-authored contributions and other sources have been kindly provided at the end as references. These were used in correlation to the section's subject and can be easily identified and suitable checked. It is noteworthy that few sections contain unpublished work of undersigned used to clarify some aspects related to the effective property under discussion and provided to enable readers to comprehend the ongoing discussions and related conclusions.

RESUMEN

El objetivo general del trabajo es proporcionar medios integrales para predecir y caracterizar las propiedades de las estructuras de compuestos basados en polímeros y refuerzos híbridos, principales que pueden producir resultados de utilidad práctica simultáneamente. Esto se logra comparando, siempre que sea posible, las predicciones teóricas de las propiedades efectivas con los datos experimentales disponibles.

Una primera parte se ocupa de los logros científicos del autor que permitieron caracterizar cuantitativamente las principales propiedades efectivas de las arquitecturas de compuestos basados en polímeros y refuerzos híbridos, basados en matrices bio, auto-desarrollados y diferentes métodos teóricos y de simulación por ordenador utilizados para la comparación. La segunda parte identifica las orientaciones futuras para la evolución y desarrollo de la ciencia y la investigación.

Los objetivos generales fueron subrayados y concisos para dar al lector una visión previa de los conceptos que serán discutidos específicamente en los siguientes capítulos. Indirectamente, apuntan hacia uno de los objetivos principales de este trabajo, a saber, proporcionar una dirección para el análisis sistemático de materiales compuestos a base de refuerzos híbridos.

SUMMARY

The main aim of this work id to provide integral methods to predict and characterize the properties of composite structures based on hybrid polymers and reinforcements, that could lead to useful results from an industrial point of view. This is addressed, if possible, by theoretical predictions of the effective properties by using the available experimental data.

The first part is focused on the scientific achievements of the author that allowed a quantitative characterization of the main effective properties of several composite architectures from hybrid polymers and reinforcements, based on bio matrices, tailor-made matrices and different theoretical and simulation methods using computer software to allow good comparison. The second part defines the future research lines to continue this initial investigation.

The main objectives are clearly defined to give the reader a sound background with the appropriate concepts that are specifically discussed in the following chapters. As a main objective, this research work makes a first attempt to provide a systematic analysis and prediction of composite hybrid structures.

RESUM

L'objectiu general d'aquest treball es proporcionar els mitjos integrals per tal de predir i caracteritzar les propietats d'estructures de compòsits basats en polímers i reforçaments híbrids, que poden produir resultats amb utilitat pràctica simultàniament. Aquest objectiu s'aconsegueix comparant, sempre que és possible, les prediccions teòriques de les propietats efectives amb les dades experimentals disponibles.

Una primera part es centra en els temes científics en què ha treballat l'autor que han permès caracteritzar quantitativament les principals propietats efectives de les arquitectures de compòsits basades en polímers i reforçaments híbrids, derivats de matrius bio, auto-desenvolupats i diferents mètodes teòrics i de simulació informàtica per a una correcta comparació. La segona part identifica les orientacions futures per tal d'establir l'evolució i desenvolupament de la ciència i investigació lligada a la temàtica de la tesi.

Els objectius generals han sigut clarament definits per tal de donar-li al lector una visió prèvia i sòlida dels conceptes que es discuteixen en capítols venidors. Indirectament, apunten cap a un dels objectius principals d'aquest treball, a saber, proporcionar una direcció per a l'anàlisi sistemàtica de materials compòsits a base de polímers i reforçaments híbrids.

Table of Contents

LIST OF FIGURES.

LIST OF TABLES.

Chapter I

Chapter I. "*State of the Art*".

I.1. Designing hybrid polymer composite materials.

Research conducted on hybrid composites, predominantly based on intermingled carbon and glass fibre fabrics, can be traced back to the early 1970s, from the work of Bunsell and Harris (1974) or Summerscales and Short (1978, 1980), that were among the first in the investigation of the mechanical properties of various material combinations in view of their prospective use as lightweight load bearing composite structures [1-3]. Since then, a variety of combinations emerged as viable architectures to produce fibre reinforced polymer (FRP) composites.

Literature is abundant in references on hybrid composite materials, generally, and polymer based, particularly. Ashby (2003, 2011) is one of the scholars who succeeded to define and formulate concisely the concept of hybrid materials – "combinations of two or more materials assembled in such a way as to have attributes not offered by either one alone" [4, 5]. In addition, he underlined the ingredients to be used in hybrid material design, including: the choice of materials to be combined, their configuration, their relative volume fraction and the scale length of the structural unit.

One may acknowledge the prevalence of three types of hybridization architectures regarded as *interlayer*, *intralayer* and *intrayarn*. The interlayer hybridization implies reinforcement mixing on the layer level while the intralayer configurations within each layer. The first architecture is the most common configuration as it handy to be manufactured. On the other hand, the latter is rather difficult to be produced but proved to yield improved mechanical properties as reported by Pegoretti et al. [6] and Fukunaga et al. [7].

In the light of above, numerous combinations emerged and studied by researchers from property prediction point of view, cost and performance, behavior under various loading conditions and application potential based on different scenarios. With respect to the latter, "the best of both", "the rule of mixtures", "the weaker link dominates" and "the least of both" were the main scenarios that emerged in

the attempting of answering the questions arose: What is a hybrid material? When is hybrid a material? How does it behave while subjected to a certain loading condition?

One of the first review on hybrid composites was written by Kretsis in 1987 [8]. The author focused especially on hybrid composites based on epoxy resins reinforced with synthetic fibers, carbon and glass, especially continuous and unidirectional oriented, from effective mechanical properties of view.

Since then, a wide range of materials was found to challenge the benchmarks. Thus, natural constitutive were preferred and leading the last decades of research as direct consequence of focused concerns about environmental issues. In addition, they naturally followed the searching for an answer to the question: "Are natural fiber composites superior to glass fiber reinforced composites?" [9-11].

One of the fundamental parameters in the hybrid polymer based composites design is the *hybrid ratio* that is acknowledged to have a direct influence on the overall performance of structure. This is intimately connected to the *hybrid effect* that is generally assessed while approaching such materials' architectures.

Noteworthy, the most comprehensive and employed definition of the hybrid effect was given by Marom et al. in 1978 [12]. According to their findings, deviation from linear rule of mixtures (RoM) can be modified to be used to predict a large spectrum of mechanical properties in addition to the failure strain. Consequently, positive and/or negative hybrid effects result from these predictions and used to quantify the examined property. The aforementioned rule is known in literature as the *linear rule of hybrid mixtures* (RoHM) and, unfortunately, has some major drawbacks as debated by Swolfs et al. (2014) [13].

There are many influencing factors that can be identified to influence the hybrid effect. High-performance composites require outstanding returns from their individual constituents, both reinforcement and matrix. Without limiting them, the nature, distribution, amount, layering pattern and individual features of the constitutive strongly influence the effective material properties. Subsequently, material selection must be tackled as sharing the same importance in the composite design. Other

parameters, such as fiber-matrix interface, inter-laminar strength and fracture toughness, can be also considered to influence the hybrid effect.

Theoretical predictions developed to address microstructure-property connection have a long and venerable history, attracting the attention of some of the luminaries of science, including Maxwell, Rayleigh and Einstein. Since their early work on the properties of heterogeneous materials, there has been an explosion in the literature on this subject, one of the outstanding contributors being Torquato (2002) [14].

In the most general sense, the overall properties of heterogeneous materials can be predicted using expressions developed based upon the variational principles, local and homogenized solutions to the problems, phase-interchange relations, exact solutions, effective medium approximations, rigorous bounds, cross-property relations, etc.

It is noteworthy that these significant advances have enabled investigators to break through the limits of models and further, to compute property estimates that depend on other requirements imposed real materials. The ability to tailor composites with unique spectrum of properties rests fundamentally on the systematic approach to relate the effective properties to the microstructure by means of accurate expressions. One can then relate changes in the microstructure quantitatively to changes in the macroscopic property.

Nonetheless, the exponential upbringing that can be seen with respect to hybrid composite materials development is driven mostly by industry pressure. Material designers and manufacturers seem to be endlessly in the search of novel combinations bounded by requirements that allow fast architecture optimization in terms of cost minimization, high performance and lightweight condition.

Hybrid polymer composites were developed mostly using thermosetting resins, ranging from epoxy to polyester and poly vinyl ester, etc. Epoxy resins and derived blends were preferred due to their versatility in use with all manufacturing technologies, good compatibility with almost all types of fibers, both synthetic and natural.

The consumption of composites, either thermoplastics or thermosetting, is controlled by user market demand. The ability to adapt these materials to economic and technical market requirements relays on the innovation in terms of both materials and processes, supplemented by adaptability to the environmental constrains (i.e. circular 3R concept - recycling, reusing and remanufacturing) as outlined, for example, by Biron (2014) [15].

These composites found their niche in engineering applications were solely two-phase constitutive lead, viewing them, mostly like an alternative instead of replacements. Thus, civil and automotive engineering, marine and aerospace, biomedical and sensing devices were several application domains of these modern composite architectures [16-20]. A balance in cost and performance can be sized behind each material design while used in aforementioned structural applications.

Certainly, the study of hybrid composite materials is a multidisciplinary endeavor that overlaps with various branches of material science, engineering, applied mathematics, etc. The ability to tailor hybrid composites with a unique spectrum of properties relies on relating the effective properties to the microstructure and correlation of experimental retrieved data with theoretical predicted values, bounded by certain processing conditions.

I.2. Material properties of hybrid polymer composites

The effective material properties of a hybrid polymer based composite depend on the reinforcements' volume fraction, geometrical parameters (e.g. length, shape, etc.), orientation and layering type, supplemented by interface interactions with the matrix system. The overall behavior of resulted hybrid material is dictated by each of and every component. The synergetic effects based on contribution of all constitutive forming the composite was outlined by Wang and Pan (2008) [21].

In addition, constitutive individual properties and their compatibility were directing towards maximum hybrid results as reported by several research groups, both theoretically and experimentally through systematic studies, challenging thus the state-of-the-art results (Faruk et al., 2012; Ahmad et al., 2004; Jawaid et al., 2011; Ashori et al., 2010) [10, 16, 22, 23].

Next, both theoretical and experimental approaches, individually or intermingled, will be discussed in the view of highlighting the significant progresses. In addition, a connection with engineering applications is aimed further to strengthen the individual research results from subsequent chapters. To be able to foster the herein author's research contribution, paper collection and ex-ante development, it will be employed a back and forth approach with respect to the scientific literature referring.

Before commencing, it is desirable to recall the comprehensive collection of micro-mechanical based models, ranging from two to multiphase systems, accompanied by graphical representation of predicted values under each composite class that was co-authored by Motoc Luca (2009) [24]. A large number of theoretical models for prediction of effective properties for two and multiphase materials were covered. These include elastic modulus, thermal and electrical conductivities and coefficient of thermal expansion, respectively.

The advent on scale transition modeling methods relays on the outstanding work of Berryman (1996, 2001, 2014), individually or co-authored, who proposed several

effective medium approximations for elastic constants of random composites to the alternative of the familiar rigorous bonds [25-27]. Furthermore, insight into the various methods enabled boosting a number of new effective medium approximations that can be viewed as natural variants and/or combinations of the existing ones.

Additionally, a comprehensive systemic approach on the overall response parameters of materials with micro-heterogeneities and defects (i.e. cracks, cavities, inclusions, etc.) was generously provided by Nemar-Nasser and Hori (1999) [28]. In summary, within the sixth chapters subdivided into sections, the basic idea of a heterogeneous *representative volume element* (RVE) and *repetitive unit cells* (RUCs) were extensively extrapolated; linearly elastic solids with micro-inclusions were tackled in such that their elastic response was captured, followed by fundamentals on elastic solids with distributed in-homogeneities, including cavities, inclusions and cracks. Furthermore, in most cases the models were accompanied by application examples.

In particular, focused approaches on *Mori-Tanaka* principles and results were tackled due to the formalism enabling interesting applications. This trend was followed by other researchers like Wu & Weng (2000), Thomsen & Pyrz (2001), Dong et al. (2005), Tan et al. (2005), Bohm & Nogales (2008), Mercier & Molinari (2009), Peng et al. (2009), Lu (2013) and recently by Liu & Huang (2014) [29-37].

Put in a nutshell, the above references fail to address directly the concept of hybrid composite materials and associated overall properties from *Mori-Tanaka* expression's point of view. On the other hand, the corresponding formalism can be extrapolated to encompass this class of hybrid composite materials as suggested by Berryman (see ref. above) or Kanaun & Jeulin (2001) [38]. Nonetheless, their findings can be ranked as fundamental in the continuously accelerating learning and developing process related to the issue.

Likewise, theories should be placed into the practical context by their theoretical underpinnings in a clear and concise manner, and illustrate their utility for the design and analysis of hybrid composite materials, generally, and polymer based particularly. An excellent reference with respect to above is the co-authored book of Aboudi (2012) [39]. They succeeded to address directly the issues of multi-scale modeling methods as

developed under a micromechanical approach, based on hierarchical, synergistic or concurrent strategies used that systematically pass information on bottom-up or top-down manners.

In summary, the micromechanical based approaches deployed were sought as a range of methods from *fully analytical* (e.g. rule of mixture (ROM) and *Mori-Tanaka*) to *fully numerical* (e.g. finite-element analysis (FEA) and molecular dynamics (MD)), or from *semi-analytical* (e.g. Generalized Method of Cells (GMC)) to *fully numerical*. The key point behind the development of all the theories presented relayed on the balance between fidelity and efficiency that was met while applied to multi-scale modeling of composite materials. Therefore, these can assist in designing the hybrid composite materials themselves as well as the structures comprised of them.

Furthermore, noteworthy can be ranked the review of Gibson (2010) with respect to the research activity and publications in multifunctional materials and structures that succeeded to identify the most appealed topics on the aforementioned [40]. Besides of establishing a road map on the hot topics focusing on multifunctional materials, including hybrid composites driven by application oriented approaches, the author urged on the "need for development of more analytical models to compliment the experiments."

Likewise, recently Lee et al. (2012, 2015) approached and adapted log-normal and generalized extreme value (GEV) *statistical functions* to predict the effective elastic moduli for multiphase hybrid composites [41, 42]. The idea of employing statistical functions to predict the material properties in composites is not a new one. The highly potential of the statistical methods relay on their versatilities, easy to be understand but difficult to be implemented due to several key factors related to the structure that must be accounted. In particular, author's theoretical and experimental platform enabled a more insightful understanding with respect to the class of hybrid composite materials, generally, and it is enough thoughtfully to allow expandability, particularly.

I.2.1. Mechanical properties of hybrid composites.

The existing analytical models for the effective mechanical properties are based or derived from the well-known *Voigt* model that served as a benchmark for validation. As mentioned before, since it is providing the upper bound for many material properties, including elastic modulus, positive and negative effects can be outlined further. The effects are deemed positive when the mechanical properties relay above the predicted trend and vice versa when the opposite occurs.

The *linear rule of the hybrid mixture* (RoHM), as it is referred the basic model from above provide acceptable predictions of the effective elastic properties for simple or simplified combinations, but the accuracy and applicability are rather limited (Teodorescu et al., 2008; Fu et al., 2002) [43, 44]. It is extremely difficult to predict the hybrid effects and overall properties, especially flexural/tensile strength and derived elastic moduli, since they depend upon the several key factors and appreciably overestimate the property under the focus.

To overcome these limitations, different researchers were either introducing empirical parameters to account for certain structure characteristics, combined several theoretical models for complex composite architectures or running finite element based simulations (Dong et al., 2015; Mishnaevsky and Dai, 2014; Dong et al., 2013; Benveniste, 2008; Afonso and Ranalli, 2005; Mori and Tanaka, 1973; Christensen, 1990; Hashin and Shtrikman, 1962) [45-52].

Noteworthy within the above is the contribution of Mishnaevsky and Dai (2014) on computation modeling techniques of hybrid and hierarchical nano reinforced polymer based composites' structure-properties relationships. They argued in favor of glass/carbon-fiber hybrid composites that exhibit a higher stiffness and lower weight and/or strength with the increase in the carbon content as compared with their counterparts. Further, addition of nano reinforcement can drastically increase the fatigue lifetime of these composites.

The effects of the reinforcement clustering, individual material properties of constitutive on the overall composite behavior under mechanical loading were

accounted by the above referred majority in terms of effect upon the elastic modulus and strength. Further, Chiang et al. (2005), Lua (2007), Teodorescu et al. (2009), Wu (2009) [53-56] proved that mechanical property improvement failed to hold in all polymer based composites. The latter can be regarded to few influencing factors that were individually identified, monitored and debated.

In materials testing, flexural strength is most commonly determined through 3-point bending test. It was reported that the flexural strength, and the inter-laminar shear strength (ILSS) are strongly influenced by the hybrid design and depend on the reinforcing fiber position (Yahaya et al., 2015; Ary Subbagia et al, 2014; Amico et al., 2010; Reiss et al., 2007) [57-60].

Carbon fiber (CF) based composites were one of the most tailored architectures due to some drawbacks of this reinforcement, including susceptibility to stress concentration due to it's to brittleness, recycling potential and associated manufacturing costs. To overcome these drawback researchers called on the hybridization procedure with direct benefits in cost and effective material properties.

Literature reports on several *synthetic/synthetic* hybrids that were developed among first to exploit the synergetic effects of the combinations. Thus, Manders and Bader (1981) reported on flexural properties of glass and carbon fibers hybrid composites [61]. According to their findings, the failure strain of carbon phase increased as the relative proportion of carbon fiber was decreased, and as the carbon fiber was more finely dispersed. They called this behavior as a hybrid effect and reported an enhancement in failure strain of up to 50%.

Further, Selmy et al. (2012) accounted 'hybridization' based on the same type of material used as reinforcement but a different shape/distribution/volume fraction such as unidirectional and random glass fibers [62]. Their findings indicated that the in-plane shear properties (i.e. shear strength and modulus) of unidirectional fiber composite can be considerably improved by incorporation of random glass fiber to proffer structural composite architectures.

Next, Ary Subagia et al. tailored different hybrid architectures out of carbon fiber (CF) and basalt fiber (BF) by various stacking the individual layers as the outer- or innermost layers using a vacuum-assisted technique [58]. They concluded that all stacking sequences exhibited a positive hybridization effect. In addition, higher flexural strength and modulus were obtained for hybrid architectures were the carbon fiber based plies were layered on the compressive side.

Hybrid polymer based composite architectures were tailored by Ahmad et al. (2004) out of glass, Kevlar and carbon woven fibers embedded within two different matrices: epoxy and polyester resins. Their results shown linear increase in tensile strength with an increase in volume fraction fabric for both polyester and epoxy based composites. In addition, the hybrid composites have shown up to more than 100% increase in modulus of polyester composites while glass fabric reinforced polyester composites showed high tensile properties [16].

Next, Valenca et al. (2015) reported on the mechanical behavior of hybrid epoxy based composites using Kevlar and glass fibers as constitutive [63]. The structural composites developed performed excellent in tensile, bending and impact tests comparatively with their counterparts. Earlier, Dutra et al. (2000) reported on impact performance of a mixture of polypropylene and carbon fibers as reinforcing elements into an epoxy matrix [64]. They argued on the improved properties of hybrids in comparison with CF based composites.

Hybrid composite architectures tailored out of basalt fibers (BF) with either glass or carbon fibers were reported previously by Czigany (2006), Che et al. (2009), Carmisciano et al. (2011) [65-67]. As forecasted, the experimentally retrieved mechanical properties are higher for hybrids out of carbon and basalt fibers comparatively with their counterparts. Fiber orientation and surface treatment were tackled and considered as influencing factors upon the mechanical properties, both stress and elastic modulus in tensile and flexures, respectively. In addition, the results point toward property improvement in case of increased fiber/matrix adhesion.

Another hybrid class further developed has been the *synthetic/natural* reinforcement type combination. These hybrids were developed to overcome the

problems associated both with synthetic and natural reinforcements. The latter are known for their susceptibility to moisture, their incompatibility with the hydrophobic polymer matrix, lack of the established manufacturing process that limits their performance and use in structural applications (Priya et al., 2006; Reis et al., 2007; Almeida et al., 2012, 2013; Dhakal et al., 2013; Mansor et al., 2013; Romanzini et al., 2013) [59, 68-73].

Experimental tensile testing procedure is often considered in conjunction with unidirectional fibers. Zhang et al. (2013) investigated the tensile and interfacial properties of few hybrid architectures tailored by different stacking unidirectional flax and glass fibers. They concluded that tensile properties of the hybrid architectures were improved with the increase of glass content. The stacking sequence was shown to influence the tensile strength, but not the tensile modulus.

A recent paper on *natural/natural* reinforced hybrid polymer composites was co-authored by Alavuuden et al. (2015) on banana and kenaf reinforcements, differently weaved, namely, plain and twill, following the work of Boopalan et al. (2013) [74, 75]. Their findings revealed that plain type reinforcements shown improved tensile properties compared to the twill type in all the fabricated composites. Furthermore, the maximum increase in mechanical strength was observed in the plain woven hybrid composites rather than in randomly oriented composites.

Scale transition and temperature dependence of the mechanical property enabled hybrid particle-fiber polymer composite analysis and overall behavior enhancements. With regard to aforementioned, the work of Li et al. (2014) can be viewed as representative for the potential in improving mechanical and thermo-mechanical properties of the fiber-reinforced composite by using multi-scale carbon hybrids [76]. They argued on the multi-scale hybridization of carbon nanotubes (CNTs) with micro-particles and about the opportunities in fostering high-performance multifunctional polymer based composites.

Further on the previous issue, the work of Lin et al. (2012) on the mechanical and wear properties of hybrid carbon fibers (CF) and nano-ZrO2 particles embedded within a polyetheretherketone (PEEK) polymer matrix can be regarded as a contribution

on structural composites [77]. In addition, nano sized particles embedded into the polymer matrix enabled stress release at the fiber/matrix interface, and thus excellent effective properties.

Besides aforementioned, Rahmanian et al. (2014) or Qin et al. (2015) tackled the issue of mechanical properties of multiscale hybrid polymer composites out of carbon fibers (CF) while Gamze Karsli et al. (2014) employed short glass fibers [78-80]. Unsurprisingly, all works report on improvements on the monitored mechanical property along with arguments in favor of synergetic effects.

Researchers tackled the *environmental influences* (e.g. moisture absorption) and *atmospheric*, *accelerated* or *thermal aging effects* upon the mechanical properties of hybrid composites during their studies aiming a comprehensive perspective on tailored materials. Among these can be mentioned the contributions of Barjasteh et al. (2009, 2012), Boualem & Sereir (2011), Burks & Kumosa (2012), Tsai et al. (2009) [81-85]. The conclusion underpinning their research resides in the unchanging or small discrepancies in the monitored effective properties due to the above mentioned external influences.

I.2.2. Dynamic mechanical properties of hybrid composites

Dynamic mechanical analysis (DMA) proved to be a useful tool in the study of polymer based composite materials' behaviour under various temperatures, frequency or external loading conditions. Measurements can be conducted either by applying a periodic load to gather the resulting deformation or by applying a constant load (or a displacement) to obtain creep (or relation) data. Information on loading modes, calibration methods, sample conditioning and particular data acquisition can be found in the comprehensive and commonly referred work of Menard (2008) [86].

Temperature-dependent dynamic mechanical properties, such as storage modulus, loss modulus and mechanical damping (i.e. loss factor), allow a closer monitoring of the level of interactions (i.e. adhesion) between the polymer matrix and

the reinforcements. In addition, *Cole-Cole* or *Cole-Davisson* plots proved to be the most expressive and useful data processing tools in sizing the constitutive influence.

Literature provides numerous references focusing on the fibre reinforced polymer composites and their dynamical material properties revealing their inherent structure related particularities and thermal history during their manufacturing (Idicula et al., 2005; Mohanty et al., 2007; Deng et al., 2007; Bai et al., 2008; Ornaghi et al, 2010; Almeida et al., 2012; Faguaga et al., 2012; Romanzini et al., 2012 and 2013) [70, 73, 87-93]. Both organic and inorganic fibres were considered as high-potential reinforcement candidates for the different polymer based composite architectures and dynamic mechanical analysis (DMA) as the most-used testing method in order to size the overall material behaviour under shock and vibrations.

Thermo-mechanical models using temperature-dependent mechanical properties of fibre reinforced polymer composites can be traced around '80s. A compressive review of these models was reported by Mahieux et al. (2001, 2002) [94, 95]. In addition, a Weibull-type function was developed to describe the elastic modulus change over the full range of transition temperatures. The model is consistent only with thermoplastic materials (e.g. PEEK, PMMA, PPS, etc.) and cover a wide range of temperatures. Other empirical models were developed by Springer (1984) or Gu and Asaro (2005) [96, 97].

Noteworthy, the majority of researchers report on both retrieved static and dynamic mechanical properties for their tailored composite samples. Surprisingly, none explicitly addressed the particular issue of similarities between experimentally retrieved values from above configurations, although, in principle, they should be the same (Lee-Sullivan et al., 2000; Shao et al., 2000) [98, 99].

Numerous research papers approaching the subject of dynamic properties of hybrid polymer based composite can be traced as experiencing an exponential increase in the last decade. Surprisingly, majorities focus upon the synthetic/natural reinforcement combinations as it was the subject preferred and developed by numerous researchers. Recently, scale transition enabled tunings with respect to the hybrid architectures as reported by Diez-Pascual et al. (2011) [100].

In addition, effectiveness of reinforcements and adhesion factor can be traced and further used to assess the effectiveness of stress/strain between the reinforcements and matrix and their interface bonding (Idicula et al., 2005; Romanzini et al., 2013) [73, 93]. The constant related to the effectiveness of reinforcements envisages that the higher its value the lower the effectiveness of the reinforcement combination. Next, it is acknowledged that composites with poor interface bonding tend to dissipate more energy than that with good interface bonding, as shown by Tan et al. (1990) [101].

I.2.3. Thermo-physical properties of hybrid composites.

Uncontrolled thermal expansion in polymer based composites, especially those designed for structural applications, can be considered nuisances that preclude precision in these architectures. To mitigate the effects, the constitutive can be selected with matching *coefficients of thermal expansion* (CTE) at interfaces or tailored so that varies within a certain range (Kelly et al., 2005, 2006) [102, 103].

References that can be traced in literature generally approach the subject of *thermal expansion* in particle reinforced composites for energy harvesting applications, power electronic, electronic packaging, sensing devices, actuators, polymer based composite architectures tailored to attain negative coefficients or to withstand extreme environments, etc. (Hatta et al., 2000; Zhao et al., 2007; Bai, et al., 2008; Tsai et al., 2009; Jefferson et al., 2009; Boualem et al., 2011) [81, 83, 92, 104-106].

Further, rather contraction effects than expansion responses from constitutive were often considered in the composite design for those architectures intended to be developed to be used in harsh environments. Carbon fibers (CF) were again among the preferences, especially for applications dedicated to high temperatures. Noteworthy, studies are scarcely in literature about the thermo-physical changes occurring in these types of reinforcements, especially within extreme temperature range. Noticeable are those conducted by Sauder et al. (2002), Pradere and Sauder (2008), Gabr et al. (2015)

[107-109]. The above covers solely the class of two-phase composites and can be used strictly to account the subject as uncovered and expandable.

Carbon fibres naturally exhibit different CTE responses along their longitudinal and transversal directions and are usually selected as reinforcements for multi-layered polymer composite structures to tailor their overall CTE. On the other hand, its counterpart, glass fibers exhibit positive CTE on both directions, longitudinal and transversal. Through 'smart' combination of reinforcements, it can be tailored an 'ideal' hybrid composite architecture exhibiting zero thermal expansion. Unfortunately, reality departs far beyond these ideal depicted scenarios.

In the herein context, Praveen et al. (2011) reported on CTE in case of a hybrid carbon-glass composite for applications at cryogenic temperatures [110]. Research conducted shown that a 80:20 relative hybrid ratio supplemented by a 30° and 0° orientation of carbon and glass constitutive, respectively, yield to a near zero overall CTE as the temperature was lowered from room temperature to 125 K.

In the light of the above, noticeable is the research of Esposito et al. (2013) with respect of polymers' CTE measurements at cryogenic temperatures with the aid of optical sensors, namely fiber Bragg grating [111]. Fiber Bragg's grating sensors were employed due to their capability to allow measurements in extreme environmental conditions as well as their high immunity toward external electromagnetic interference factors. The procedure can be accounted for hybrid polymer composites' characterization as reliable.

Attempts for overall CTE dependence on fiber orientation was carried out by Tezvergil et al. (2003) on particle/fiber hybrid polymer composites [112]. The ANOVA analysis revealed strong dependences between the fiber orientation and temperature range particular to each hybrid specimen. In addition, their findings suggest that the anisotropic nature of fiber-reinforced composites exists also in connection to the CTE values.

Among earliest published contributions on the particle/fiber-reinforced hybrid composite architectures' CTE belong to Dzenis (1989) and Camacho et al. (1990) [113,

114]. Accompanying theoretical predictions covered the influences of fiber aspect ratio, isotropic and anisotropic fiber materials, planar, three-dimensional or arbitrary fiber orientation, solid spherical reinforcements. Agreement between predicted values and experimental values was argued. Their hybrid structures were designed for very high speed integrated circuit (VHSIC) board applications.

Further, scale transition enabled particle/particle hybrid composite development out of micron size silicon dioxide (SiO2) and graphitized carbon nano-fiber (CNF) particles, respectively, as reported by Jang et al. (2011) [115]. The effect of filler loading was investigated with respect to both mechanical and thermal stability of the hybrid composite materials. Their findings revealed that the addition of 3% weight fraction of SiO2 particles along with 3% weight fraction of CNF improved damping loss factors by 15.6% at room temperature and thermal stability with up to 15% from retrieved diminished CTE values.

Entirely nano-sized particles tailored as hybrid particle/particle polymer composite architectures were developed and investigated by Jin and Park (2012) [116]. They monitored the thermal stability in alumina (Al_2O_3) and silicon carbide (SiC) nano-particles embedded within a DGEBA resin, in addition to dynamic mechanical and curing behavior, followed by thermal mechanical properties as the filler content increased. Their findings revealed that the coefficient of thermal expansion of hybrid composite samples at the glassy and rubbery regions decreased with the increase of the filler content.

Modeling and numerical predictions of thermal expansion of entirely fibrous composites were tackled for various reinforcements' shape and orientation, different material combination, and accounting fiber/matrix interactions by Price et al. (2006); Papanicolaou et al. (2009); Nayak et al. (2009); Tsukamoto (2011), Dzenis (1989) [113, 117-120].

More recently, Lu (2013) approached the aforementioned subject in his attempt to clarify some confusing aspects concerning of the *Mori-Tanaka* model for CTEs [35]. Corrections were introduced by using derived expressions of the initial model followed

by comparison with other models. Accompanying debate favors the *Mori-Tanaka* model, and a practical expression was proposed to the prospective users.

Another property accounted in composite material development and characterization is *thermal conductivity*, especially for applications aiming power electronics, microelectronics, energy harvesting and storage, sensors and transducers, etc. (Alsina et al., 2005; Han et al., 2011; Mallick et al., 2011; Otiaba et al., 2011) [121-124].

In the light of above, a comprehensive work was carried out by Lee et al. (2006) that investigated various inorganic fillers including aluminum nitride (AlN), wollastonite, silicon carbide whisker (SiC) and boron nitride (BN) with different shape and size, alone or in combination [125]. Their findings substantiate the effects of hybridization toward the increase of thermal conductivity due to the enhanced connectivity offered by structuring filler with a high aspect ratio. Next, for given filler loading, the use of larger particle and surface treated filler resulted in composite materials with enhanced thermal conductivity.

Out of aforementioned, several references tackled the modeling or numerical predictions' available methods to further aid thermal analysis of the polymer based composite architectures under the focus. Among them, micromechanics theoretical models are prevailing and considered among the best quantitative predictors of the overall composite material property considered.

Noteworthy, the contribution of Sevostianov (2012) can be ranked as comprehensive, proven the cross-property connection approach on thermal expansion and thermal conductivity [126]. Its mathematical development covered a wide range of reinforcements, proven different shape and orientation, enabling quantitatively characterization of microstructures involving mixtures of diverse inhomogeneities. In addition, he debated on the limitation induced by familiar models developed by Turner (1946), Kerner (1956), Thomas (1960), Schapery (1968), Fahmi and Ragai (1970), Van Fo Fay (1971), Tummala and Friedberg (1970), Sevastianov (2007), etc. [24], [127]. The results were consistent with experimental data available in literature and aforementioned approaches.

Thermal conductivity of particle reinforced polymer composites were extensively investigated by Hatta and Taya (1991) who's theoretical models are among the best predictors for this material property [128, 129]. Further, more comprehensively can be ranked the paper of Bigg (1995) who extended the above concepts to spherical and irregular shape fillers [130]. In addition, experimental methods, including steady and unsteady state techniques were also reviewed in the light of thermal conductivity retrieval, especially for applications like heat exchangers where is of primary importance.

Thermal conductivities of hybrid epoxy composites reinforced with different particle fillers were investigated by various researchers, such as: Choi & Kim (2013) who used aluminum oxide and aluminum nitride fillers, Teng et al. (2012) that approached the issue by using functionalized multi-walled carbon nano-tubes and aluminum nitride or Zhou et al. (2010, 2013) that employed hybrid multi-walled carbon nano-tube and micro silicon carbide fillers or flake graphite and carbon nano-fillers. Kandare et al. (2015), on the other hand, reported on epoxy composites based on carbon fibers mixed with nano-inclusions (e.g. silver and graphene) by exploiting the synergy of latter [131-135].

In addition, in the work of Pak et al. (2012) was tackled the synergistic effect sizable in the thermal conductivity overall property of thermoplastic composites reinforced with boron nitride and multi-walled carbon nano-tube fillers, while Kumar Reddy et al. (2014) reported on cow dung powder filled glass-polyester composites [136, 137].

With respect of above, despite the attempts in upbringing effective thermal conductivity enhancement on investigated *particle-particle* or *particle-fiber* thermosetting composites, to exploit the synergetic effects due to particle reinforcement compatibilities and to argue against the effectiveness of proposed combination, one might observe that scale transitions do not necessarily represent a viable solution in terms of the application potential.

Further, remarkable can be raked the contribution of Chen and its co-authors (2015) on thermal conductivity enhancement as a result of hybridization in polymer

based composites [138]. They developed a two-step analytical model for the effective thermal conductivity prediction of epoxy composites containing hybrid single-walled carbon nano-tubes (SWCNTs) and graphite nano-platelets (GNPs) fillers [138]. Their results proved to be high consistent with reported data, and synergetic effects were envisaged into debate around the hybrid ratio.

Previously, Goyal et al. (2012) were investigated the electrically conductive thermal interface materials reinforced with hybrid graphene-metal particle fillers [139]. The experimental retrieved values shown that nano-particle size graphene fillers were responsible for the highly enhancement of the effective thermal property and this particular finding is important for the thermal management of advanced electronics and optoelectronics devices.

Through-thickness and out-of-plane thermal conductivities of 3D woven carbon fiber reinforced polymer composites were investigated by Schuster and his co-workers (2008) [140]. Theoretical modeling by the finite-element method was also employed to enhance their predictive expressions and experimental results. Next, challenging can be sought the perspective of considering thermal conductivity as a design aspect to be varied by fiber architecture and equal to mechanical design criteria such as Young's modulus or strength.

The above resulted from previous contributions of Krach and Advani (1996), Kulkarny and Brady (1997), Thomann et al. (2004), Turias et al. (2005), etc. [141-144]. These references fail to address directly the subject of effective thermal conductivity estimation or predictions, being of importance if further developments on the issue it will be tackled. Generally, they aimed thermal conductivity property recovery for two-phase polymer based composites, reinforced with unidirectional or commingled fibers, experimentally and theoretically.

I.2.4. Electrical properties of hybrid composites

Inasmuch as the property is sharing the same importance in hybrid composite design and applications and despite the scarcity of reports in literature, knowledge on it

has important implications for the optimal design of composites. The latter are particularly important in developing functional composites that differ from structural ones in the sense that their properties are quite different from those of the matrix materials and reinforcements, and it is far from that based on the law-of-mixture type formula. Composite materials that are exhibiting a "coupling" behavior are often referred to as *smart composites* or *multi-functional materials* (Newnham et al., 1978) [145].

First of all, there is necessarily to clarify the meaning of the *electronic composite* as most comprehensively defined by Taya (2008) like a material: "whose function is primarily to exhibit electromagnetic, thermal, and/or mechanical behavior while maintaining structural integrity" [146]. Therefore, not only electronic behavior should be sought during investigations but its physical and coupling behavior must be included. In addition, referring to its co-authored papers, the theoretical models developed accounted for the percolation and microscopic conduction mechanism irrespective of the reinforcements type, shape, size and volume fraction [147].

The properties of electronic composites can be tailored to meet specific applications, like those in electronic packaging: printed circuit boards (PCBs), thermal interface materials (TIMs), or like micro-electromechanical systems (MEMS) and BioMEMS where their functions are multi-fold: active sensing and housing.

To the best of author's knowledge, tenuity on the relaxation processes *modeling* techniques applied to hybrid polymer based composites can be found. Beyond these shortcoming El Hasnaoui et al. (2014) reported on dielectric properties of an epoxy-resin matrix with randomly dispersed carbon black nano particles in various amounts [148]. The analysis of the temperature dependence of electric permittivity using the *Vogel-Tammam-Fulcher* and *Havriliak-Negami* formalisms revealed the existence of carbon black/matrix interaction.

Early stages on electronic composite development focused on using mainly carbon black (CB) as conductive filler embedded within a high-density polyethylene (HDPE) matrix (Novak et al., 2005) or the combined effect while mixing with carbon fiber in polyethylene or polyethylene/polypropylene blends or other polymer matrices (Shen et al., 2011; Jin et al., 2013; Othman et al., 2013; Puertolas & Kurtz, 2014) [149-153].

In addition, noteworthy are the *particle-fiber* hybrid architectures tailored out of synthetic fibers, including carbon and glass mixed with carbon black. Moreover, recent scientific contributions approached the synthetic/natural combinations under the *fiber-fiber* category (e.g. PP/jute yarn commingled fabric) (Wichmann et al., 2006; Lonjon et al., 2012; Yamamoto et al., 2012; Gejo et al., 2013) [154-157].

Furthermore, following the work of Yang et al. (2007) on electrical properties of different hybrid carbon fiber reinforced plastics (CFRP), Yao et al. (2008) reported on dielectric constants on epoxy based composites tailored out as a combination of basalt and Kevlar fibers [158, 159]. Their experimental data agreed with the predicted results, and a positive hybrid effect was reported in all composites. Once again, carbon and Kevlar fibers proved outstanding competitors both individually or in combination with other types of materials.

Noteworthy, Zhan et al. (2011) reported on an unusual combination among chicken feather and glass fibers and related electrical properties, identifying as having potential application in printed circuit boards (PCBs) [160]. In addition, they argued on the manufacturing costs and sustainability of the chicken feather fibers' presence within their tailored hybrid composite architectures.

A comprehensive review was carried out by Thomassin et al. (2013) on polymer/carbon based composites as electromagnetic interference (EMI) shielding materials [161]. The paper was divided into five sections focusing on: electromagnetic theory and the main parameters that influence the related property of the materials, description and classification of various materials envisioned for reaching high EM absorption performances with respect to the different carbon fillers, combination and/or comparison of the latter with other fillers, and finally description of few composite architectures.

Scale transition enabled dielectric relation processes monitoring in hybrid composites tailored from carbon nano-tubes (CNT), carbon black (CB) and carbon nano-fibers (CNF). For example, Al-Saleh and Saadeh (2013) reported on the electrical properties and electromagnetic interference shielding effectiveness in the X-band frequency range, underlining that no synergy outcome on their overall conductive

properties was found, while Zheming et al. (2010) reported on reduction in electrical resistivity and percolation threshold along with increase on the graphite oxide content [162, 163]. Opposite, da Silva et al. (2013) succeeded to outline the synergetic effect with respect to the electrical conductivity of hybrid composites based multi-wall carbon nano-tube (MWCNT) reinforced blend of poly-vinylidene fluoride (PVDF) and poly-pyrrole (PPy) polymer matrix [164].

Additionally, Yang et al. (2011), Yu et al. (2011), Zhang et al. (2012), Salinier et al. (2013), Yan et al. (2014), Motaghi et al. (2014) and recently Yan et al. (2015) tackled and generously reported on synergetic effects in hybrid carbon fillers reinforced polymer composites [165-170]. In summary, they reported excellent electric performance in temperature response, energy efficiency and operation within temperature range at given applied voltage in addition to enhanced dielectric properties.

Changes in material use patterns and the corresponding opportunities along the value-chains, fostered green composites as the main issue of intensive research in the last decade. Essentially, as debated in the previous sections, an insight on the effective dielectric properties of green hybrid composites was tackled. Thus, Jayamani et al. (2014) reported on dielectric constant, dissipation factor and dielectric loss factor of jute/bamboo natural fibers reinforced with polypropylene and unsaturated polyester hybrid composites [171]. Moreover, they further argued against the influence in increased jute volume fractions on the monitored dielectric properties, on the irrelevance of the polymer matrix contribution and alkali treatment of the natural fibers.

I.3. General remarks.

The previous sections aimed to address the main challenges on the route of development high performance polymer composite materials out of various constitutive combinations and architectures, including issues on synthesis, characterization and property modeling or simulation. Reflections on their overall behavior, interferences and synergies with direct consequences on their balanced properties should carefully be considered further while tailoring their architectures.

As the industry demand is skyrocketing around synthetic materials that impair supremacy either with natural or 3^R materials (i.e. recycled, reused, recovered), scientists acknowledged the importance of hybridization for both research and industrial purposes.

In this regard, experts view on the challenges of existing and future trends on the approached herein subject may help to overcome the gaps along each road map set individually or within a mix of accustomed and innovative issues.

The opportunities for these improvements can lie within: design, recycling, manufacturing processes, multi-scale approaches, availability, cost, substitution, etc. To promote understanding, inter- and intra- effective communication and interaction with outstanding worldwide research achievements and outcomes, focused actions should be employed to enable paradigm changes.

A sustainable development approach towards hybrid composite materials' deployment and 'smart' management tackles all underlined challenges in a comprehensive way by taking into account: a balance of economic, social and environmental aspects, a life cycle perspective and the direct implication of relevant actors (e.g. researchers, industry players, etc.).

Chapter II

Chapter II. Objectives.

II.1. Research general objectives.

Motivated by aforementioned outlined contributions, trends and research concerns, supplemented by a wide variety of applications, the herein contribution complied with the general quest for high-performance materials tailored as hybrid composite architectures envisaged by the mainstream field of research.

Further, it is considered to comply with the prevailing paradigm underpinned by the research community and acknowledged and accepted by business leaders and entrepreneurs proven the generated data. However, translated into practice these might give rise to some lock-in situation due to dogmatic views of different interest groups. Consequently, a balanced disposal in approaching the herein scientific information is both encouraged and desirable.

Therefore, the present contribution *primary aims* to provide and foster a research framework on high-performance polymer based hybrid composite materials and their retrieved effective material properties by comprehensive characterization to enable structural and/or other emerging engineering applications.

II.2. Research specific objectives.

More specifically, the herein PhD thesis strives to address:

Objective 1 – issues to tackle in relation to hybrid polymer based composite architecture design, e.g. identifying cut-offs with respect to the material selection and compatibility issues attainment, expanding and enlargement novel micromechanical based relationships to be used in conjunction with the effective material property addressed, underline of potential transition within the multi-scale transition through simulation and modeling, etc.

Objective 2 – facilitating understanding of employed material characterization method and/or set up in conjunction with particular hybrid polymer based composite architectures in order to ensure mutual awareness, knowledge transfer and fostering between scientific researchers, specifically, and industry players and other actors, generally.

Objective 3 - providing input to further debates on hybrid polymer based composite materials' synthesis and characterization, full implementation of the existing state-of-art in the particular field approached or related scientific domains through smart specialization of various stakeholders (e.g. young researchers, master and doctoral students, industry specialists, etc.).

In order to achieve these objectives, the herein scientific contribution will feature, inter alia:

1. An update on the scientific achievements and experts' views on the challenges of existing and future trends in hybrid polymer based composite materials, prior and post published references of the herein author.
2. Outlines of the inter-linkages between hybrid composite materials' design, manufacturing and characterization on future prospective applications, on the role of scientific data availability, understanding and use in the world-wide context of research and innovation.

3. Providing pointers to the systemic approach applied while tackled the herein subject, balanced views and expanded research description developed throughout the individual chapters into a fashionable and contemporary manner.

Chapter III

Chapter III. Design of Experiments.

III.1. Introduction.

Taking into account the general objectives stated in the previous chapter, the experimental research carried out was centered both on different hybrid polymer based composite architectures' manufacturing and testing with the aim of wide range of effective material properties' retrieval.

Due to the complexity and availability of the research equipments, the experimental research related to the individual material property under the focus was carried out in several locations, as follows:

- Department of Mechanical and Materials Engineering, Polytechnic University of Valencia, Spain.
- Faculty of Materials Science and Engineering, 'Transilvania' University of Braşov, Romania.
- Fraunhofer Institute for Applied Polymer Research PYCO, Teltow, Germany.

III.2. Hybrid polymer based composites - architectures and synthesis.

The manufacturing aspects were tackled by tailoring few hybrid polymers based composites' architectures based on their constitutive features. The hybrid architectures were designed by differently stacking 4 and 9 layers of synthetic and natural fabrics, respectively. The hybrid polymer composite architectures were developed using the following manufacturing technologies:

- Conventional vacuum assisted resin transfer molding (VARTM) process for the 4 layers stacked architectures.

- Temperature controlled closed molding pressing for the 9 layers stacked architectures.

Reinforcements used to develop the hybrid polymer based composites can be assigned to the class of the most employed type of synthetic engineering materials: *carbon* and *basalt*. Further, the 'green' aspect was addressed by selection of *flax* as the most suited reinforcement. All of them were plain 1/1 weave fabrics, since the architecture of textiles was not considered as subject of interest and influencing factor with this contribution.

These constitutive were selected to balance the overall properties of hybrid composite architectures. Other selection criteria were accounting for their availability, individual material properties and compatibility issues already shown with a wide range of applications (see previous chapter). Finally, the cost-effectiveness issue can be viewed as a subject of interest indirectly addressed. The latter will be not developed or exploited explicitly, individually or related to one of the effective material properties, even it concerns the herein undersigned researcher's interest.

III.2.1. Types of constitutive.

As aforementioned, different types of reinforcements was deployed, namely: carbon-fiber (n. CF), basalt (n. BF) and flax (n. FF) fabrics were selected as fiber reinforcements (see **Table III.2.1**). The content (i.e. volume fraction) of each constitutive was determined accordingly to the previous versions of ASTM D3171: 2015 [172].

Table III.2.1. Material data of the present composite reinforcements.

	Carbon fiber (KDK 8003)	**Basalt fiber**	**Flax fiber**
Fabric areal weight (g/m²)	200 ± 10	475 ± 10	175 ± 10
Fabric thickness (mm)	0.30 ± 0.05	0.35 ± 0.05	0.40 ± 0.05
Young modulus (GPa)	241	105	60
Commercial trade name	SIGRATEX®	-	-
Supplier	SGL Technologies GmbH	Deutsche Basalt Faser GmbH	Leinenweberei Hoffmann GmbH

Different thermosetting polymer resins were selected and/or formulated to deliver the hybrid laminate architectures based on several criteria addressing the compatibility aspects, applications potential, manufacturing issues and costs effectiveness. All blends were formulated as derivatives of diglycidyl ether of bisphenol F (n. DGEBF) commercial epoxy resins (see Table III.2.2) and used to deliver hybrid architectures of 4 and 9 stacked layers, respectively.

Thus, the DGEBF epoxy (i.e. Epikote™ 04434) resin was cured with its delivered hardener under a ratio of 100 to 45 parts by weight of each constituent for the 9 stacked layers' configuration whereas for the 4 layer was used an epoxidized linseed oil (n. ELO) (supplied by Traquisa S.A, Spain) with an epoxy equivalent weight of 178 g equiv^{-1}. The resins were chosen either due to their wide availability and adequacy in the first case (i.e. including its high thermoforming stable laminate manufacturing) or as new formula delivery.

The green epoxy resin was formulated by using a glutaric anhydride (n. G 3806) agent to aid the cross-linking process (from Sigma Aldrich, Germany) and maleinized linseed oil (n. MLO) as plasticizer-compatibilizer (from Vanderputte, Belgium) characterized as posing a viscosity of 10 dPa at 20 °C and an acid value of 105-130 mg KOH g^{-1}. Several mixing by volume were formulated to the ELO:G:MLO blend (50:50:0, 50:30:20 and 50:40:10) and used with subsequent constitutive.

In addition, the other blend of thermosetting resin was formulated by mixing a bisphenol A (n. BA) dicyanate ester pre-polymer (n. CE), supplied as 75% solid in methyl ethyl ketone (MEK) with the DGEBF epoxy resin (Epikote™ 862) into a 70:30 (vol.%) ratio.

Table III.2.2 summarizes supplier's individual material data on the epoxy and cyanate ester polymer resins, respectively.

Table III.2.2. Individual physical properties of the polymer systems.

	Cyanate ester resin (Primaset™ BA 230 S)	**DGEBF epoxy resin (Epikote™ 862)**	**DGEBF epoxy resin (Epikote™ 04434)**
Glass transition temperature (°C)	320 (by DMA)	270 (by DSC)	up to 200 (by TMA)
Viscosity @ 25°C (mPa·s)	450 ± 100	740 ± 150	800 ± 150
Density @ 20°C (g/cm³)		1.18 ± 0.02	1.14 ± 0.02
Curing agent	Bisphenol A (BA)		Epikure™ 04434
Supplier	Lonza Ltd	Momentive	Momentive

III.2.2. Manufacturing of composite stacking.

4 layers stacked architectures.

A conventional Resin Transfer Molding (RTM) technique was considered for the ELO blend based specimens (dimensions: 300 mm x 300 mm) manufacturing by aid of a Hypaject MKII supplied by Plastech Thermoset Tectonics Ltd. (Gunnislake, UK) under identical process conditions as those reported by Samper et. al. [173, 174]. The processing conditions of laminate composites are summarized in **Table III.2.3**.

The gel time for each resin blend was estimated by the aid of plate-plate oscillatory rheometry in an AR-G2 (TA Instruments, New Castle, USA) within 90° - 120° C temperature range. The evolution of the phase angle between the applied dynamic

stress and the corresponding dynamic deformation was monitored and accounted to indicate the curing phases. The controlled variables were 0.1% strain at a constant frequency of 1 Hz. A temperature value of 100° C was considered an optimum value for the ELO based blends cross-linking since provides a balanced curing cycle.

The overall fiber loading fluctuated within 55.3 ± 0.5 wt. % for all configurations while the sample thickness ranged from 4 to 4.5 mm. Good-quality surfaces were obtained in all composite specimens with exceptions of those for which the flax reinforcements were layered as the outermost surfaces. With respect to the later, accounting their inherent property (i.e. hydrophilicity), a roughness appearance was obtained.

With respect to the stacking sequence, in the case of the hybrid architectures, symmetrical stacked sequences were delivered in terms of the synthetic and natural constitutive. Thus, the following codes were considered for the stacking sequences: BF/FF/FF/BF and FF/BF/BF/FF, respectively. To address further comparisons, BB and FF were layered individually to deliver reference specimens.

Table III.2.3. Process conditions of ELO based composites [173, 174]

Parameter	**Set value**
Resin injection temperature (°C)	60
Resin injection pressure (kPa)	100
In mold cavity pressure (kPa)	95
Curing cycle	
Temperature (°C)	100
Time (h)	3.0
De-molding temperature (°C)	30

9 layers stacked architectures manufacturing

The hybrid composite laminates (dimensions: 310 mm x 310 mm) were produced by stacking individually 9 either entirely natural and/or synthetic reinforcement based prepreg sheets. The prepregs were manufactured *in situ* after previously retrieving and optimizing the novel blend and standard polymer pre-polymerization conditions.

ISO 15034:1999 standardized procedures were used to determine the resin flow while ISO 15040:1999 was used to evaluate the gel time for each resin system, individually.

A temperature-controlled oven was used to compress and fully cure the composite plates at different constant temperatures, distinctively for each resin, at 50 kN for one hour. Thus, a temperature of 180 °C was selected for the CE&DGEBF epoxy based hybrid composites, and 120 °C for the DGEBF epoxy resin. The laminates based on the DGEBF epoxy resin were further post-cured for 1 hour at 170 °C, as recommended by the supplier.

The overall fiber loading fluctuated as shown in Table and an average of 5 % of resin flow was measured, after lamination, for all hybrid composite plates. Single type and hybrid composite laminates, five individual specimens for each polymer resin, posing high-quality surfaces were obtained. Sample thickness ranged from 2.5 to 3 mm depending on stacking configuration.

With respect to the stacking sequence, in the case of the hybrid architectures, the higher strength materials (i.e. CF, BF) were layered as the outermost, external and external/middle layers. Flax fibers were layered in between due to their poor material properties comparatively with the other reinforcements used herein. Thus, asymmetric and symmetric architectures were delivered for these particular synthetic epoxy based hybrid composites.

Table III.2.4 lists the stacking layering codes used to further address the 9 layers hybrid composite architectures as well as their individual and total volume fraction within the final laminate configurations.

Table III.2.4. Details on hybrid composites stacking sequences, assigned codes and volume fractions.

Stacking sequence	**Laminate codes**	**Reinforcements volume fraction (vol. %)**				**Total fiber loading (vol. %)**	
		CE&DGEBF		DGEBF		CE&DGEBF	DGEBF
		nf	*sf*	*nf*	*sf*		
□□□□□□□□□	9FF	45	-	40	-	45	40
■□□□□□□□■	BF/7FF/BF	21	14	21	14	35	35
■□□□■□□□■	BF/3FF/BF/3FF/BF	13	17	19	21	30	40
■□□□□□□□■	CF/7FF/CF	18	17	24	11	35	35
■□□□■□□□■	CF/3FF/CF/3FF/CF	19	11	23	12	30	35

■ synthetic reinforcement (*sf*); □ natural reinforcement (*nf*)

III.3. Testing methodologies and equipments.

III.3.1. Mechanical properties.

Flexural properties were retrieved in accordance with SR EN ISO 14125:1998 standard using a mechanical testing machine INSTRON model 3369 (Instron, USA) running in a 3-point bending mode with a length span of 48 mm, using a 10 kN load cell. A bending rate of 1.5 mm/min was used to take the measurements and an average value from five representative samples for each composite class is reported. All mechanical tests were conducted at room temperature (approximately 21 ± 2 °C). Flexural strength and modulus were retrieved as claimed by the ISO 178:2010 standard.

III.3.2. Dynamic mechanical thermal characterization.

Dynamic mechanical properties were retrieved in accordance with ASTM D5023-07 using a RSA6 analyzer from Rheometric Scientific (TA Instruments, USA) running in a 3-point-bending mode at an oscillating frequency of 1 Hz and length span of 25 mm. The hybrid composite specimens were scanned in the "dynamic temperature ramp mode". The Rheometric Orchestrator® software was used to operate the instrument and analyze the experimental data. The storage (E') and damping factor (tan δ) of the individual hybrid composite specimens were acquired at temperatures ranging up to 250 °C, at a heating rate of 4 K/min to avoid all artifacts. Two successive scans were applied to each specimen under study.

III.3.3. Thermo-physical properties.

Thermal expansion.

Thermal expansion tests were performed on a differential dilatometer DIL 420 PC/1 (Netzsch GmbH, D), in accordance with ASTM E228-11 and DIN 53752-A standards - dynamic heating ramp was set out a temperature mode, temperature range – between 25°C and 250°C, heating rate of 1 K/min. The software includes semi-automatic routines for correction of the sample holder expansion, as well as, computation of the expansion coefficients, onset and peak temperatures, inflection points, rate of expansion etc.

Thermal conductivity.

Thermal conductivity tests were performed LFA 447 HyperFlash™ device (Netzsch GmbH, D), within 25°C – 125°C (e.g. 9 stacked layers) and 25°C – 200°C (e.g. 4 stacked layers) temperature intervals, respectively according with the ISO 22007-4:2008 standard procedures. Samples were covered back and forth with a thin layer of graphite to enhance their emission/absorption properties. Thermal conductivity data can be referred as through-thickness values and represents the mean of recorded values out of five single shots on each point considered. The standard deviation of the five shots was less than 1.5%.

III.3.4. Thermal stability and fire retardant properties.

Thermal stability was studied by thermogravimetric analysis on the specimens. The measurements were performed by aid of a STA 449 F3 Jupiter® (Netzsch GmbH, D) at a heating rate of 10 K/min, in liquid nitrogen atmosphere at 20 mL/min flow rate, in accordance with ISO 11358-1:2014. Dynamic mode was deployed in the heating step within the selected 25°C – 850°C temperature range. Alumina crucible was used for each

individual specimen excerpt. The weight loss was recorded in response to temperature increases. *Fire retardant properties* were performed according to ISO 5660-1:2015 standard procedures.

III.3.5. Dielectric properties.

Dielectric properties were retrieved by the aid of high precision dielectric analyzer (Alpha analyzer, Novocontrol Technologies) in combination with a control temperature system in the temperature range 25°C - 180°C, in steps of 5 K/min and consecutive isothermal frequency sweeps (101 – 107 Hz).

III.3.6. Scanning electron microscopy (SEM).

Scanning electron microscopy (SEM) - Morphology was investigated by an EVO MA 25 (Zeiss, D), at room temperature, running in 500x magnification mode. The prevailing images, after sputtering the samples with a thin layer of gold, were further subjected to analysis in order to qualitatively characterize the fiber–matrix interfaces.

III.3.7. General considerations and specifications.

Generally, the aforementioned mentioned values under each experimental device's setup considerations were preserved and used in case of both hybrid particle-fiber and fiber-fiber polymer composites architectures.

Variations from previous were considered while monitoring and sizing the influence of the experimental environment and running conditions upon the effective properties and performances of hybrid polymer based samples under consideration.

Variations in experimental set-ups and specimen geometry were individually addressed and considered for the hybrid composites under debate (e.g. tensile replaced by compression in particle-particle hybrid composites samples, etc.).

In temperature related overall properties, the reported data corresponds to the second or to the next thermal cycles, irrespective to the temperature programs selected to run the measurements. The reasons behind this will be revealed in the corresponding chapter.

Chapter IV

Chapter IV. Theoretical Micromechanical based Approaches.

IV.1. Introduction.

Theoretical predictions of hybrid composites' effective material properties are currently under extensive approaches due to the requirements involving expertise and subject understanding. Due to heterogeneous nature of these types of materials, scale transitions from macro to micro and reverse are employed by the instrumentality of mean-field homogenization methods.

Thus, micro to macro transition needs the presence of a *representative volume element* (RVE) containing all inclusions that better describe the hybrid composite structure, sufficiently large to represent the underlining heterogeneous microstructure and a homogenization method to find the macro constitutive response of the previous.

Two distinct courses of actions were followed to predict the effective material properties of the hybrid polymer based composites under the focus:

- numerical predictions by the aid of a professional multi-scale modeling software platform from e-Xstream Engineering;
- numerical predictions based on theoretical models by the aid of commercially available software (e.g. Excel from Microsoft Office, PTC Mathcad, Matlab, Maple, Mathematica, etc.).

It is beyond the purpose of the herein thesis to debate on the advantages and disadvantages on using the aforementioned, even several mentions were made in the articles referred within this chapter.

A large collection of micromechanical models was extensively presented, augmented and debated by the herein contributor in one of her co-authored book [24]. Particular theoretical models were selected and presented next based on their frequency in use and not on their accuracy or accompanying mathematical formalism, while others only referred to as listed in **Table IV.1.1**.

Table IV.1.1. Expressions of theoretical models used in hybrid composites properties predictions.

Hybrid composite architectures	**Property predicted**	**Theoretical model**	**References**
Hybrid particle-particle polymer composites	Mechanical	Mechanics of Materials, Mori-Tanaka, RoHM	[24], [182], [183]
	Thermo-physical (thermal expansion)	Mori-Tanaka, Double inclusion	[24], [181], [184], [185], [186], [187], [188]
	Electrical	Maxwell, Clausius-Mossoti, Milton, Pal, Bruggeman, Hashin-Shtrikman	[24], [177], [180], [189], [190]
Hybrid particle-fiber polymer composites	Mechanical	Milton, Mechanics of Materials, Halpin-Tsai, RoHM	[24], [173], [183]
	Dynamic mechanical	Mori-Tanaka, Halpin-Tsai	[191], [192]
	Thermo-physical (thermal expansion and conductivity)	Mechanics of Materials, Maxwell, Levin-Hashin-Shtrikman, Hashin-Rosen, Christensen, Chamis, Ziebland	[179], [193], [194],[195]
Hybrid fiber-fiber polymer composites	Thermo-physical	Shapery, Hopkins-Chamis, Geier, Mori-Tanaka	[176], [178]

IV.2. Effective elastic modulus.

The micromechanical models were developed mainly in terms of reinforcement and matrix volume fractions even the weight fraction is more favorable to be applied in industry since the manufacturing equipments normally uses gravimetric feeding systems. Nonetheless, the simple relationship between the volume and weight fractions in single phase composite materials can be written as follows:

$$V_f = \frac{\frac{W_f}{\rho_f}}{\frac{W_f}{\rho_f} + \frac{W_m}{\rho_m}} \qquad \textbf{Equation IV.2.1}$$

where V_f is the fibers's volume fraction, W_f is the filler's weight fraction whereas W_m is the matrix weight fraction, ρ_f and ρ_m representing the filler's and matrix materials density.

On the other hand, for a hybrid composite architecture, the individual filler contribution inside the overall reinforcement's volume fraction can be determined by using the following expressions:

$$V_{f1} = \frac{\frac{W_{f1}}{\rho_{f1}}}{\frac{W_{f1}}{\rho_{f1}} + \frac{W_{f2}}{\rho_{f2}} + \frac{W_m}{\rho_m}} \quad \textbf{and} \quad V_{f2} = \frac{\frac{W_{f2}}{\rho_{f2}}}{\frac{W_{f1}}{\rho_{f1}} + \frac{W_{f2}}{\rho_{f2}} + \frac{W_m}{\rho_m}} \qquad \textbf{Equation IV.2.2}$$

where V_{f1} and V_{f2} are the volume fraction of the individual fillers embedded with the polymer system.

Rule of the hybrid mixtures (n. RoHM) is one of the simplest predictors that can be used for preliminary design situations where precision and accuracy of the properties are not of primary importance. In order to predict the effective elastic modulus of the hybrid composites the individual elastic modulus of phases should be determined first and then incorporated into the RoHM equations.

Rule of mixtures (n. RoM) ***and rule of hybrid mixtures*** (RoHM) were used to predict the effective stiffness of individual substrates; solely FF reinforced composites as well as combined FF/BF or FF/CF architectures, respectively. Expressions were stated in terms of volume faction of the composite constituents to facilitate further use, even the weight fraction of the individual reinforcements and matrices were deployed:

- RoM for natural-fiber reinforced composites

$$E_c = E_{nf} V_{nf} + E_m \left(1 - V_{nf}\right) \qquad \textbf{Equation IV.2.3}$$

- RoM for synthetic-fiber reinforced composites

$$E_c = E_{sf} V_{sf} + E_m \left(1 - V_{sf}\right) \qquad \textbf{Equation IV.2.4}$$

- RoHM for natural/synthetic hybrid composites

$$E_c = E_{cnf} V_{cnf} + E_{csf} V_{csf} \qquad \textbf{Equation IV.2.5}$$

The relationships between the volume fraction and weight fraction for the individual composite systems to be used in the RoM expressions are:

$$V_{nf} = \frac{W_{nf} / \rho_{nf}}{W_{nf} / \rho_{nf} + W_m / \rho_m} \quad \text{and} \quad V_{sf} = \frac{W_{sf} / \rho_{sf}}{W_{sf} / \rho_{sf} + W_m / \rho_m} \qquad \textbf{Equation IV.2.6}$$

in the case of individual substrates based on natural (n. *nf*) or synthetic reinforcements (n. *sf*), where V_{nf} and V_{sf} represent their fiber loading, W_{nf} and W_{sf} the corresponding weight fraction, and ρ_{nf} and ρ_{sf} their material density, where W_m and ρ_m are the matrix weight and density, respectively.

On the other hand, for the hybrid composites the individual fiber volume fraction can be estimated using the following expressions:

$$V_{nf} = \frac{W_{nf} / \rho_{nf}}{W_{nf} / \rho_{nf} + W_{sf} / \rho_{sf} + W_m / \rho_m} \text{ and}$$

$$V_{sf} = \frac{W_{sf} / \rho_{sf}}{W_{nf} / \rho_{nf} + W_{sf} / \rho_{sf} + W_m / \rho_m}$$

Equation IV.2.7

thus enabling prediction of the relative hybrid volume fraction of the natural- and synthetic based composite systems. Accordingly, the expressions used were:

$V_{cnf} = \frac{V_{nf}}{V_t}$, $V_{csf} = \frac{V_{sf}}{V_t}$ and $V_t = V_{nf} + V_{sf}$, respectively, where V_t is the total reinforcement volume fraction.

Positive and negative hybrid effect can be further defined and used to quantify any positive or negative deviation of the retrieved elastic modulus of the hybrid composite from the predicted value using RoHM equation [12]. With respect to the elastic strength of the hybrid composite architecture, it can be estimated in the same manner using the above concept.

IV.3. Effective complex elastic modulus.

A *multi-step homogenization scheme* was developed to predict the effective dynamic-mechanical properties (i.e. E-modulus and viscosity) in case of herein particle-fiber polymer based composites, consisting of two homogenization steps after decomposition. The multi-step method is capable of delivering excellent predictions when the right choice of the homogenization schemes is made.

Other theoretical models that can be deployed to roughly estimate the dynamic mechanical properties are the *rule of mixtures (RoM)* and/or *inverse rule of mixtures (iRoM)*. Literature acknowledges them as the *Voigt* and *Reuss* models. These models provide the lower and the upper limits of the predicted elastic values that bound the other predicted and/or retrieved values.

Accordingly, the complex modulus and damping factor of a composite material out of two constitutive are expressed as following:

$$E_c^* = E_r^* V_r + E_m^* V_m \qquad \textbf{Equation IV.3.1}$$

$$\tan\delta_c = \frac{E_r' V_r \tan\delta_r + E_m' V_m \tan\delta_m}{E_r' V_r + E_m' V_m} \qquad \textbf{Equation IV.3.2}$$

in case of the *Voigt* or *RoM* model, whereas

$$\frac{1}{E_c^*} = \frac{V_r}{E_r^*} + \frac{V_m}{E_m^*} \qquad \textbf{Equation IV.3.3}$$

$$\tan\delta_c = \frac{(\tan\delta_r + \tan\delta_m)(E_m' V_r + E_r' V_m) - (1 - \tan\delta_r \tan\delta_m)(E_r' V_m \tan\delta_r + E_m' V_r \tan\delta_m)}{(1 - \tan\delta_r \tan\delta_m)(E_m' V_r + E_r' V_m) + (\tan\delta_r + \tan\delta_m)(E_r' V_m \tan\delta_r + E_m' V_r \tan\delta_m)}$$

Equation IV.3.4

in case of the *Reuss* or *iRoM* model, whereas E^*, V and $\tan\delta$ stand for the complex modulus, volume fraction of individual constitutive and mechanical loss factor, respectively. Next, for hybrid composite architectures, the above can be used as

expressed in the previous section in case of the elastic modulus derived from *rule of hybrid mixtures* (RoHM).

Inter alia, the bounds are particular useful because they are usually exact under certain conditions, can be used for comparison purposes against the experimental data and provide a unified framework to study other types of effective properties.

IV.4. Effective thermal properties.

Rule of mixtures (RoM) and *rule of hybrid mixtures* (RoHM) will be deployed to predict thermal conductivities of epoxy based 9 stacked layers composites. In the line with the approach developed in section 3.1, expressions will be stated in terms of the volume faction of the composite constituents to facilitate further use even the weight fraction of the individual reinforcements and matrices were deployed:

- RoM with natural-fiber reinforced composites

$$k_{nfc} = k_{nf} V_{nf} + k_m \left(1 - V_{nf}\right) \qquad \textbf{Equation IV.4.1}$$

- RoM with synthetic-fiber reinforced composites

$$k_{sfc} = k_{sf} V_{sf} + k_m \left(1 - V_{sf}\right) \qquad \textbf{Equation IV.4.2}$$

- RoHM with natural/synthetic hybrid composites

$$k_c = k_{nfc} V_{cnf} + k_{csf} V_{sfc} \qquad \textbf{Equation IV.4.3}$$

In the above expressions letters and indices state as following: k for thermal conductivity, in W/mK, V for constitutive volume fraction, *nfc* for natural reinforcement composite, *nf* for the natural reinforcement, *sfc* for the synthetic fiber composite, *sf* for the synthetic reinforcement, *c* for the final hybrid architecture and *m* for the polymer matrix, respectively.

Chapter V

Chapter V. Measured properties on composites.

V.1. Mechanical properties.

In composite materials' testing, especially concerning the hybrid architectures, flexural properties (i.e. E-modulus, strength and strain to failure) are widely retrieved through 3-point bending experimental configurations as specified by ASTM D7264/D7264 M:2015 while tensile properties in accordance with ASTM D3039:2014 [175, 176]. The subsequent data were retrieved by approaching the above investigation setup but not limited to these.

V.1.1. Effect of hybridization on effective flexural properties.

The behavior of developed 9 stacked layers hybrid composite laminates under flexural loading is shown in **Figure V.1.1** and **Figure V.1.2**, (a) and (b). As can be seen, irrespective of the resin system and stacking sequences, the flexure failure mechanisms are more complicated in the hybrid composites compared to the solely FF reinforced laminates; the latter experience higher linear variation in load vs. deformation, which can be regarded as the elastic behavior of the specimens.

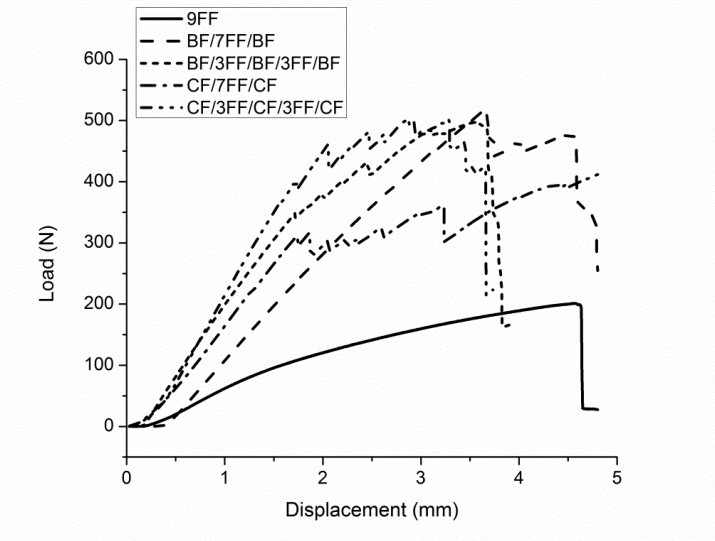

Figure V.1.1. Load vs. displacement curves of the laminates based on novel CE&DGEBF epoxy resin.

Through hybridization, the load vs. deformation curve changes from linear to more prolonged nonlinear variations for all hybrid specimens due to damage caused by bending and the resins' brittle nature [177]. Furthermore, the higher slope of the deformation curve corresponds to the increased number of synthetic fiber reinforced plies, irrespective of the resin system, that turns on providing the highest values of the flexural properties. The latter can also be determined from the values listed in Table and data plotted in **Figure V.1.3**.

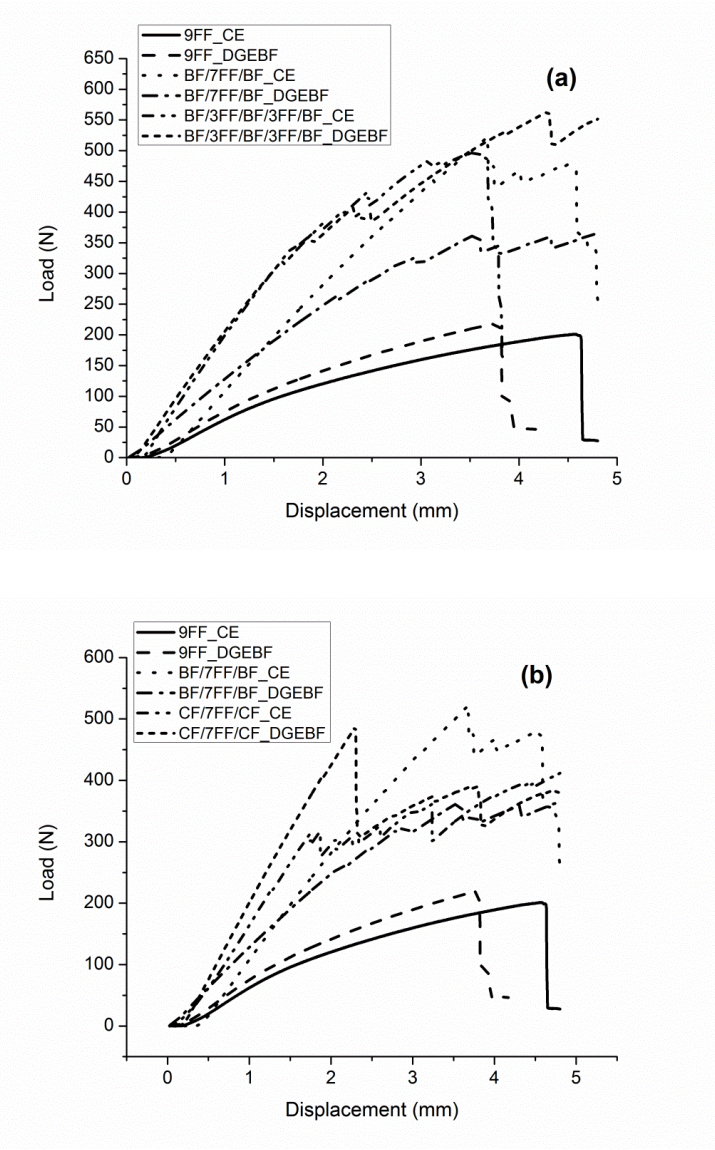

Figure V.1.2. Load vs. displacement curves of laminates (a) with different BF plies or (b) same BF and CF plies stacking sequences.

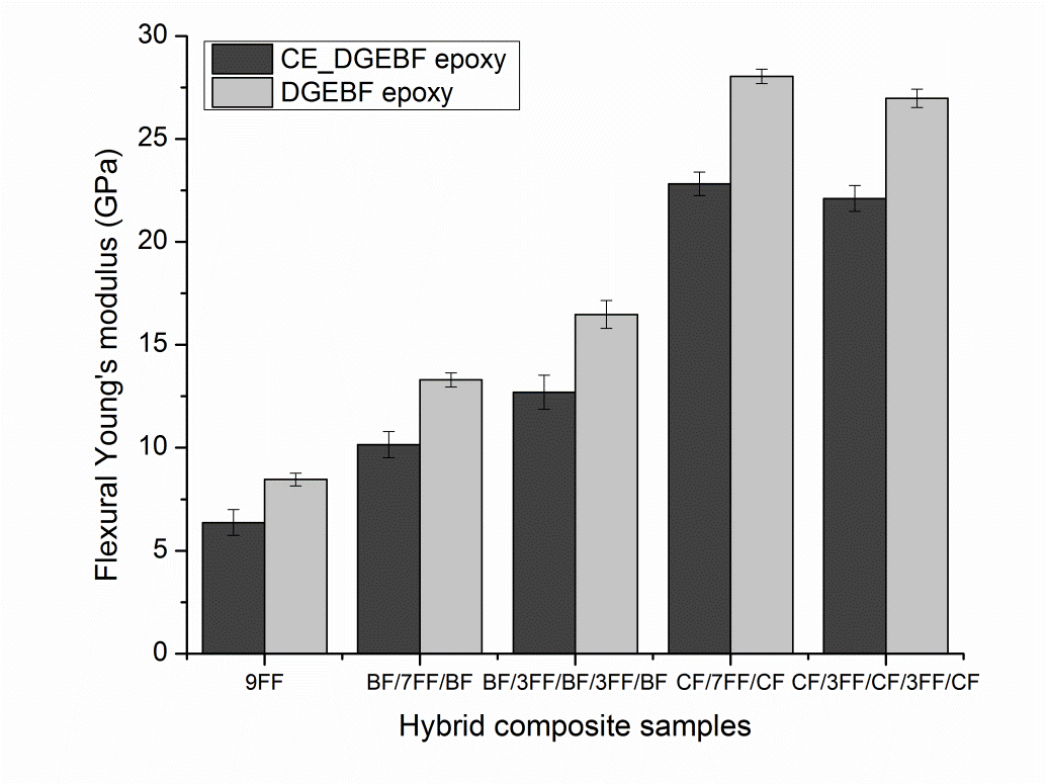

Figure V.1.3. Young modulus in flexure retrieved for all 9 stacked layers composite specimens.

Flexural properties of hybrid laminates under focus can be regarded to depend mainly on the stacking sequence, individual reinforcement material and polymer matrix. Thus, the flexural strength increases with the increase of the rigid phase content in comparison with solely FF composites, irrespective of the resin system employed.

The flexural properties of the hybrid laminates under focus can be regarded as depending mainly on the stacking sequence, individual reinforcement material and polymer matrix. Thus, the flexural strength increases with the increase in the rigid phase content in comparison with solely FF composites, irrespective of the resin system employed.

Table V.1.1. Flexural properties of NFRP and hybrid composite laminates.

Matrix system	Laminate codes	Flexural modulus (GPa)	Flexural strength (MPa)	Strain at break (%)	Max. load (N)
CE & DGEBF epoxy	9FF	6.37 ± 1.03	133.09 ± 12.02	3.55 ± 0.26	208 ± 9.22
	BF/7FF/BF	10.15 ± 0.64	217.92 ± 24.31	4.33 ± 0.67	461 ± 44.18
	BF/3FF/BF/3FF/BF	12.70 ± 0.83	252. 92 ± 20.11	3.28 ± 0.16	544 ± 47.20
	CF/7FF/CF	22.82 ± 0.57	317.30 ± 23.16	3.89 ± 0.25	438 ± 34.29
	CF/3FF/CF/3FF/CF	22.11 ± 0.63	330.43 ± 25.15	2.89 ± 0.28	549 ± 36.20
DGEBF epoxy	9FF	8.46 ± 0.31	169.55 ± 14.77	2.79 ± 0.27	226 ± 17.03
	BF/7FF/BF	13.29 ± 1.34	251.65 ± 7.61	4.07 ± 0.36	411 ± 19.98
	BF/3FF/BF/3FF/BF	16.47 ± 0.67	317.59 ± 23.63	3.74 ± 0.56	552 ± 36.46
	CF/7FF/CF	28.04 ± 0.35	350.95 ± 12.92	3.16 ± 0.65	467 ± 21.51
	CF/3FF/CF/3FF/CF	26.97 ± 0.44	358.15 ± 34.79	2.18 ± 0.10	488 ± 56.62

Furthermore, as expected, the CF based composites exhibit the best mechanical performance over the other hybrid architectures, irrespective of the polymer resin used and their stacking sequence. Positive departures are obtained for all BF and CF reinforced hybrid composites, either symmetrically or non-symmetrically stacked, in connection with flexural strength and/or elastic modulus.

For example, the overall elastic moduli of BF hybrid composites give rise to an increase in the property of approximately 45% and 65% for all resin systems compared with solely FF laminates. On the other hand, in CF based architectures, the synergetic effects even are positively accentuated, highlighting once again the efficacy of this type of reinforcement.

Little discrepancies were found between the symmetrical and unsymmetrical architectures and between one resin system and the other, particularly the different individual and total volume fractions of reinforcements. Thus, property improvement increments of approximately 113% and 110.5%, for symmetrically and non-symmetrically stacked CF reinforced CE&DGEBF composites, were obtained compared to FF laminates.

Switching to the DGEBF resin-based architectures, the property improvement changes were to approximately 107% and 105%, respectively.

In addition, the above discrepancies in the flexural modulus clearly reveal the incompatibilities between the FF and resin systems, thus causing improper wetting and poor adhesion. The latter is due mainly to the hydrophilic nature of the FF that was used without any prior surface modifications and whose -OH groups and other volatile residues impede the fiber/matrix adhesion efficiency. This can be evidenced while embedded in the CE&DGEBF resin, which is a more complicated structure and highly sensitive to moisture.

Relatively high differences were recorded in the CF hybrid composites similarly stacked but embedded in a different matrix material. The deceptive results in this case can be attributed to a lower-quality interface with the CE&DGEBF matrix.

V.1.2. RoM or RoHM vs. experimental data.

The RoM and RoHM predictions were carried out based on material data listed in **Table III.2.1** and **Table III.2.2**. The mechanical properties of the novel blend and DGEBF epoxy resin were retrieved from the *in situ* fully cured batch: 2.35 ± 0. 21 (GPa) for the CE&DGEBF resin, 2.15 ± 0.11 (GPa) for the DGEBF resin system.

In addition, the volume fractions of the reinforcements were predicted function of weight fractions of the constitutive and the laminates. The individual volume fraction of the natural/synthetic reinforcements and total volume fraction assigned to the different resin systems were summarized in **Table III.2.4**.

In **Figure** V.1.4. RoM and RoHM based stiffness prediction for all 9 stacked layers architectures.

e V.1.4 was shown the effect of the stacking sequence, the individual fiber and the matrix materials on the predicted elastic stiffness using the RoM and RoHM expressions in Eq. (3.1)-(3.3). An increase in the effective mechanical properties with the

increase in the reinforcement loading can be emphasized by closely looking at the plotted data.

Hybrid laminates based on the CE&DGEBF epoxy resin show the same trend as the incorporation of synthetic fibers. Since every combination reveals the same values of the total volume fraction (i.e. 35% and 30%, respectively) differences underline the effectiveness of the individual synthetic materials in favor of CF.

Next, the hybrid effect for all combinations employed can be categorized based on data plotted in **Figure V.1.5**. As expected, solely FF reinforced laminates reveal a negative effect irrespective of the matrix system, since their RoM based predictions are higher than the experimental values. It is widely acknowledged in the literature that the linear RoM provides the upper values in stiffness prediction among the micro-mechanical based theoretical models [14].

On the other hand, RoHM enables predictions that differ less from the retrieved values. This is one of the major reasons for its frequent use in effective property estimates [12, 22]. In this case, negative hybrid effects are revealed by both the BF based hybrid composite architectures used with the CE&DGEBF epoxy resin system (i.e. -20.2% and -14.3%). These are turned to positive effects while using the DGEBF epoxy resin but with very small differences from their predicted values as the synthetic fiber content increases (i.e. 9.3% and 2.4%, respectively).

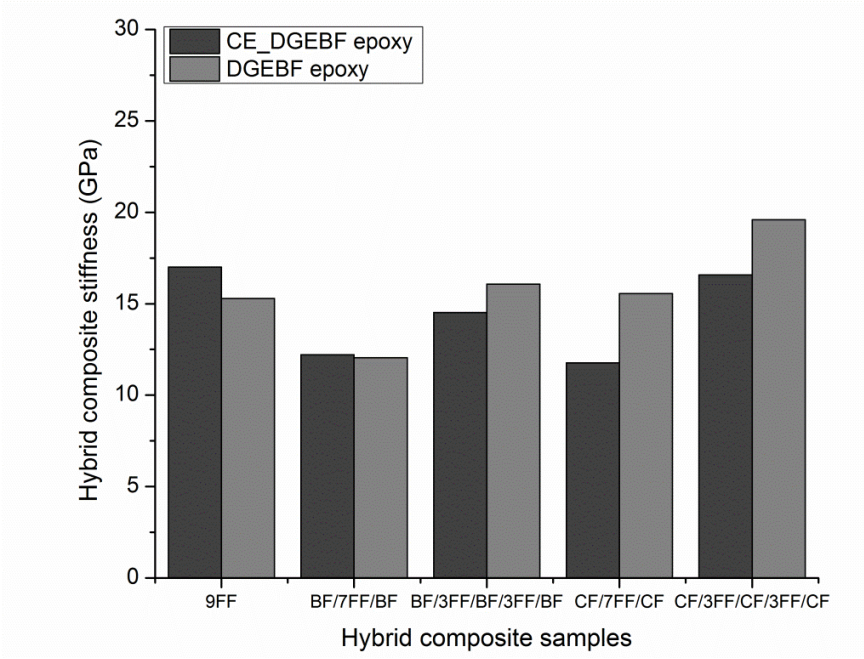

Figure V.1.4. RoM and RoHM based stiffness prediction for all 9 stacked layers architectures.

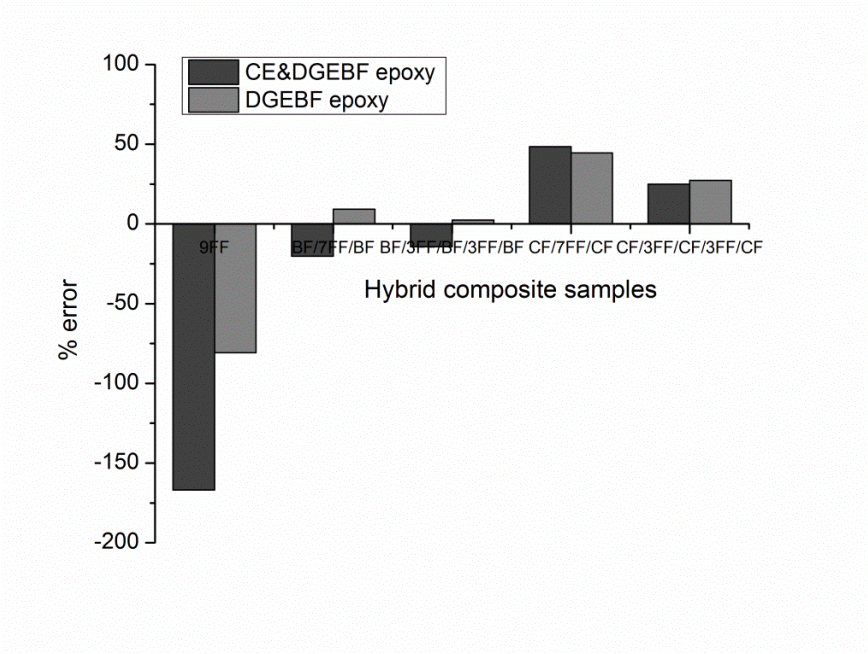

Figure V.1.5. Percent error to be used in hybrid effect ranking of 9 stacked layers laminates.

In addition, in all CF based hybrid architectures, irrespective of the resin system, positive hybrid effects are obtained while determining the constitutive synergetic status. Based on the experimental data and predicted values, consistency in

the differences for each combination based on one type of resin to the other can be seen. This underlines once again the effectiveness of CF as reinforcement in all hybrid architectures and the prevalence of its material properties to the overall predicted.

In addition, individual material properties were highly responsible for the relative error values between the predictions and the estimates. Since the materials came from different suppliers and were acquired in distinct loading conditions, they should be considered only as general indicators.

V.2. Dynamic mechanical properties

Dynamical mechanical analysis represents one of the most comprehensive testing methods of polymer based composite materials. Its temperature and frequency-dependent parameters (e.g. storage and loss modulus, mechanical damping) allow close monitoring of the fiber–matrix interactions within a large range of temperature values or different excitation frequencies. Furthermore, it represents a good indicator regarding the curing and/or post-curing conditions and their effects upon specimens.

As it was previously stated, the main *influencing factors* upon the effective material properties of polymer based composites, generally, and hybrid ones, particularly, have to be identified by looking to the composites: architecture, constitutive (e.g. volume fraction, orientation, materials, etc.), manufacturing technology, prior and post-processing of individual or overall structure and last to the experimental conditions selected.

The latter out of aforementioned influential factors and consequently, sources of errors associated with experiments envisages: type of load, frequency, clamp, specimen geometry, temperature program, etc.

According to ISO 6721-1:2011, the *storage modulus* E' represents the stiffness of a visco-elastic material and is proportional to the energy stored during a loading cycle while the *loss modulus* E" is defined as being proportional to the energy dissipated during one loading cycle.

The *loss factor* tan δ is the ratio of loss modulus to storage modulus. It is a measure of the energy lost, expressed in terms of the recoverable energy, and represents mechanical damping or internal friction in a viscoelastic system. The loss factor tan δ is expressed as a dimensionless number. A high tan δ value is indicative of a material that has a high, non-elastic strain component, while a low value indicates one that is more elastic [178].

V.2.1. Epoxy based composites.

V.2.1.1. Storage modulus (E')

In Figure V.2.1, (a) and (b) were plotted the temperature variation of this modulus E' for all 9 stacking sequences considered and both resin systems. As it can be seen, two transitions (i.e. glass and leathery to rubbery) and three different states (i.e. glassy, leathery and rubbery) can be identified for the herein unsaturated polyester thermosetting resin used as matrix material.

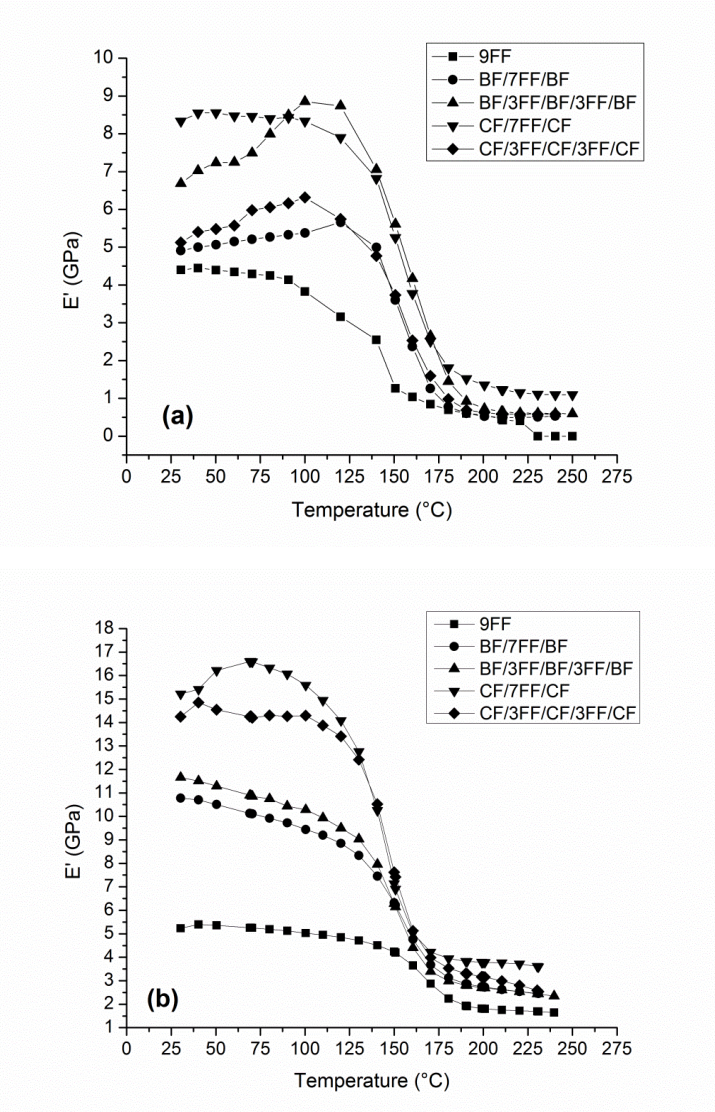

Figure V.2.1. Storage modulus (E') curves for the 9 layers architecture based on (a) CE&DGEBF epoxy blend and (b) DGEBF epoxy resins.

Graphical representations reveal relatively small departures from linearity of all the E' recorded values in the temperature range up to 120 °C irrespective of stacking sequence and individual fiber and matrix types. This can be regarded again as the hydrophilic nature of FF and -OH groups and other volatiles that impede a good fiber–matrix interface adhesion.

Moreover, it might be regarded that the discrepancies between FF and BF/CF tend to dispute their supremacy in the overall performance of hybrid composites. The latter can be evidenced especially in the case of the high number of synthetic reinforcement based plies within the hybrid composite structures.

Additionally, in the glassy plateau, the storage modulus experiences a decrease while replacing BF with CF, for both resin systems. On the other hand, in the rubbery plateau, this reverses and can be regarded as the CF behavior with temperature and the matrix's cross-linking density [179].

Furthermore, the slope of the glass transition varies within each hybrid composite architecture class and from one resin system to the other. Thus, composites reinforced only with FF exhibit a relative small slope during transition and, consequently, polymer flows before their end. On the other hand, BF reinforced hybrid laminates exhibit lower slopes during this glass transition compared with their counterpart CF architectures, irrespective of the resin system used.

Next, when the temperature increases the *leathery* polymer state, is being reached. This is compromising intact primary bonds and broken secondary polymer bonds that are causing both a drop in the dynamic mechanical modulus and an increase in the viscosity.

As the temperature is raised further, between 175° up to 250 °C, the primary and secondary bonds remains unchanged as previously, but the molecular structure get entangled. In this case, the rubbery state is roughly well captured in the experimental data. Since the experiment was stopped at 250 °C, any further variations ascribed to the rubbery-decomposition process were not included and thus, omitted from the plots.

V.2.1.2. Damping factor/loss tangent (tan δ)

As one of the important parameters that provide a balance between the elastic and viscous phase of polymer based composite materials, this material property reveals the influence of the constitutive, in terms of type, distribution and compatibilities upon the damping behavior of the structures.

The damping behavior of hybrid laminates can be determined from the tan δ values (i.e. the loss/damping factor) represented in **Figure V.2.**2, (a) and (b), defined as the ratio between loss modulus (E'') and storage modulus (E'). As can be seen, the transition temperatures obtained from the tan δ curves are in the range 145 °C to 180 °C for 9 stacked layers composites and have a negative shift compared to that of neat resins.

Further, there are no huge discrepancies in the T_g values for the same synthetic fiber type and resin system but different stacking sequence apart from a negative shift while replacing BF with CF. The latter is consistent with the aforementioned relating to the CF behavior with the temperature increase without ranking it as a negative effect.

One can obviously determine the influence of the synthetic/natural reinforcement and stacking sequence on the damping behavior of the overall hybrid laminates by overlapping the tan δ curves for individual resin systems. For example, in the CE&DGEBF based laminates, higher peak values in the tan δ curves were obtained for BF reinforced architectures regardless of the stacking sequence compared with their CF counterparts (see **Figure V.2.2a**).

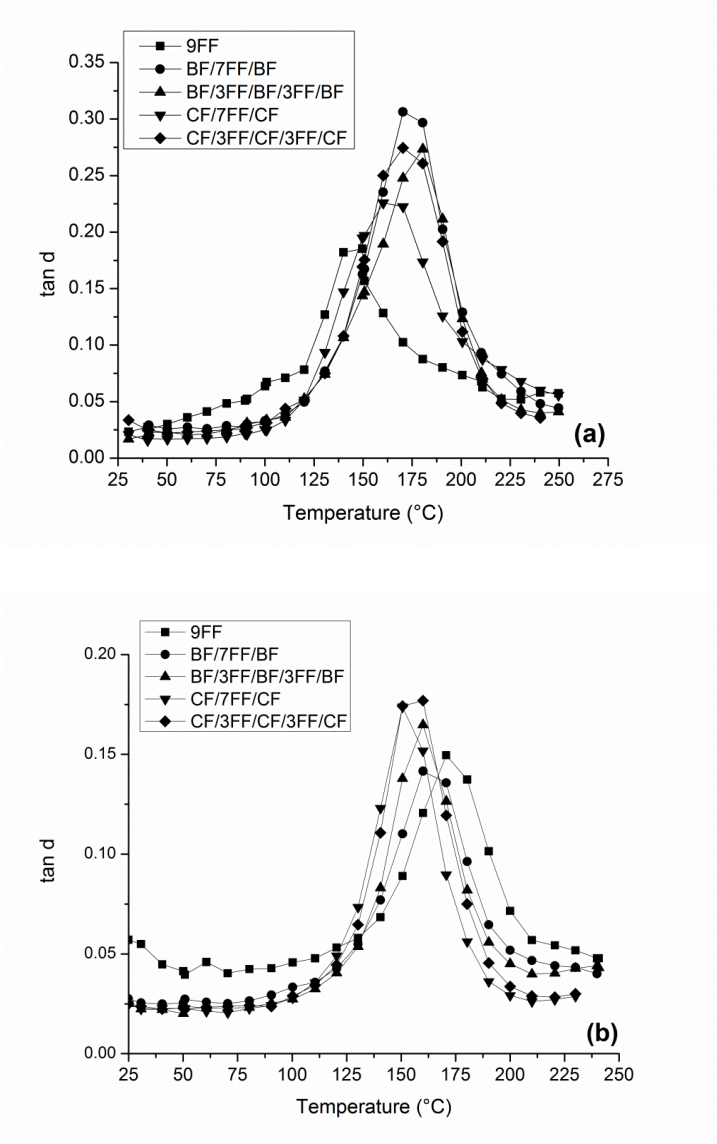

Figure V.2.2. Loss factor (tan d) vs. temperature dependencies in case of 9 stacked layers composites based on (a) CE&DGEBF epoxy blend and (b) DGEBF epoxy resins.

The aforementioned do not hold for the DGEBF based laminates, where the roles of the basalt and carbon fibers reverse (see **Figure V.2.2b**). The main reason for this behavior is that FF exhibits a "desiccating" role within the hybrid configuration due to the above influencing factors that impede the fiber–matrix adhesion efficiency. On the other hand, these differences should be sought in modifying the conformation and orientation of the polymer chain segments as a result of interfacial adhesion.

Furthermore, CE &DGEBF resin was found to be sensitive to the presence of -OH groups. This was outlined during the first thermal conditioning scan of the hybrid laminates when two loss peaks were present. The second loss peak is a relaxation peak that should be associated with the polymer curing effects and the cross-linking degree, a peak that disappears in the second scan. This is consistent with the findings of Karad et al. [180], reported herein, from experimentally reproducible reasons in the answer to possible questions.

Neither post-curing conditioning of 1 hour at 180 °C for the CE&DGEBF based laminates, nor further conditioning at prepreg levels help in the removal of the second relaxation peak from the first thermal run. The latter reveals only the composite laminates' thermal history and is not used in the assessment of damping properties.

Furthermore, BF and CF seem to behave differently while subjected to temperature variations, despite other similarities that transform the first into an alternative attractive solution.

In **Table V.2.1** was listed the Tg values retrieved from the damping factor and loss modulus curves. These values are usefully in assessing the hybrid composite's behavior in shock and vibrations as recommended by ASTM D 4065:2001 [181].

Furthermore, the importance of Tg relays on its practical significance since provides information regarding the thermal limits in use of structures or components, their frequency and temperature-dependent damping, influence of the constitutive on the mechanical properties, degree of curing or post-curing, etc.

Table V.2.1. Peak height and Tg temperatures (from tan δ and E″ curves).

Resin system	Sample architecture	Peak height of tan δ curve	Temperature [° C]	
			Tg from tan δ	Tg from E″
CE & DGEBF epoxy	9FF	0.155	176.24	
	BF/7FF/BF	0.261	173.28	
	BF/3FF/BF/3FF/BF	0.229	174.55	
	CF/7FF/CF	0.190	166.12	
	CF/3FF/CF/3FF/CF	0.247	171.27	
DGEBF epoxy	9FF	0.149	170.7	
	BF/7FF/BF			
	BF/3FF/BF/3FF/BF			
	CF/7FF/CF			
	CF/3FF/CF/3FF/CF			

The different roles of the matrix or fiber types and stacking sequence in the overall damping behavior of the hybrid composites were evaluated using the reinforcement *effectiveness coefficient* C (from Eq. (4.1)) and the *adhesion efficiency factor* A (using Eq. (4.2)) [73]:

$$C = \frac{\left(E'_g / E'_r\right)_{composite}}{\left(E'_g / E'_r\right)_{resin}} \qquad \textbf{Equation V.2.1}$$

where E'_g and E'_r are the storage modulus values retrieved from the glassy (50 °C) and rubbery (225 °C) plateaus, respectively,

$$A = \frac{1}{1-V_t}\frac{tan\delta_{composite}}{tan\delta_{resin}} - 1 \qquad \textbf{Equation V.2.2}$$

where $tan\delta_{composite}$ and $tan\delta_{resin}$ are the relative damping of the composite and resin at the glass transition temperature, and V_t is the overall reinforcement volume fraction. As can be seen, both estimators are temperature dependent.

Table V.2.2 lists the values of these performance estimators for all 9 stacked layers architectures herein for further comparison purposes. Based, on the above, it can

be determined that the reinforcement effectiveness coefficient (C) increases with increments in the synthetic reinforcement layers, irrespective of the polymer resin system.

Differences can be determined from one resin system to the other in the sense that the highest values are obtained for the DGEBF resin based combinations. The latter reveals a better fiber–matrix adhesion and thus improved dynamic mechanical properties. Furthermore, small discrepancies were found with respect to the reinforcement efficiency in the symmetrical BF and unsymmetrical CF hybrid composites based on DGEBF resin.

Table V.2.2. Effectiveness coefficient C (25 to 250 °C) and adhesion factor A (at Tg).

Stacking sequence	**Effectiveness coefficient C**		**Adhesion factor A**	
	CE & DGEBF epoxy	DGEBF epoxy	CE & DGEBF epoxy	DGEBF epoxy
9FF	0.051	0.142	-0.648	-0.263
BF/7FF/BF	0.055	0.206	-0.458	-0.287
BF/3FF/BF/3FF/BF	0.061	0.221	-0.532	-0.196
CF/7FF/CF	0.040	0.198	-0.576	-0.141
CF/3FF/CF/3FF/CF	0.046	0.256	-0.529	-0.090

On the other hand, the adhesion factor A exhibits interesting behavior if represented as a function of temperature (see **Figure V.2.3**, (a) and (b)) and not individually analyzed based on the values listed in **Table V.2.2** or predicted using **Equation V.2.2**. Thus, not only is temperature sensitive but it reveals the same trend as the tan δ curves for each hybrid composite architecture since it is a sort of normalized curve.

Moreover, as shown above, all hybrid composites based on the DGEBF resin system reveal improved fiber/matrix adhesion compared to that of the CE&DGEBF resin based systems. This inadequate adhesion of the latter can be regarded as the

already mentioned influencing factor underlining that both resin systems perform better at room temperature.

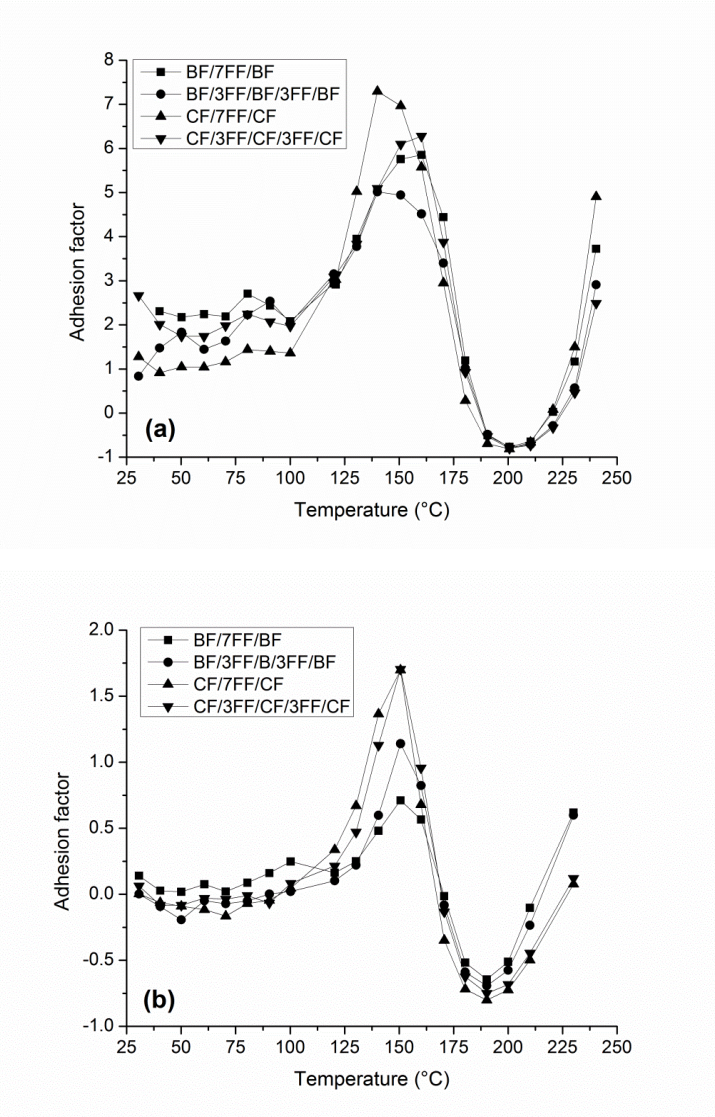

Figure V.2.3. Adhesion factor of 9 stacked layers composite architectures based on (a) CE&DGEBF epoxy blend and (b) DGEBF epoxy resins

Consequently, it can be stipulated that a composite architecture with an inadequate fiber–matrix interface will tend to dissipate more energy while subjected to dynamic loading conditions. Measures should be taken to overcome these inaccuracies, such as one of the presumed fiber/matrix interaction modifications at the molecular

level through plasma etching, wet or dry oxidation or other non-oxidative treatments, etc.

In relation to above, noteworthy is the recent contribution of Szebenyi et al. [182] on the 3D-printing assisted inter-phase engineering that set up a new route on how to overcome the poor adhesion issue prior laminates manufacturing by aid of 3D printing without deterioration the initial material properties. .

Furthermore, data on the adhesion factors for all specimens irrespective of the matrix used are consistent with the peak height values from the tan δ curves. Namely, from **Figure V.2.2b** for example, a lower peak height in the tan δ curves yields an improved interface adhesion seen in the lower values plotted in **Figure V.2.3b** or summarized in **Table V.2.2**.

V.2.1.3. Cole-Cole plots.

The heterogeneity of the 9 stacked layers hybrid specimens herein was investigated using the *Cole–Cole diagrams*. In **Figure V.2.4**, (a) and (b) can be seen the Cole–Cole plots of the loss modulus (log E″) as a function of the storage modulus (log E′) for the neat resins as well as for 9 stacked layers composite structures. Departure from the ideal semicircular shape can be sized in all specimens regardless of the resin system, especially in laminates with a higher number of BF/CF plies.

In these cases, heterogeneity of the combinations reveals the different synergetic effects that are more accentuated with DGEBF based hybrid composites, especially in CF reinforced architectures. This fails to hold for hybrid laminates based on the CE&DGEBF resin system, regardless of the synthetic reinforcement and stacking sequence, despite the recorded/predicted adhesion efficiency values.

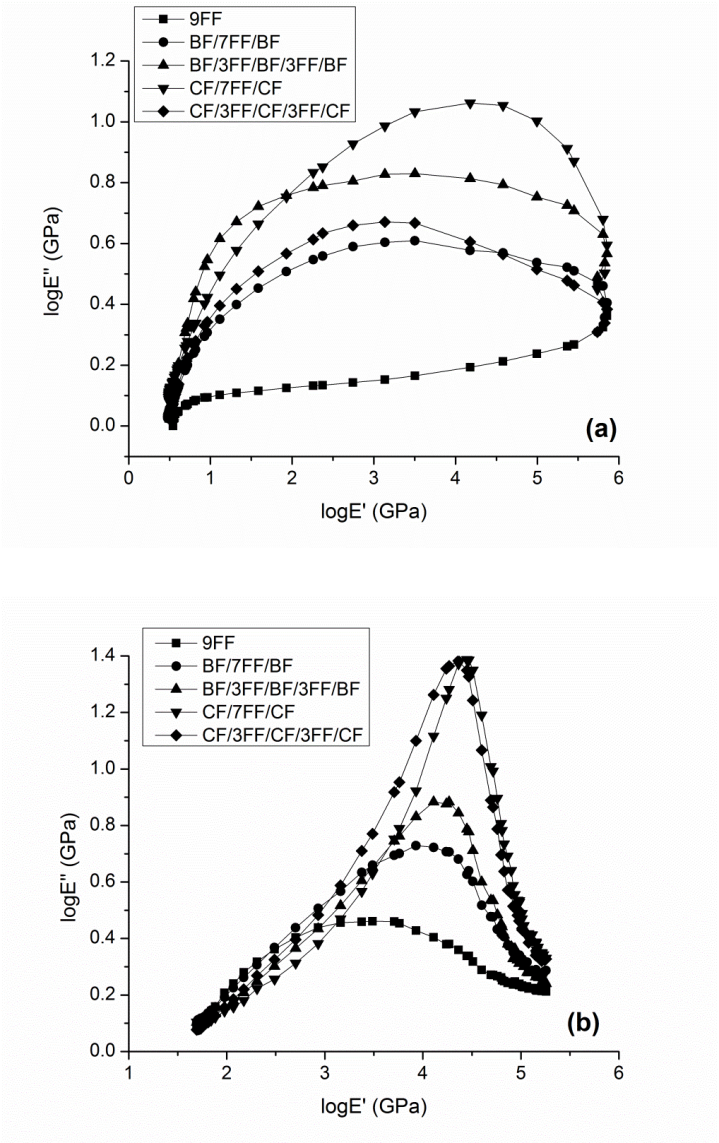

Figure V.2.4. Cole-Cole plots of 9 stacked layers composites based on (a) CE&DGEBF epoxy blend and (b) DGEBF epoxy matrices.

V.2.2. Epoxidized linseed oil based composites.

V.2.2.1. Storage modulus (E')

Prior any debate on the dynamic properties of epoxidized linseed oil (ELO) tailored resin systems, a 3-point-bending mode at oscillating frequencies of 1 Hz and 10 Hz, respectively, at a length span of 25 mm were deployed for experimental data acquisition. In **Figure V.2.5** is being plotted the temperature variation of storage modulus E' for the 4 stacked sequences of BF and FF reinforcements, respectively, embedded within the novel ELO tailored polymer resin as an ELO:G:MLO blends under 50:40:10 ratio. The frequency dependence is also plotted in the following Figures.

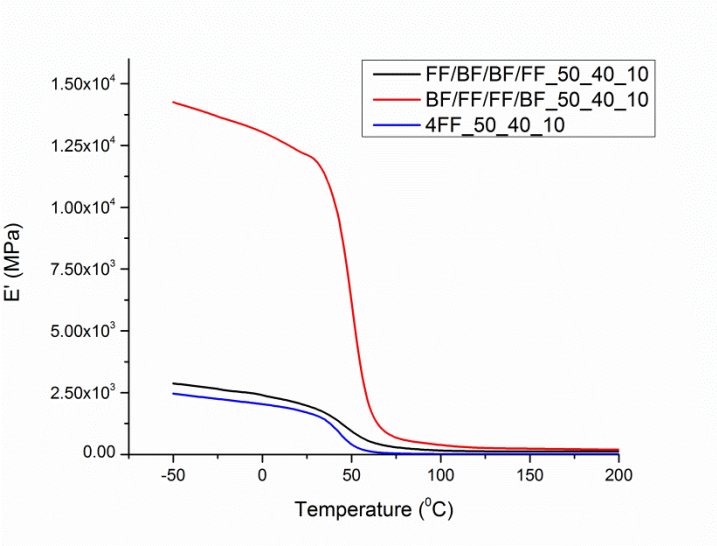

Figure V.2.5. Storage modulus evolution with temperature increases in ELO based composites.

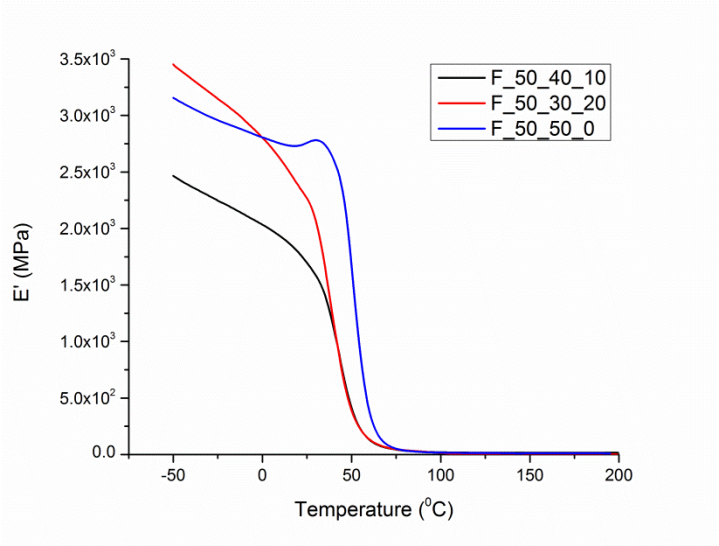

Figure V.2.6. Storage modulus evolution in various ELO blends based FF reinforced composites.

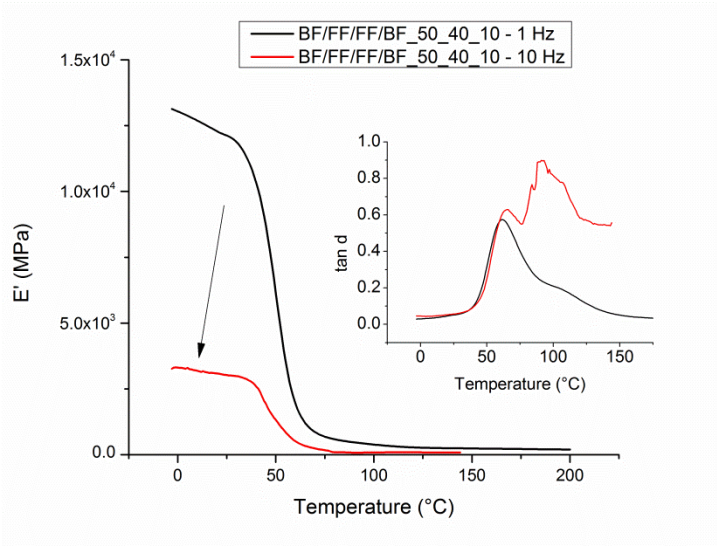

Figure V.2.7. Frequency dependent storage modulus with hybrid BF/FF/FF/BF composites.

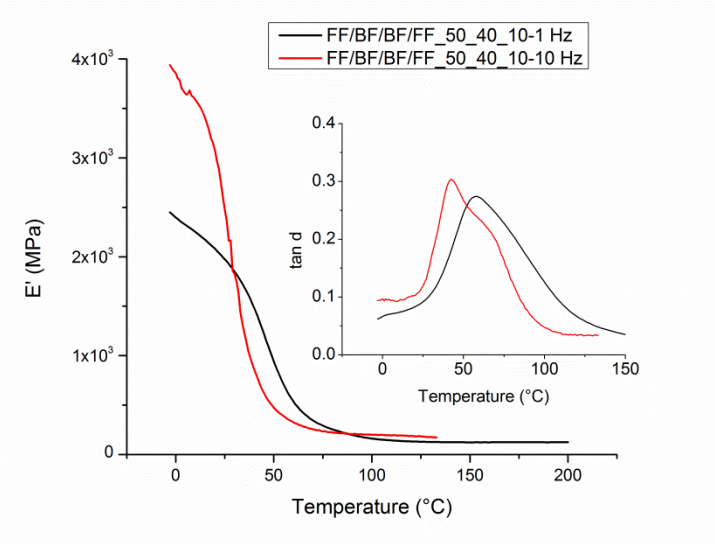

Figure V.2.8. Frequency dependent storage modulus with hybrid FF/BF/BF/FF composites.

V.2.2.2. Damping factor/loss tangent (tan δ)

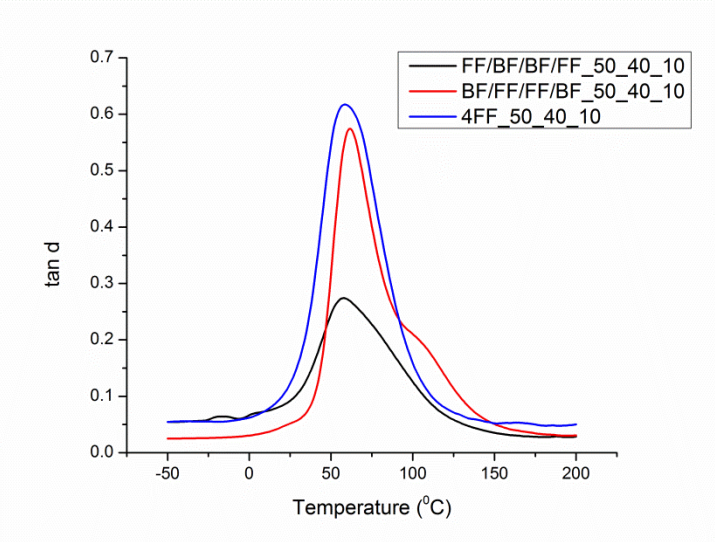

Figure V.2.9. Plot evolution of the damping factor with temperature increases in ELO based composites.

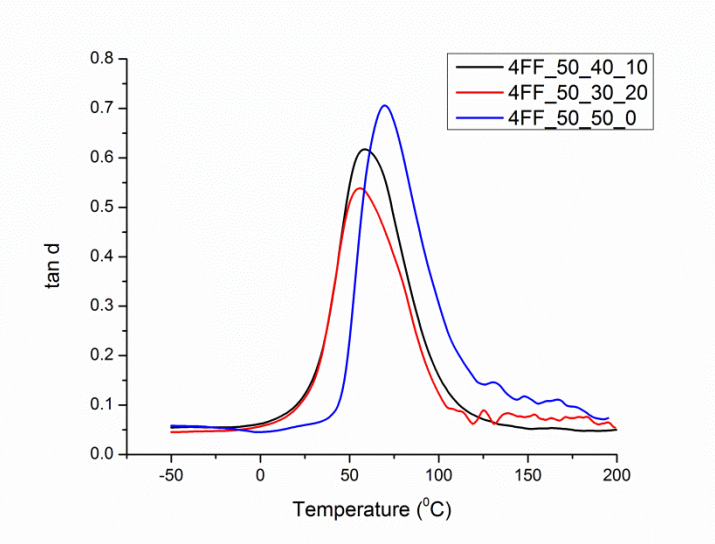

Figure V.2.10. Damping factor evolution in various ELO blends based FF reinforced composites.

V.2.2.3. Cole-Cole plots

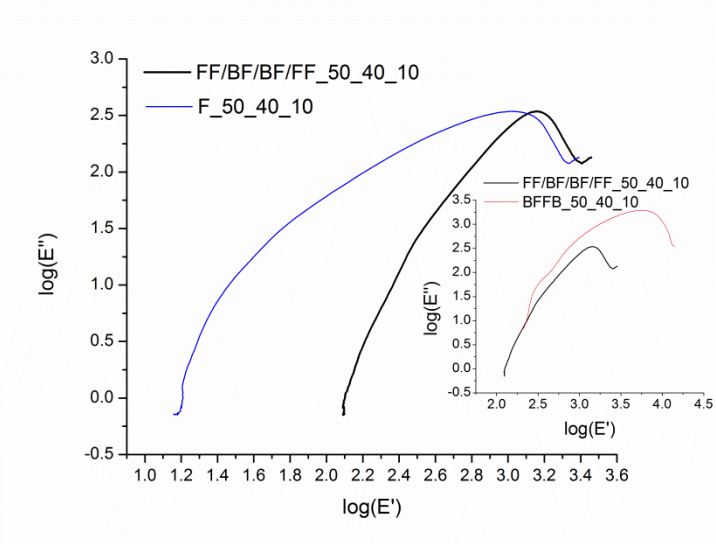

Figure V.2.11. Cole-Cole plots of various ELO blends based FF reinforced composites.

V.3. Thermo-physical properties

The influencing factors as acknowledged from previous chapters will be closely monitored and referred herein. These include information on laminates: architecture, constitutive (e.g. volume fraction, orientation, materials, etc.), manufacturing technology, prior and post-processing of individual specimens and last to the experimental conditions selected.

The latter out of aforementioned influential factors and consequently, sources of errors associated with experiments envisages: temperature program, specimen geometry, thermocouple position with respect to the specimen, specimen layering, etc.

The experimental measurements are being considered to comply with the general principles stated with the last amendments on ASMT E 473:2014 [183] and principles stated with ASTM E831:2014, ASTM D696:2008 or ISO 11403-2:2012 on thermal measurements, generally and linear expansion, particularly [184-186]. In addition, since the specimens are being subjected to various environmental conditions (e.g. water immersion, moisture, low temperature environments, etc.) some other standards are being accounted to apply, namely ASTM D570:98 (2010) E1 and ASTM D5229/D5229 M:2014 [187, 188].

V.3.1. Thermal expansion.

The dilatometer used for this work was equipped with a fused silica sample holder and pushrod. The contact force of the pushrod was 2.5 N. The temperature measurement at the sample was done using a type E thermocouple. The system's influence was diminished using the calibration correction. The calibration run was carried out under the same conditions as used for the specimens.

The samples' length was about 25 mm. Each individual sample was tested in a controlled air atmosphere between 25 °C and 250 °C at a heating rate of 1 K/min following two successive runs. The first one removes thermal history particular about

specimens' manufacturing while the second run enabled to retrieve the thermal property foreseen.

Differences on the CTE values retrieved at room temperature are relatively small and can be regarded to thermal stress induced during the manufacturing, residue removal from the specimens' surface (e.g. wax, surface conditioners, etc.) and air trapped at the surface as the result of the polymerization process.

V.3.2. Thermal conductivity.

This material property is particular important while designing composite panels or structures acting as thermal insulators (e.g. civil engineering, transport, aerospace, encapsulated electronic devices, etc.). The measuring principle is rather simple but effective and provides a quick retrieval of the property. In addition, since *thermal effusivity* represents another important parameter to be accounted in thermal related design processes, proven the practical significance (i.e. measure of the material's ability to exchange thermal energy with its surroundings) it was accounted as well herein.

As specified previously, the measurements for thermal conductivity were carried out by deploying a LFA 467 HyperFlash® device from Netzsch GmbH operated in the range between 25 °C and 200 °C, using an acquisition rate of 25 °C. Experimental data provided represents the average values of five measurements acquired for every individual temperature point with a standard deviation less than 1.5%.

V.3.2.1. Epoxy based composites.

In **Figure V.3.1** and **Figure V.3.2** were plotted the experimental results gathered for the 9 stacked layers epoxy based composite samples under investigation. As it can be seen, in all cases, there is a linear trend in the variation revealing an increase of the through-thickness thermal conductivities along with expanding temperature.

The reader should recall the fact that through-thickness thermal conductivities represent the lowest values comparatively to their counterparts retrieved from in plane measurements. In addition, small values on through-thickness thermal conductivities limit heat dissipation from the composite panels and thus restricting their application potential.

In addition, solely FF reinforced laminates, irrespective of polymer matrix, exhibits an insulating character comparatively with the hybrid laminates.

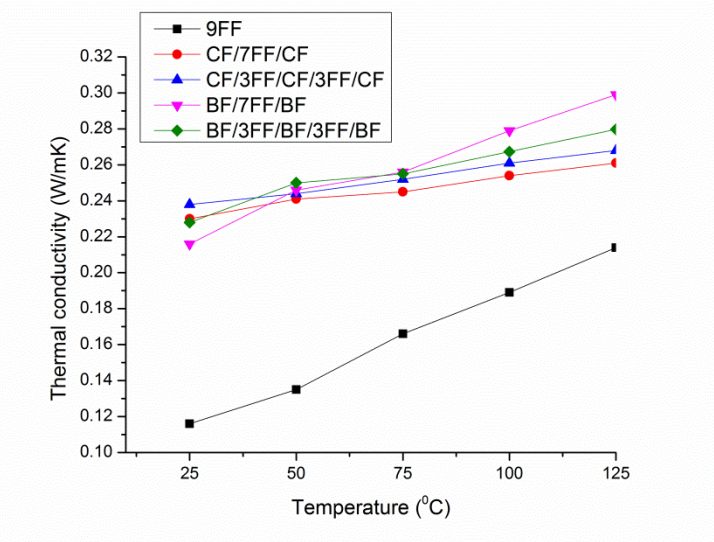

Figure V.3.1. Thermal conductivities with CE&DGEBF based 9 stacked layers composites.

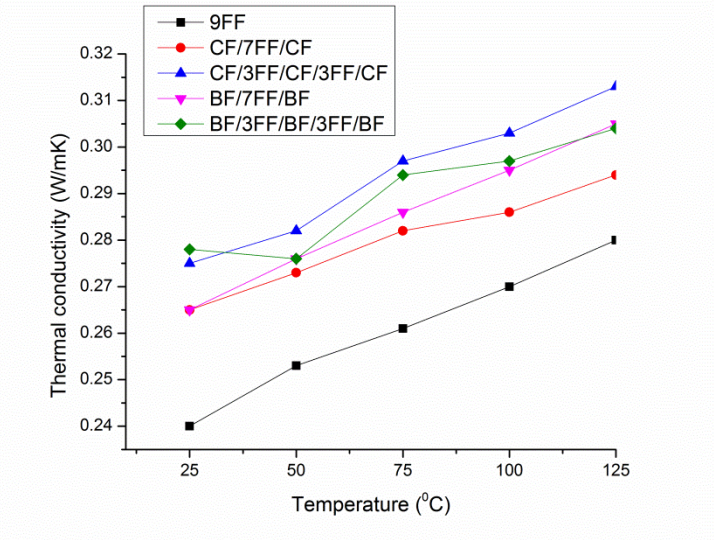

Figure V.3.2. Thermal conductivities with DGEBF based 9 stacked layers composites.

A *thermal conductivity enhancement factor* (i.e. TCEF) can be defined as relative error between the retrieved hybrid specimens' and epoxy polymer matrices thermal conductivities to further enabling materials characterization. In Fig. and Fig. were plotted the corresponding percentages, showing an increasing tendency in terms of efficiency due to hybridization and deployment of more either BF or CF layers within the hybrid polymer architectures.

V.3.2.2. ELO based composites.

In **Figure V.3.2** are being represented the thermal conductivities and specific heat values retrieved for 4 stacked layers specimens delivered as basalt fibers reinforced composites based on different ELO polymer resins (50: 40:10 and 50:30:20) accordingly on their hardener and plasticizer-compatibilizer % vol. content.

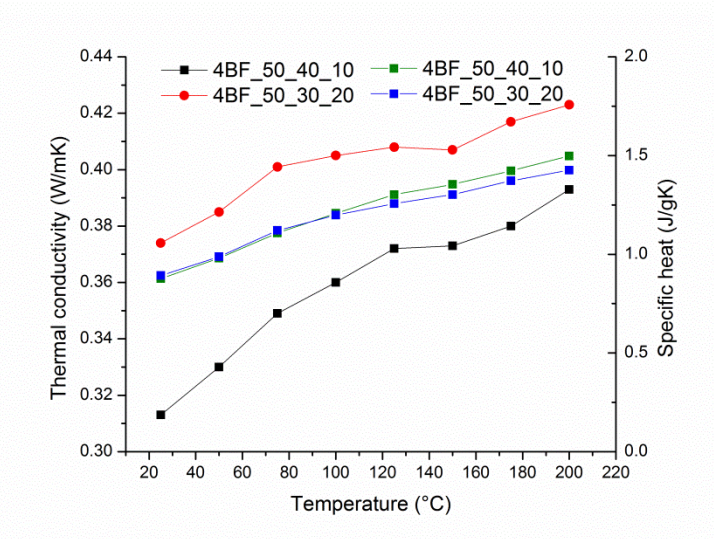

Figure V.3.3. Thermo-physical values in 4 basalt layers ELO based composites.

V.4. Morphology of composites.

Excerpts of SEM images were collected for the 9 stacked layers architectures of hybrid polymer composite specimens to reveal the synergetic effects on their morphology. The morphologies highlight better the previous findings, particularly with regard to fiber/matrix adhesion. Figures clearly evidence the weak adhesion between the CE&DGEBF resin and FF and BF/CF fibers due to the high sensitivity of CE resin to -OH groups and other volatiles present in the untreated fibers.

Moreover, different types of interactions can be outlined in these composites, irrespective of the resin type but dependent on the nature of the fiber. These are interactions between the fiber bundles and interactions between the cells of natural fiber. The latter is of particular importance because it can cause inter-fibrillar failure and uncoiling of the helical fibrils, and thus diffuse matrix cracking in practical applications [189].

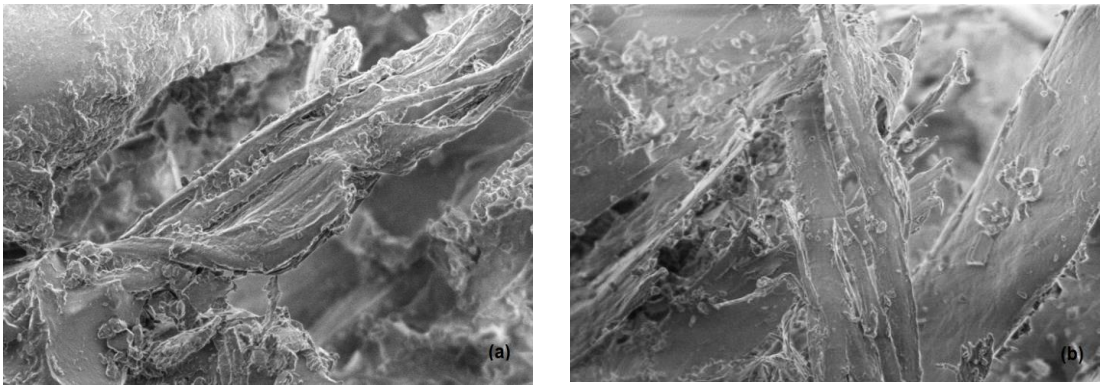

a) b)

Figure V.4.1. SEM images corresponding to a) 9 FF reinforced CE&DGEBF epoxy hybrid composite and b) FF reinforced DGEBF epoxy hybrid composite.

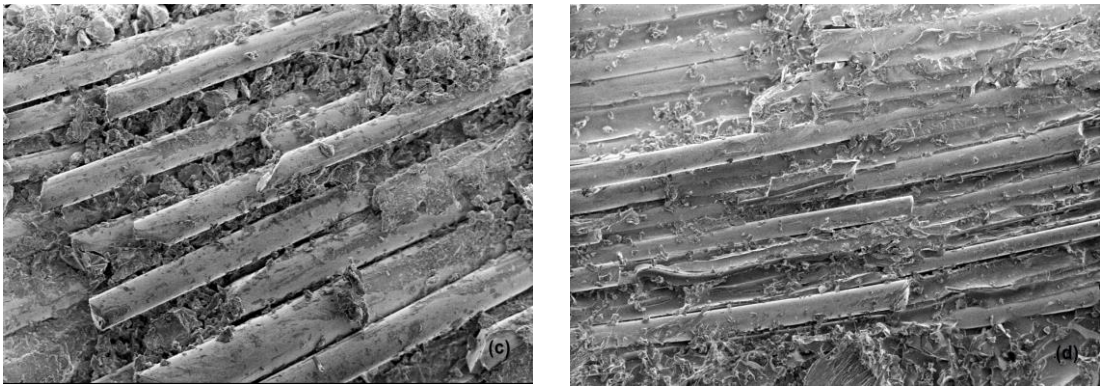

a) b)

Figure V.4.2. SEM images corresponding to a) BF/3FF/BF/3FF/BF reinforced CE&DGEBF epoxy hybrid composite b) BF/3FF/BF/3FF/BF reinforced DGEBF epoxy hybrid composite.

a) b)

Figure V.4.3. SEM images corresponding to a) CF/3FF/CF/3FF/CF reinforced CE&DGEBF epoxy hybrid composite b) CF/3FF/CF/3FF/CF reinforced DGEBF epoxy hybrid composite.

Chapter VI

Chapter VI. Results and Discussion.

This chapter contains original results and the corresponding discussion related to the following research works, published in international journals. Some of the previous Figures and Tables are shown again to give coherence to the text.

- Effects of fibre orientation and content on the mechanical, dynamic mechanical and thermal expansion properties of multi-layered glass/carbon fibre-reinforced polymer composites.
- Particle reinforced composites' elastic properties retrieval by aid of laser generated ultrasound waves.
- Thermal properties comparison of hybrid CF/FF and BF/FF cyanate ester based composites.

VI.1. Effects of fibre orientation and content on the mechanical, dynamic mechanical and thermal expansion properties of multi-layered glass/carbon fibre-reinforced polymer composites.

VI.1.1. Introduction.

A competitive market situation supplemented by exponentially increasing technological advents are continuously pushing the demands for novel material combinations that would pose excellent to outstanding properties in terms of mechanical, dynamical, thermal or dielectric ones, unrestricted solely to high performance, high-strength or lightweight structures. Advanced multi-layered composite architectures appear to be one of the answers, especially for structural engineering applications driven by design factors like manufacturing costs, weight, environmental conditions or material compatibilities. Hybrid composites can be considered as another research path under the focus and extensive development and unfortunately, the source of confusion in a relatively large number of research articles, demanding further clarification and standardization.

Research conducted on hybrid composites, predominantly based on intermingled carbon and glass fibre fabrics, can be traced back to the early 1970s, from the work of Bunsell and Harris [1] or Summerscales and Short [3], that were among the first in the investigation of the mechanical properties of various material combinations in view of their prospective use as lightweight load bearing composite structures. Since then, a variety of combinations emerged as viable architectures to produce fibre

reinforced polymer (FRP) composites. However, research conducted to retrieve the mechanical properties has largely been limited to configurations in which fibres have been intimately mixed within the matrix or stacked having various ply lay-up sequences [8].

The success key for developing advanced multi-layered polymer based composite architectures is to enhance the failure strain of their constitutive. The selection of the constitutive materials, their structural or geometry-related parameters, has a significant influence on the overall composite failure strain. Based on the aforementioned specificities, extensive studies were carried out with respect to the effects of different fibre fabrics multi-layering sequencing on the overall tensile and flexural properties of polymer based composites [190-194]. When considering the mechanical characteristics, flexural strength was the most common retrieved from three-point bending tests and reported. In the work of Mujika [195] it was reported discrepancy on the elastic modulus in bending while switching from three to four point bending configuration for different polymers based composite architectures. Although some investigations on the advanced polymer composites behaviour in failure have been carried out [196], published articles scarcely reported tensile and flexural properties in view of the unidirectional carbon and glass fibre multi- layered polymer based composites concerning the differences due to the presence, content and orientation of carbon fibres. The latter can be regarded to industrial data protection and may have been unreleased for public on large.

Dynamic mechanical analysis proved to be a useful tool in the study of polymer based composite materials' behaviour under various temperatures, frequency or external loading conditions. Temperature-dependent dynamic mechanical parameters, such as storage modulus, loss modulus and mechanical damping, allow a closer monitoring of the level of interactions between the polymer matrix and the reinforcements, and the derived Cole-Cole or Cole- Davisson plots proved to be the most expressive and useful data processing tools in sizing the constitutive influence.

Literature provides numerous references focusing on the fibre reinforced polymer composites and their dynamical material properties revealing their inherent

structure related particularities and thermal history during their manufacturing [197]. Both organic and inorganic fibres were considered as high-potential reinforcement candidates for the different polymer based composite architectures and dynamic mechanical analysis (DMA) as the most-used testing method in order to size the overall material behaviour under shock and vibrations. Furthermore, it should be emphasised that carbon fibres were the most preferred reinforcements due to their outstanding material properties unattained so far by any other type of materials. This enabled a wide-range of engineering applications ranging from aerospace to marine, civil engineering to transport, sporting goods to automotive industry, etc.[192, 198-200]

Next, the multi-layering concept allowed the advent of an entry in the polymer based composite material class and opened new research directions of studies. Extensive experimental studies were carried out and reported within literature on these types of materials, aiming the understanding of their structural behaviour while subjected to different design and loading constraints [201-203].

Further, rather contraction effects than expansion responses from constitutive were often considered in the composite design for those architectures intended to be developed to be used in harsh environments [204]. Supplementary, negative overall CTE response was retrieved for composite benchmarks (e.g. GFRP) whose polymer resins were exhibited low elastic modulus and high expansion material properties. A representative example of the aforementioned can be the glass fibre/polypropylene system developed by Ito et al. [205]. Carbon fibres naturally exhibit different CTE responses along their longitudinal and transversal directions and are usually selected as reinforcements for multi-layered polymer composite structures to tailor their overall CTE. Supplementary, several studies were reported in literature on the multi-layered polymer composites' material properties changes if pre-conditioned under extreme environments [83, 206, 207].

The herein contribution presents a comparative study centred on the design, development and material characterization of some tailored multi-layered polymer composite architectures reinforced with different content of uni-directional (UD) carbon and random glass fibres. The elastic and dynamic mechanical properties, along with

their thermo-physical changes, were monitored and recorded within a temperature range below and beyond the glass temperature of the unsaturated polymer resin employed as the matrix material, and next analyzed and debated. Supplementary, it will emphasize the differences on the effective material properties under the focus due to the orientation of the UD carbon constitutive with respect to the general reference system. Moreover, the content of the UD carbon fibres ply-ups, that are balancing symmetrical or unsymmetrical the overall composite design, will be considered for further explanations.

VI.1.2. Experimental research.

VI.1.2.1. Materials selection and specimens preparation.

The composite specimens have been manufactured as a 5-ply laminate with different volume fraction ratio of the reinforcement materials – glass fibre chopped strand mats (n. GF; MultiStratTM Mat ES 33-0-25, Johns Manville, USA) and UD carbon fabrics (n. CF; Panex® 35 UD300, Zoltek Co., H). The reinforcements were bounded together by an unsaturated polyester resin (Synolite 8388-P-1, DSM Composite Resins, CH) and further cured at room temperature for 24 h before cut into specimens for the experimental tests. The curing agent methyl ethyl ketone peroxide (MEKP) was purchased from AKZO Nobel (Butanox M-50, NL). The multi-layer composites were labelled according to their relative volume fraction with the structure as GF:CF(100:0), GF:CF(60:40) and GF:CF(80:20), respectively, keeping constant the overall fibre loading (35 vol.%). All samples were cut in accordance to account for the 0° and 90° different carbon fibre orientation.

VI.1.2.2. Material testing procedures.

Mechanical testing. Tensile and 3-point bending loading were performed to assess the mechanical properties in accordance with SR EN ISO 527-1:2000 and SR EN ISO 14125:1998 standards. LS100 and LR5K Plus devices from Lloyd Instruments (UK) were used to retrieve the stress/strain dependencies, followed by elastic modulus, yield stress, ultimate strength recovery procedures to preliminary asses the multi-layered reinforced polymer composites' toughness. The final experimental data were statistically processed out of those recorded for each 10 representative specimens used.

Dynamic mechanical thermal analysis (DMA). The dynamic mechanical thermal analyses were performed using a DMA 242 C analyzer (Netzsch GmbH, D) running in a 3-point-bending mode at an oscillating frequency of 1 Hz. The storage modulus (E′) and loss modulus (E″) as well as the damping factor (tan δ) of each composite specimen were retrieved under the following conditions: a temperature range from – 40 ^{o}C up to 150 ^{o}C at a scan rate of 3 ^{o}C/min, a controlled atmosphere due to the

liquid nitrogen used as a cooling agent. The samples were shaped having 60 mm in length and 10 mm in width, while the thickness were individually measured as dependent on the layering sequence.

Thermo-physical changes. Thermo-physical changes of specimens were performed on a differential dilatometer DIL 420 PC/1 from Netzsch GmbH (D), in accordance with ASTM E228- 11 and DIN 53752-A standards. The specimens were shaped into rectangular bars of 25 mm in length and 5 mm wide while the transversal external surfaces were polished to guarantee plan- parallel surfaces for precise positioning within the measuring head. The temperature mode was set up as a dynamic heating ramp trend from 25° C up to 250° C. The heating rate imposed was 1° C/min.

VI.1.3 Results and discussion.

VI.1.3.1 Mechanical properties.

There is evidence that the individual constitutive fibre content has an influence on the composite's failure strain. The UD carbon fibres content increase and their different orientations with respect to the reference system led to a shift in the overall fracture event curve. A shift was encountered in the load-deflection curves retrieved from flexure tests on the GF:CF(100:0) and the GF:CF(80:20) specimens, on both directions of carbon fibre orientation as shown in **Figure VI.1.1**

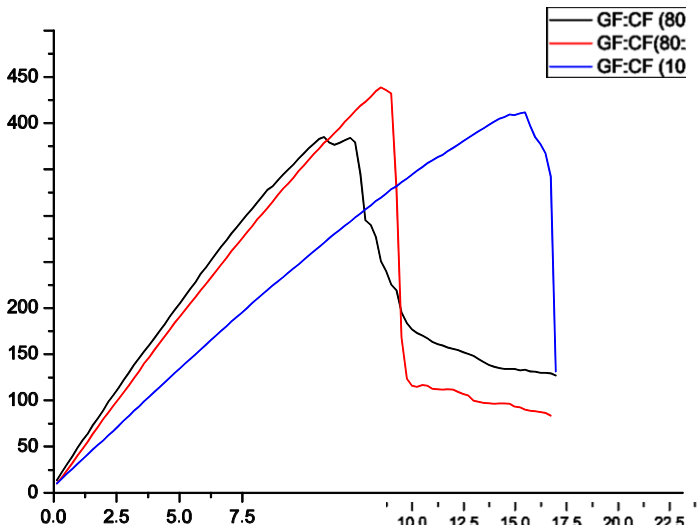

Figure VI.1.1 Load versus extension curves of the GF:CF(100:0) and GF:CF(80:20) composites in flexure.

The composite elastic modulus is another dependent material property on the fibre volume fraction; the experimental flexural modulus is much lower than the tensile modulus as the content of UD carbon fibres increases. This it can be seen from data provided in **Table VI.1.1** The decrease in the flexural modulus can be regarded as a shear-deformation effect within these

multi-layered polymer composite specimens, being one of the failure mechanisms that are particular about these types of materials. Furthermore, the effective

elasticity modulus in flexure can be correlated with the fibre's length, especially for the UD carbon fibres. The aforementioned is acknowledged in the technical literature to dominate this elastic property [8].

Table VI.1.1 Tensile and flexural mechanical properties accounting for different content and orientation.

Sample architecture	UD CF orientation	Tensile		Flexural	
		Strength (MPa)	Modulus (GPa)	Strength (MPa)	Modulus (GPa)
GF:CF(100:0)		116.17±0.04*	4.81±0.03	38.10±0.04	4.68±0.03
GF:CF(80:20)	0°	295.6±0.03	14.64±0.09	26.15±0.05	4.74±0.07
	90°	95.8±0.02	7.60±0.05	32.40±0.04	4.23±0.07
GF:CF(60:40)	0°	331.37±0.01	16.21±0.07	108.12±0.05	4.48±0.05
	90°	93.15±0.04	7.22±0.05	118.14±0.04	4.21±0.04

* Standard error.

Inconsistencies between the experimental values, proven various UD carbon fibres orientation and number of layers, can be ranked as being relatively low for data retrieved based on the flexure tests in comparison with the tensile tests where a severe drop of approximately 50% in the elastic modulus was found to occur for the same composite architecture but different UD carbon fibre orientation. Moreover, the discrepancies between the multi-layer composites' overall strength are evenly more accentuated, especially in the composite architectures with longitudinal (0°) oriented UD carbon fibres. The effective mechanical properties of these advanced composites are being also influenced by the capacity of stress transferring between the fibre-matrix interfaces and fibres' different breakage mechanisms. Further inside on the above is beyond the purpose of the present study.

In **Figure VI.1.2** was plotted the maximum bending stresses of the reference, and the multi-layered composite specimens considered in the herein study. Data scattering can be regarded to the increase of the carbon fibre reinforced content, different orientation directions and less to the uncontrolled random distribution of the glass fibres

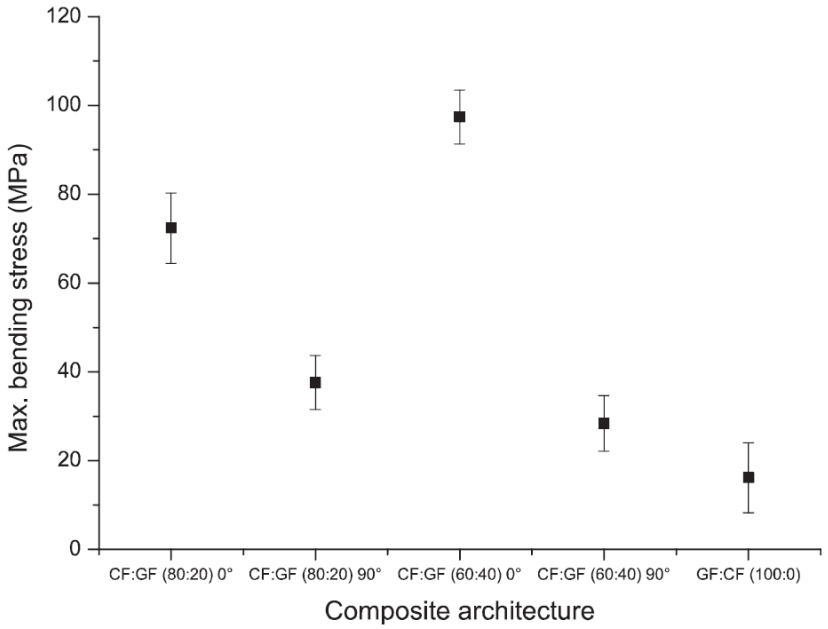

Figure VI.1.2. Mean maximum stress values in flexure retrieved for the multi-layered composites.

VI.1.3.2. Dynamic mechanical thermal analysis (DMA)

Dynamic mechanical properties (DMA) of the multi-layered fibre reinforced polymeric composites can be regarded to reveal the same dependencies on several influencing factors as their benchmark, such as: material-related dependencies - nature of the matrix material, constitutive material type; structure-related dependencies - layer architecture (e.g. reinforcing fibre orientation), number of layers, nature of fibre-matrix interfaces; loading conditions – frequency, temperature range, type of load and temperature history [197].

In this section, a detailed analysis will be made with respect to the dynamic mechanical properties of the multi-layered polymer composite specimens investigated, and some of the above-mentioned influencing factors will be closely monitored and ranked on the retrieved experimental data.

Storage modulus (E').

The storage modulus is closely related to the load-bearing capacity of a material and is analogous to the flexural modulus measured as per ASTM-D 790 [197]. **Figure VI.1.3** reveals the effect of temperature dependence of the storage modulus of GF:CF(100:0) and the multi-layered composite architectures under the focus. Accordingly, one might observe that E′ values decrease as the number of the UD carbon fibre ply-ups increases and changes their orientation with respect to the general reference system. The latter can be regarded to the fact that the modulus of elasticity (i.e. Young's modulus) of the UD carbon fibre is much lower in the transversal direction than in the longitudinal direction. Addition of carbon fibre ply-ups was expected to lead to an increase of the E′ modulus of these architectures of polymer based composites. Nonetheless, based on these simple observations, UD carbon fibres can be viewed as behaving better in standalone configurations than in combined multi-layered structures but are proving once again that their presence may contribute significantly to an efficient stress transfer within the structure as well as from the fibre constitutive to the matrix.

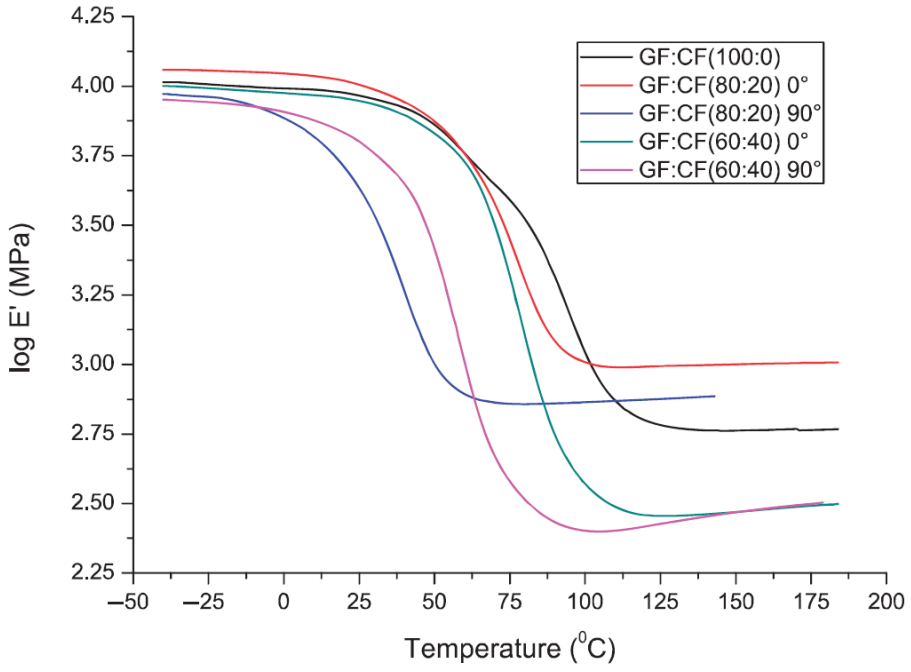

Figure VI.1.3. Temperature dependence of log E′ curves for all composites under the study.

As temperature increases, close to glass transition temperature (Tg), the E' of the reference and multi-layered composites experience a sharp decrease indicating that the materials are passing through the glass/rubbery transition stage. Further, above Tg, the storage modulus of the GF:CF(100:0) is lower than that of GF:CF(80:20), having UD carbon fibres both 0° and 90° oriented but higher than that of GF:CF(60:40), of same type. The aforementioned can be regarded to the increases in molecular mobility of the polymer chains above Tg temperature, as well as to the UD carbon fibre content and temperature dependence.

Loss modulus (E").

Generally, the loss modulus represents the viscous response of the polymer based materials or can be a measure of energy dissipated as heat/cycle under deformation [197]. As in the case of the storage modulus, the loss modulus preserves the same tendency of high values over the temperature range for reduced numbers of carbon fibre ply-ups embedded within the multi-layered composite architecture (see **Figure VI.3.4**). A discrepancy can be observed throughout the transition region, especially for the maximum E" in case of GF:CF(60:40) and GF:CF(100:0) specimens. This can be attributed to the inhibition of the relaxation process within the composite structures with the addition of the UD carbon fibres as a supplementary phase. However, GF:CF(80:20) multi-layered composite architecture has resulted in higher E" values within temperature range above it's Tg.

Below the Tg values of each specimen, the E'' curve for GF:CF(100:0) composite is closer to the curve retrieved for the GF:CF(80:20) architecture, whereas after these values, is getting nearer to the curve retrieved for the GF:CF(60:40) combination, proven the longitudinal orientation of the UD carbon fibres. In **Table VI.1.2** was listed the glass transition temperature values retrieved from the E" curves, for all the specimens involved in the present study, revealing once again the influence of the number of UD carbon fibre ply-ups and orientation. Glass temperature values retrieved using aforementioned curve types were reported within literature to be more realistic

compared to those obtained from damping factor plots and their associated experimental values [203].

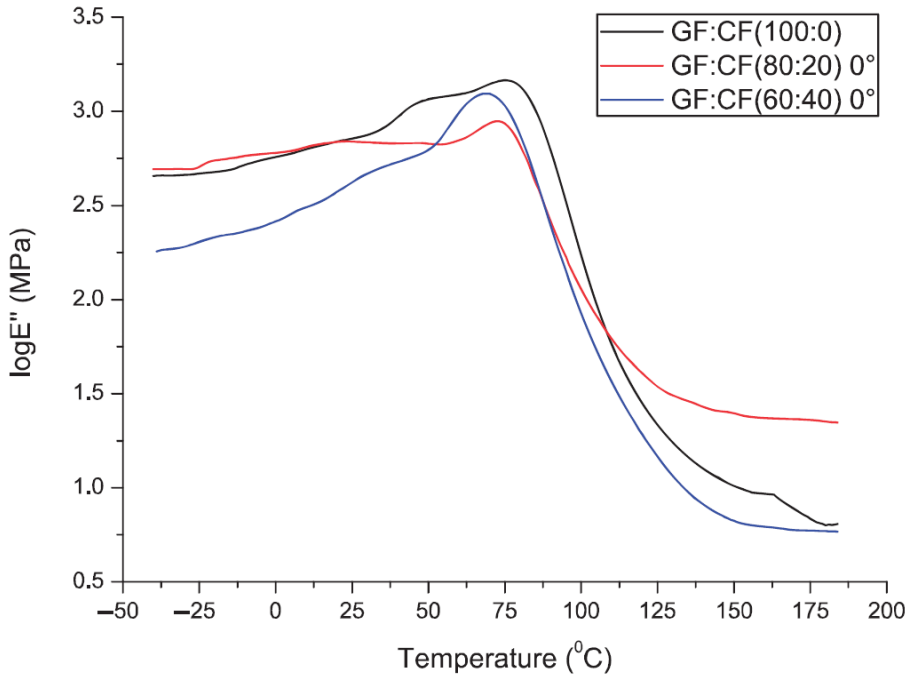

Figure VI.1.4. Temperature dependence of log E'' curves for composite specimens with 0° oriented UD carbon fibres.

Table VI.1.2. Peak height and glass transition temperatures (from tan δ, E'' and dL/L0 curves) of multi-layered composite architectures.

Sample architecture	**UD CF orientation**	**Peak height of tan δ curve**	**Temperature [°C]**		
			Tg from tan δ	**Tg from E″**	**Tg from onset dL/L0**
GF:CF(100:0)	-	0.3762	91.2	89.0	52.0
GF:CF(80:20)	0°	0.3030	87.4	85.0	55.0
	90°	0.3241	88.4	83.6	55.0
GF:CF(60:40)	0°	0.5182	86.2	81.3	58.0
	90°	0.4782	88.0	83.4	59.0

Damping factor (tan δ).

The material loss factor or loss tangent is related to the impact resistance of a material and depends, as has already been shown in literature, on the applied frequency [197]. The damping properties of the investigated polymer based composite materials provide the balance between the elastic and viscous phases of the individual architectures. Generally, the higher tan δ peak values the better the material performances are in shock and vibrations, whereas the lower tan δ peak values the higher the load-bearing capacity properties are of the polymer based composite materials. It is widely acknowledged that a peak in tan δ curve represents an energy-absorbing transition, whereas the area beneath represents the amount of energy absorbed [197].

In **Figure VI.1.5(a)** was plotted the tan δ curves function of temperature, accounting for different UD carbon fibre content and orientation, whereas in Table 2 was provided the tan δ peaks and Tg values retrieved from tan δ for all the combinations considered. **Figure VI.1.5(b)** represents a detailed excerpt from the tan δ curves to reveal the influence of the UD carbon fibre content and orientation.

It is interesting to note that the loss factor experience, in almost all cases, a positive small shift as the UD carbon fibre content and orientation change. These positive shifts in Tg values show the effectiveness of the GF and CF fibres as reinforcing agents and will be not linked to any post-curing effects. For example, in case of GF:CF(60:40) multi-layered composites the shifting of Tg to higher temperatures may be associated with the decreased mobility of the polymer chains by the addition of supplementary carbon fibre ply-ups. Based on the diminishing in the tan δ, an improved fibre/matrix interface bonding behaviour can be observed in case of GF:CF(80:20) architecture while compared to the GF:CF(100:0) specimen. Moreover, in case of 90° UD carbon fibre configurations, the same tendencies hold with respect to the tan δ variations.

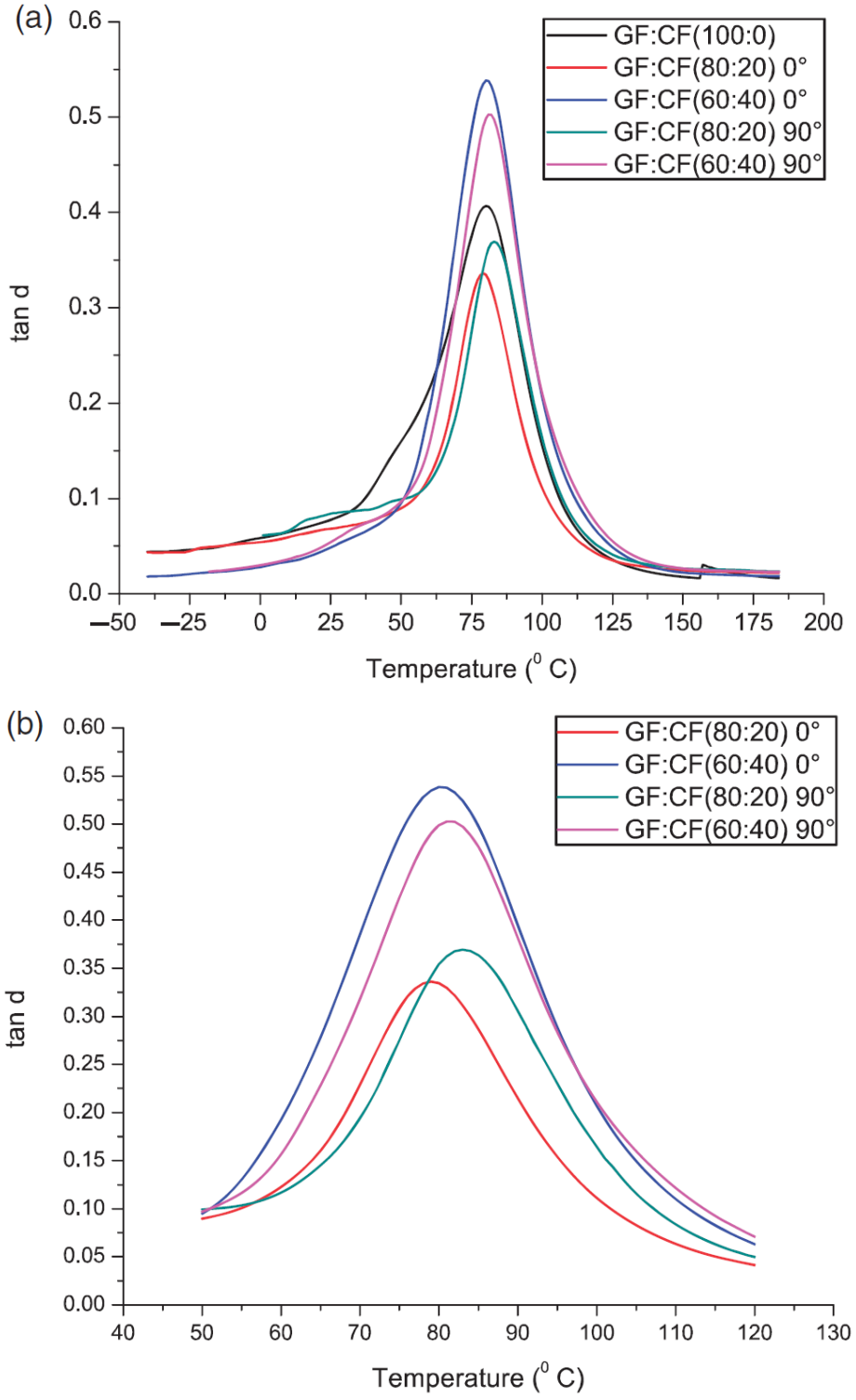

Figure VI.1.5. (a). Temperature dependence of tan δ curves for all the composite specimens under discussion, (b). Zoom around tan δ peaks accounting for different UD carbon fibre content and orientation within the multi-layered composite architectures.

Cole-Cole plots.

Generally, these types of graphs are reported to be good indicators of the homogeneity of the structures subjected to dynamical loading. Departure from the ideal circular shape reveals the heterogeneity of polymer based systems [197].

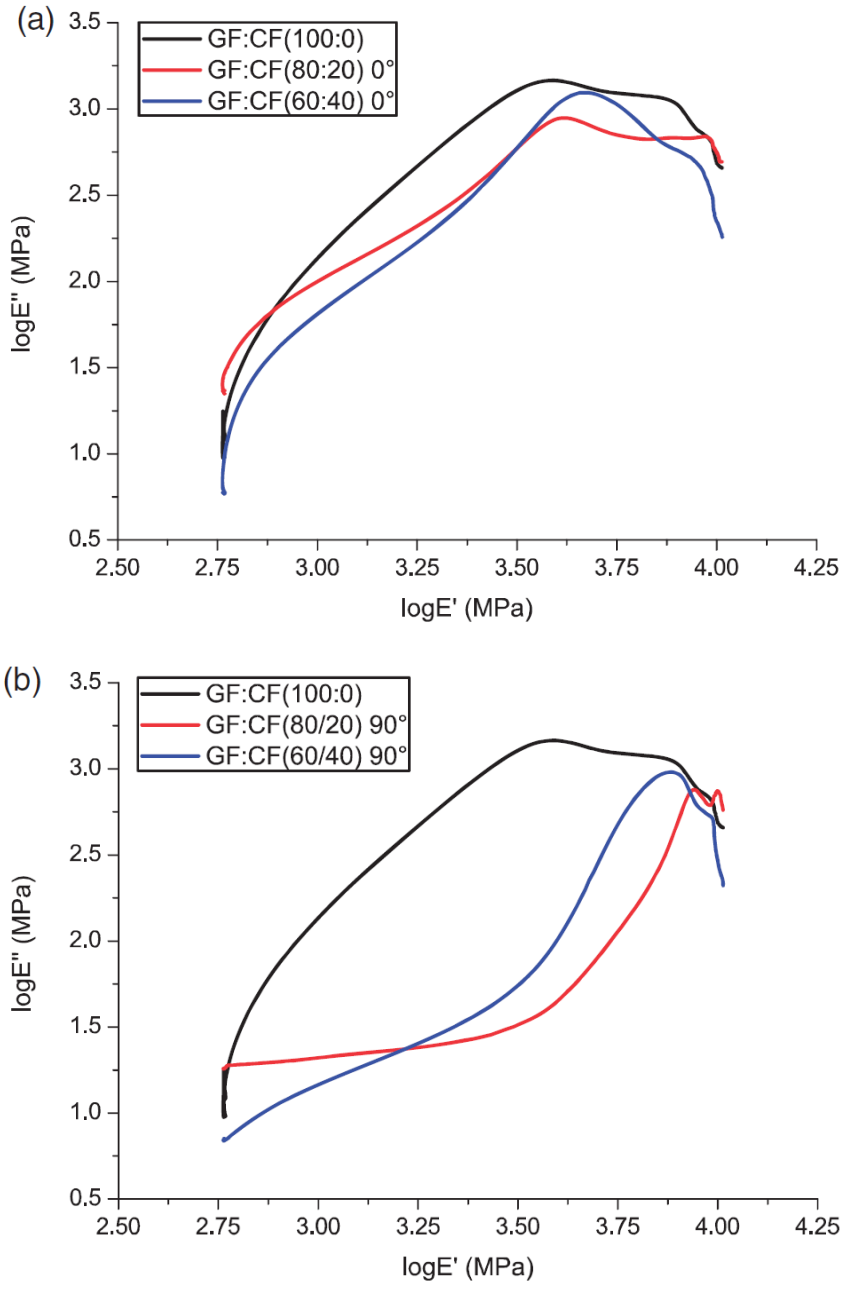

Figure VI.1.6. (a). Cole-Cole plot of the composites with different content and 0° orientation of UD carbon fibres. Figure 6(b). Cole-Cole plot of the composites with different content and 90° orientation of UD carbon fibres.

Figures VI.1.6, (a) and (b) shows the Cole-Cole plots of the loss modulus (E″) as a function of the storage modulus (E′) for the reference and multi-layered composite structures accounting for different UD carbon fibre content and orientation. As it can be seen, both content and orientation of the UD carbon fibre contribute to the Cole-Cole plot shape changes. While in case of the 0° disposed UD carbon fibres, the changes give rise to imperfect semicircular shapes to the Cole- Cole plots, for their reverse configuration (i.e. 90°), the form of plots changes to an irregular shape. These imperfections indicate that there is heterogeneity among the glass and carbon fibres, as well as the polymer matrix material. Consequently, the content and orientation of constitutive, supplemented by their individual material properties influence the shape of the Cole-Cole plots, thereby the tailoring process regarding the dynamical mechanical properties of these multi-layered composite architectures.

VI.1.3.3 Thermo-mechanical analysis (CTE).

The instantaneous coefficient of thermal expansion (CTE) as well as the thermal strain field recorded for the polymer based composite specimens herein can be viewed in **Figure VI.1.7** and **Figure VI.1.8**, respectively. These are accounting for different orientation and content of the UD carbon fibre constitutive. Supplementary, as it can be seen from **Figure VI.1.7**, the different layer architectures induce the occurrence of little peaks (i.e. noise) in the instantaneous overall CTE field over the temperature range, departing from the linear variation for temperatures higher than Tg values. These can be associated to the weak cross linked network of the unsaturated polymer matrix herein, to the transitions from the glassy state to the rubbery state as well to the different fibre/matrix interfaces.

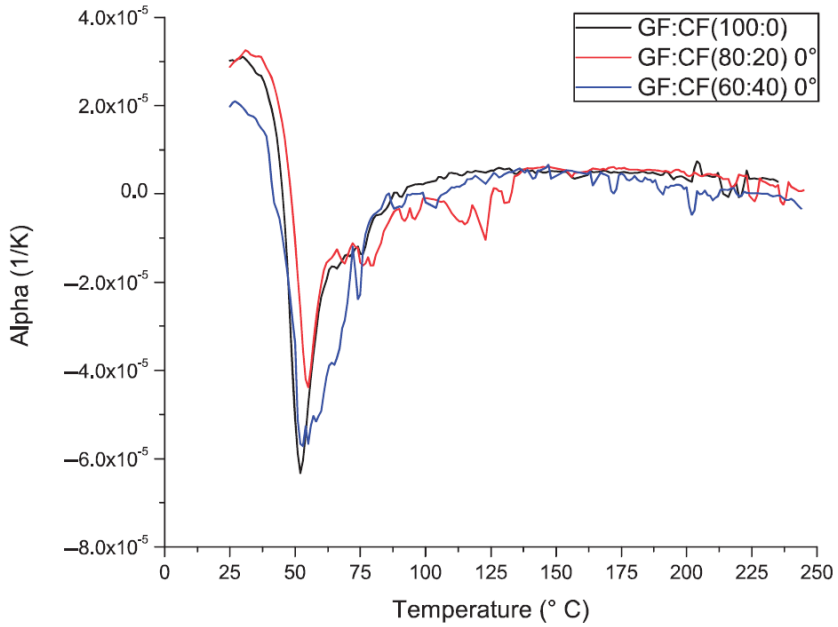

Figure VI.1.7. Instantaneous overall CTE temperature variations accounting different content and 0° orientation of UD carbon fibres within the composite architectures.

With respect to dimension changes, the differences in the recorded variations reveal the influence of both UD carbon fibre content and orientation. One interesting observation that must be underlined herein, concerns the similarities revealed by the GF:CF(80:20) with 90° UD oriented carbon fibres and GF:CF(60:40) with 0° UD oriented carbon fibres during the temperature rise. It seems that the specimens exhibit almost identical behaviour in terms of dimension change over the temperature range, as shown in **Figure VI.1.8**, and relatively close instantaneous CTE values within the same interval. This may be useful while manufacturing costs come as one of the major issues in the structures design and applications development.

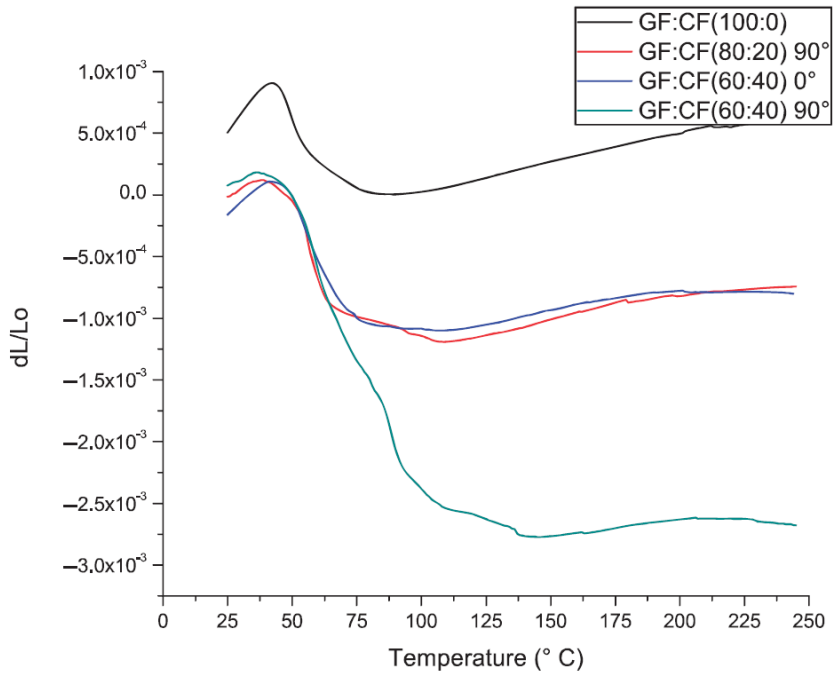

Figure VI.1.8. Thermal strain fields evolution from the composite specimens under the study.

Concerning the Tg values retrieved from the onset in the dL/L0 curves, these are lower than the ones retrieved from the DMA runs, as has been reported also in **Table VI.1.2**. As it can be seen from the table, a shift of approximately 30° C from the DMA reported values was recorded for all values retrieved for the multi-layered composite specimens. This can be assigned mainly to the experimental device working principle that cannot be ranked as providing the best results concerning the Tg values comparatively with the DMA method. Any further debate on this issue is beyond the purpose of the herein article. It must be pointed out that the DIL measurements give good indicators on the compatibility of the reinforcements with the matrix materials as well as on the influence of the individual constitutive on the overall material properties of the composite architecture.

VI.1.4. Conclusions.

These architectures of advanced polymer reinforced composites exhibit unique material properties while compared with the benchmark polymer composites, either glass or carbon fibre reinforced. They were developed to replace the benchmark polymer composites in engineering applications where the manufacturing cost and weight are key issues in the lightweight structure's design.

High flexural properties and high-tensile strength were retrieved in case of GF:CF(60/40) multi- layered composite architecture. The increase in the carbon fibre reinforced content was found to contribute further to the improvement of the structural strength, both in tensile and flexure mode. Furthermore, carbon fibres reinforced ply-ups are revealing improved stress transfer behaviour between fibres and polymer matrix as compared to their concurrent (i.e. glass fibres based). Further studies should be considered to investigate the stress transfer mechanisms among the individual layers and fibre to matrix interfaces.

Furthermore, the GF:CF(60/40) architecture was found to exhibit improved resistance if subjected to shock and vibrations comparatively with the reference. It was also shown that the UD carbon fibre content and orientation with respect to the general reference system contribute to the shape changes in the Cole-Cole plots.

The instantaneous CTE responses were also found to be influenced by the UD carbon fibre content and orientations. Besides, the influence of the constitutive individual material properties on the effective CTE was also underlined and revealed in the retrieved experimental curves.

The automotive industry was identified as the primary industry that can benefit from the use of this advanced polymer based composite structures. One may also include the aerospace or marine structural components, sporting goods manufacturing, etc. proven the presence of the carbon fibre constitutive within the composite architectures and supplementary, their yearnings for development of lightweight structures.

Nevertheless, the advent of advanced polymer based composite architectures based on particle/particle, particle/fibre or fibre/fibre multiple tailoring largely opened

the combination possibilities and allow outstanding achievements with respect to their effective material properties, manufacturing technologies and costs as well as their wide-spread application areas.

Article

JOURNAL OF COMPOSITE MATERIALS

Journal of Composite Materials
0(0) 1–11

DOI: 10.1177/0021998314532151
jcm.sagepub.com
SAGE

Effects of fibre orientation and content on the mechanical, dynamic mechanical and thermal expansion properties of multi-layered glass/carbon fibre-reinforced polymer composites

Dana Luca Motoc[1], Santiago Ferrandiz Bou[2] and Rafael Balart Gimeno[2]

Abstract

Multi-layered glass and carbon-reinforced polymer composites may exhibit unique properties comparatively with the benchmark, proven they are being tailored bounded by several requirements. The paper herein approaches issues on the influence of the various contents and orientation of UD carbon fibre constitutive on the mechanical, dynamical and thermal expansion if embedded along with glass fibres in different stacking sequencing within an unsaturated polymer resin. The results show that the architectures with the highest content of carbon fibres (e.g. GF:CF(60:40) – 0° and 90°) provide the best tensile and flexural properties, and behave better under dynamical loading conditions and temperature variations, no matter the orientation directions. In addition, it was shown that a thorough understanding can be attained, with respect to the UD carbon fibre content, and different orientations influence on the overall composite material properties, taking into account the data retrieved from dynamical and thermal expansion runs.

Keywords

Mechanical, dynamic mechanical, thermal expansion, orientation, carbon fibre, glass fibre, polymer, composite

Introduction

A competitive market situation supplemented by exponentially increasing technological advents are continuously pushing the demands for novel material combinations that would pose excellent to outstanding properties in terms of mechanical, dynamical, thermal or dielectric ones, unrestricted solely to high performance, high-strength or lightweight structures. Advanced multi-layered composite architectures appear to be one of the answers, especially for structural engineering applications driven by design factors such as manufacturing costs, weight, environmental conditions or material compatibilities. Hybrid composites can be considered as another research path under the focus and extensive development, and unfortunately, the source of confusion in a relatively large number of research articles, demanding further clarification and standardization.

Research conducted on hybrid composites, predominantly based on intermingled carbon and glass fibre fabrics, can be traced back to the early 1970s, from the work of Bunsell and Harris[1] or Summerscales and Short,[2] that were among the first in the investigation of the mechanical properties of various material combinations in view of their prospective use as lightweight load-bearing composite structures. Since then, a variety of combinations emerged as viable architectures to produce fibre reinforced polymer (FRP) composites. However, research conducted to retrieve the mechanical properties has largely been limited to

[1]Department of Material Science, Transilvania University of Brasov, Romania
[2]Department of Mechanical and Materials Engineering, Polytechnic University of Valencia, Romania

Corresponding author:
Dana Luca Motoc, Transilvania University of Brasov, 29 Eroilor Av., Brasov 500036, Romania.
Email: danaluca@unitbv.ro

VI.2. Particle reinforced composites' elastic properties retrieval by aid of laser generated ultrasound waves.

VI.2.1. Introduction.

Ultrasonic material testing has been widely used for decades due to its versatility and handling facilities. Numerous techniques emerged and proved viable in assisting the material characterization and inspection. Noteworthy is the last review of Chimenti (2014) on air- coupled ultrasonic material characterization devices, techniques and applications [208]. In addition, the emphasis is on how to overcome the limitation inherent to these experimental configurations, followed by carefully examination of the outstanding work of Hosten (1998, 2008) and his collaborators [209, 210].

Laser generated ultrasound emerged as one of the air- coupled material characterization methods. A laser source operated in the thermo-elastic regime generates ultrasound waves through thermal expansion while used at the low- power level. Opposite, at the high-power level, the laser source operates in the ablation regime and gives rise to vaporization of a small amount of material.

Numerous researchers tackled the issue of ultrasound wave generation from a laser source by fully operating it on the ablative and the19rmo-elastic regime. Viewed as one of the major contributors in the field of laser generated ultrasound, Karabuthov (1998, 2000, and 2010) is continuously surprising the scientific world. Contributions are targeting the use of laser generated ultrasound to recover the elastic coefficients in unidirectional graphite- epoxy composites or layered materials [211-213].

Next, all references contain theoretical approaches in addition to the experimental recorded signals. Agreements between experimental recorded and theoretical reported values are found.

Technical difficulties associated with the recording of ultrasonic field are overcome by use of high sensitive optical detectors and proper material recovery techniques. An understanding of generated wave propagation from different distributed (i.e. point, linear) sources is advisable before commencing the properties' recovery procedure, as suggested by Pan et al. (2006) or Audoin (2001, 2008) in their sharing contributions [214-216].

Thereto, noteworthy is to underline the approach of sensitivity issue while tackling the recovery of elastic coefficients from laser generated ultrasound waves within polymer composites with string anisotropy [217, 218]. Since the phase or group velocities of ultrasonic bulk waves are deployed within an inverse procedure, the latter can be examined by extensive simulations [219-221]. These are illustrating the effect of input data distortion and incompleteness while converting the velocities type.

Finite-element method (FEM) is being used due to its versatility and flexibility in modelling complicated geometries and loading conditions. Several contributions are tackling the issue of FEM usage to simulate the distribution of displacement and stress fields generated within an isotropic or viscoelastic specimen by a dynamic thermal source resembling the laser generated ultrasound [222, 223]. The input data values account the finite spatial and temporal shape of the laser pulse, optical penetration and temperature dependence of material properties.

The paper aims to approach the issue of laser ultrasound pulses from a source running in ablative mode, linearly distributed over the surface of an epoxy based composite specimens. The recovered elastic coefficients using a numerical procedure developed within the Laser Group from University of Bordeaux are further used as input data into an FEM based environment.

In addition, the temporal and spatial range of the linearly distributed laser source was deployed to enable stress and strain field contours during the transient thermal analysis carried out.

Debate on similarities between finite element method aided simulated displacements and experimentally recorded is being approached and closely investigated. The primary aim is to demonstrate the feasibility of FEM aided simulation usage in laser ultrasonic non-destructive material characterization.

VI.2.2. Materials and methods.

VI.2.2.1. Materials.

By embedding different volume fractions of alumina particles within an epoxy resin using a hot compressing technique enabled specimens' manufacturing. The polymer resin is available under the Hexcel MY 750 trademark while the hardener under HY 907, from Hexcel Corporation (Dublin, CA). The polymer matrix can withstand high temperatures like those generated by a laser source. The mixture was pressed at specimens' final dimensions of 100x8 mm2 as cylindrical shapes.

Composite specimens differ in terms of fillers' volume fraction point of view. They are labelled relative to filler content, as following: sample 1 – 45%, sample 2 – 40% and sample 3 – 35%, respectively.

Table VI.2.1 lists the polymer resin's properties as they were further used as input in the simulation environment.

Table VI.2.1. Polymer matrix properties used in simulation.

Physical properties	Value
Young's modulus [GPa]	3
Shear modulus [GPa]	1.09
Poisson's ratio	0.38
Glass transition temperature [°C]	160

VI.2.2.2. Experimental technique.

A Nd:YAG laser source, emitting at 1064 nm, was used to generate the ultrasonic waves in short pulses having 20 ns duration. The medium power output is typically ranging from 10 to 250 mJ per pulse. The collimated optical beam is focused

onto the composite specimen by means of a cylindrical lens. The latter enable to generate a line source dimension for the ultrasonic waves within the composite specimens. Ablation occurs at the side facing the laser source, marking it slightly, as can be seen in **Figure VI.2.1.**

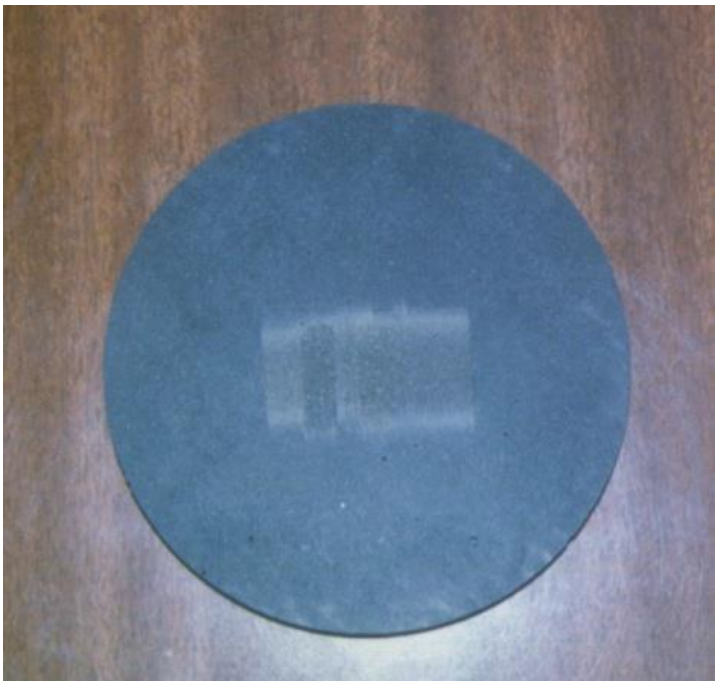

Figure VI.2.1. Laser ablation signature on specimens' surface.

From a conceptual perspective, this can be represented as a force normal to the surface of the specimen. Furthermore, this type of source generates a high- amplitude bulk longitudinal wave on the receiver side.

Detection is carried out by aid of a Mach-Zender laser interferometer probe, heterodyne type. The bandwidth extended up to 10 MHz. The reflectance of the specimens' surface does not enable a proper use of the heterodyne probe, requiring thus the use of a thin aluminium foil to increase the signal to noise ratio.

The signals were further amplified and sent to a computer connected to the transducer for further data processing.

VI.2.3. FEM modelling of transient response.

A coupled transient thermo-dynamical analysis enabled laser generated ultrasound problem approach within ANSYS 12.0 simulation environment [224]. First, a thermal element was used to simulate the thermal field. Then, the stress and displacement fields are simulated by replacing the above with a structural element (VISCO 88) that accounts for the viscous-elastic behaviour of the polymer matrix.

The initial and boundary conditions for modelling are set as follows: the initial temperature is assumed to be the ambient temperature. The load is considered linearly distributed over 25 mm, as focused by the cylindrical lens. Moreover, heat convection and thermal radiation are neglected.

The laser energy is 18 mJ and pulse rise time at the specimen surface is taken to be 20 ns. The maxim temperature achieved for a pulse width of 20 ns is about 618 °C, high enough to get ablation on specimen surface. Temporal and spatial resolution of the finite model is critical to the convergence of the numerical results [222].

VI.2.4. Results and discussions.

This section contains explanations on stiffness coefficients' recovery procedures followed by a discussion on simulation results gathered from FEM analysis.

The composite specimens' stiffness coefficients are recovered in two steps: (a) processing of group velocities from signals collected on the receiver side; (b) use of a numerical scheme developed to enable stiffness coefficients' recovery.

VI.2.4.1. Elastic coefficients from measurements.

The numerical recovery of the elastic coefficients from experimental velocities and amplitude of bulk modes from the laser source is already ascribed in reference papers [209, 225-227]. The elastic stiffness coefficients C_{ij} are defined in an axis system such as that direction 1 is the normal to the specimen and directions 2 and 3 are lying in the plane.

In the particle reinforced viscoelastic specimens, like those herein, two main elastic coefficients must be identified – C_{11} and C_{12}, the third being estimated from a dependency between the other ones.

The well-known elastic stiffness matrix for isotropic media in Voigt notation is:

$$C_{ij} = \begin{bmatrix} C_{11} & C_{12} & C_{12} & 0 & 0 & 0 \\ 0 & C_{11} & C_{12} & 0 & 0 & 0 \\ 0 & 0 & C_{11} & 0 & 0 & 0 \\ 0 & 0 & 0 & C_{44} & 0 & 0 \\ 0 & 0 & 0 & 0 & C_{44} & 0 \\ 0 & 0 & 0 & 0 & 0 & C_{44} \end{bmatrix} \quad (1)$$

Since in isotropic media only two waves are propagating through, longitudinal and shear, their velocities may be related to the material's properties.

The relationships between longitudinal and shear velocities and elastic coefficients in isotropic media are as follows:

$$v_T = \sqrt{\frac{C_{11} - C_{12}}{2\rho}} \qquad (1)$$

$$v_L = \sqrt{\frac{C_{11}}{\rho}} \qquad (2)$$

where ρ is the density of polymer based composite material and C_{ij} the stiffness coefficients from above.

From numerical scheme implementation, the stiffness coefficients are derived employing the Christofell equations that related each recorded velocity phase to these [210, 212].

On the other hand, stiffness coefficients recovered from group velocities is not straightforward as previous. Since there are no equations available, several methods for solving this inverse problem exist in literature [227].

In connection with above, the algorithm proposed by Deschamps and Bescond departs from the Cagniard-de Hoop method employed usually to relate the proposed change in variable and solving the expression of Christofell afterward. They identified a simple relationship between the group velocity and waves' time of arrival and deployed further.

In **Table VI.2.2** is listed the experimental values retrieved after using an optimized numerical recovery procedure as described above.

The values are consistent with the fillers' volume fraction embedded within the polymer composite. Small discrepancies exist between the recovered elastic coefficients in directions 2 and 3. These discrepancies are neglected and can be regarded to the manufacturing conditions and sensitivity of the experimental devices. Nevertheless, these characterize the quality of stiffness coefficients recovery process from group velocity data.

The stiffness coefficient C_{11} is recovered from the longitudinal transverse wave velocity propagating in the direction of epicenter direction, whereas C_{12} from velocities

of waves travelling in transversal direction. Noteworthy, the recovered values are ascribed to room temperature recorded signals since they depend upon temperature.

Table VI.2.2. Elastic coefficients recovered from measurements at room temperature.

Sample	Elastic coefficients	
	C_{11}	C_{12}
Sample 1	22.3 ± 0.85	6.52 ± 0.3
Sample 2	21.6 ± 0.63	5.75 ± 0.3
Sample 3	20.7 ± 0.48	6.50 ± 0.4

VI.2.4.2. FEM simulation of stress/displacements fields.

A numerical recovery procedure and modelling of laser generated ultrasound is employed to aid elastic coefficients' retrieval of polymer based composite specimens. The temporal shape of the laser pulses is accounted, also.

In **Figure VI.2.2** and **Figure VI.2.3** is being plotted the displacements' field recorded along the main direction of laser pulse loading within samples 1 and 3. These were simulated to cover the entire temporal range between incidence and emergence on the receiver side.

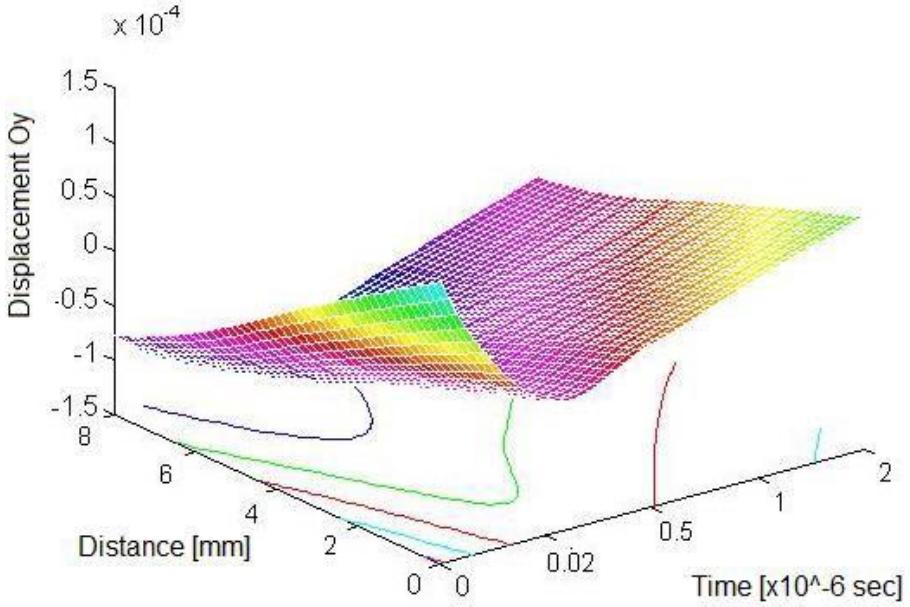

Figure VI.2.2. FEM simulated displacement field from sample 1.

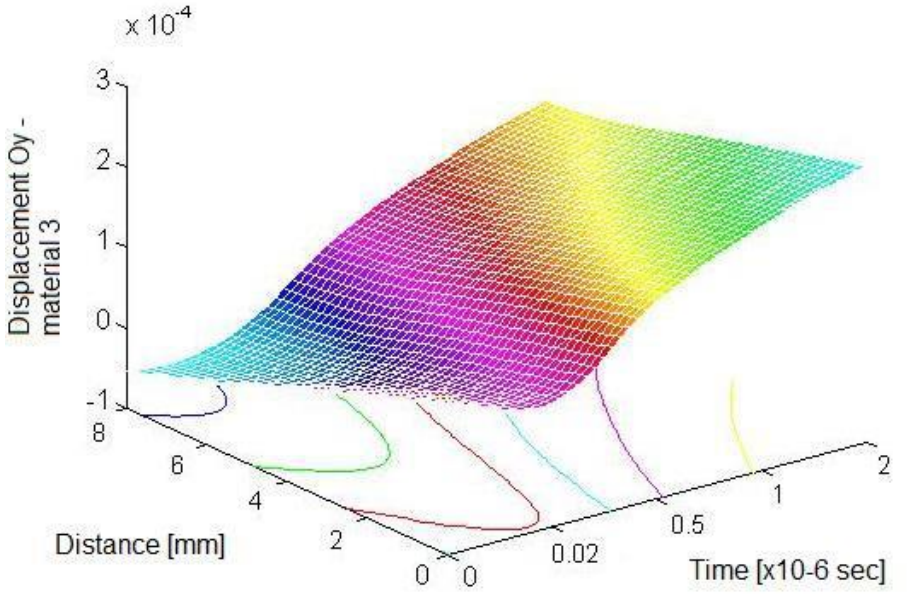

Figure VI.2.3. FEM simulated displacement field from sample 3.

A closer look to the above variations, both in time and penetration distance of the laser pulses reveal their consistency with the experimental recorded displacement field.

In all specimens, a negative spike is recorded within 20 ns associated to the extern load temporal range. The same trend is being recorded experimentally along the epicentre as a distinguished feature in the longitudinal component of the ultrasonic wave front. This is associated to the thermal stress generated by incidence of the laser pulse that causes surface heating and expansion.

The magnitude of this spike is strongly affected by the mass evaporated during the pulse interaction with sample's surface.

In Figure **VI.2.4** and Figure **VI.2.5** is represented the total strain fields within samples 1 and 2 along their thickness and within temporal range set to cover pulse propagation.

The following graphical representations and contour plots reflect the loading conditions, both temporal and thermal. Noteworthy, these follow the vertical and horizontal distribution of the external load that can be translated in terms of ultrasonic wave as longitudinal and transversal/surface propagation modes.

As previously described, thermal stresses are generated within the sample by laser heating. **Figure VI.2.6** captures this effect, including also the dynamic response due to a very short temporal range of the laser pulse. Both elastic and thermal stress develops nearby the sample surface and propagates downward.

Plot from **Figure VI.2.7** better depict the influence of the precursor on the in-plane stress field while its amplitude increases with the optical penetration depth. The contours of the in-plane stress indicate that it is compressive with a maximum recorded at 20 ns from load action and move further inside the sample's thickness.

The similar contour tendencies can be seen in the in- plane stress elastic field variation, both time and specimen distance from source side. This is outlined in **Figure VI.2.8**.

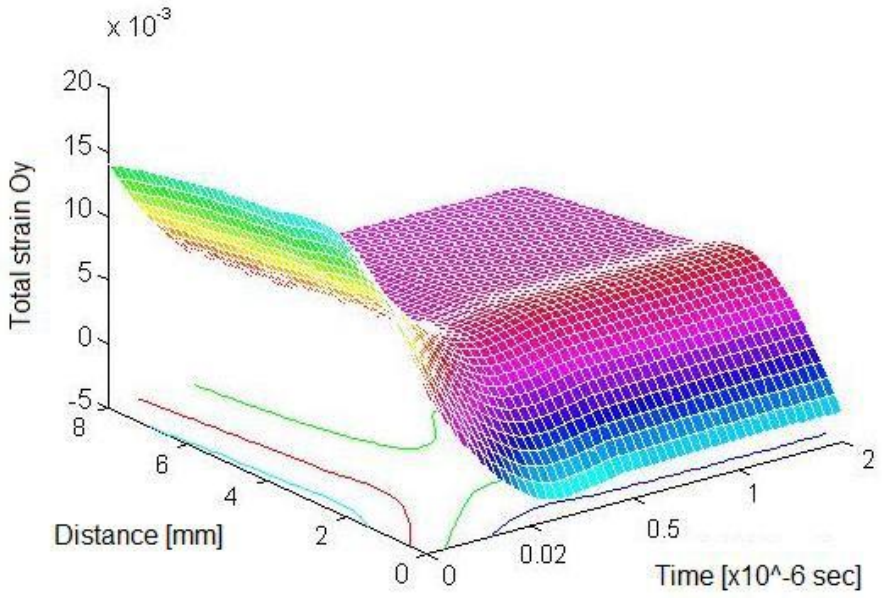

Figure VI.2.4. Total strain fields generated within sample 1.

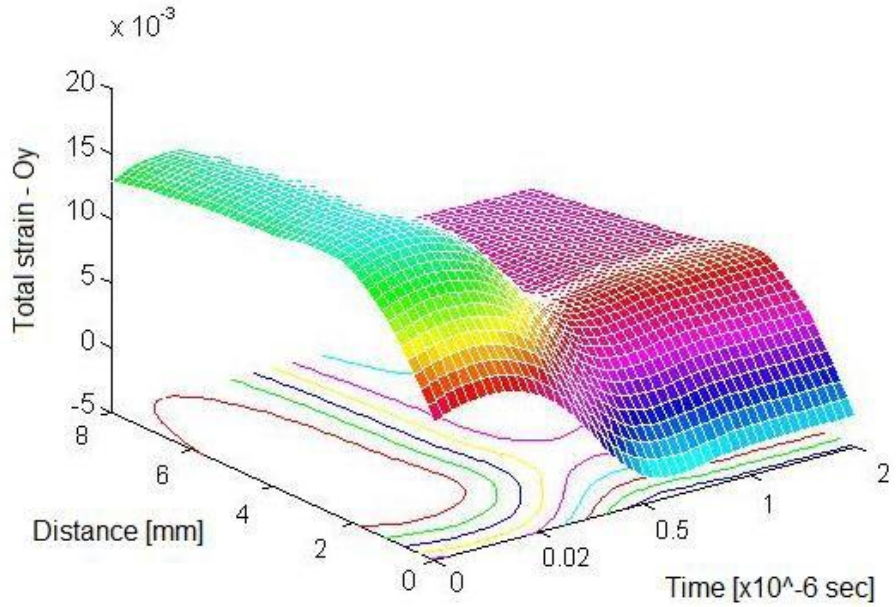

Figure VI.2.5. Total strain fields generated within sample 3.

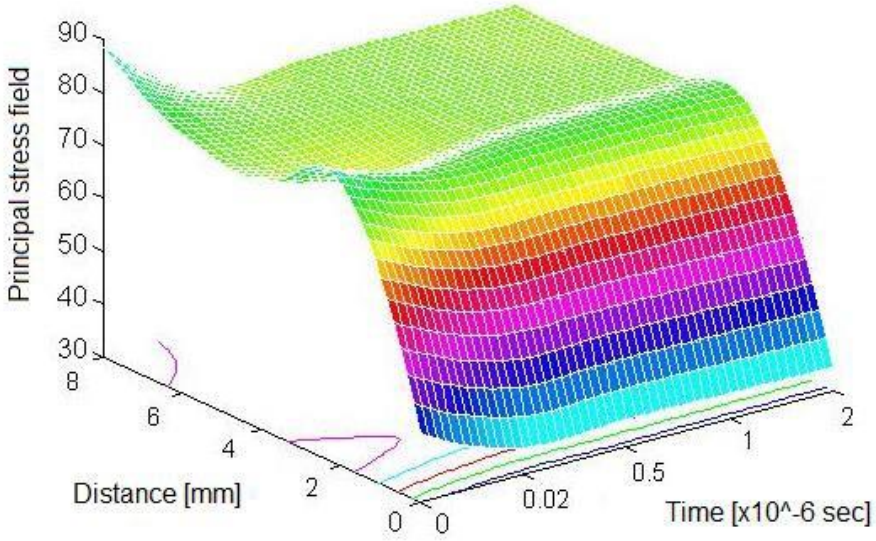

Figure VI.2.6. Total stress fields generated within sample 1.

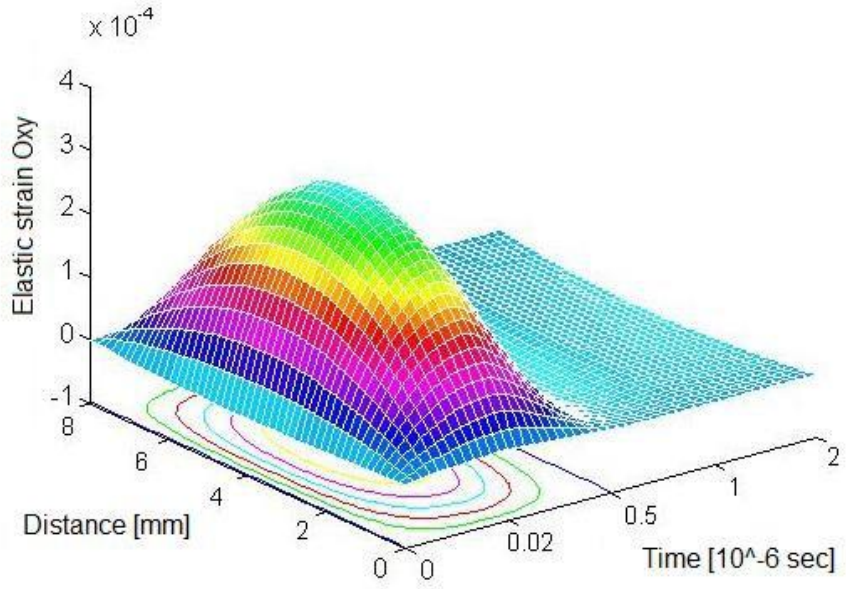

Figure VI.2.7. In-plane elastic strain field within sample 1.

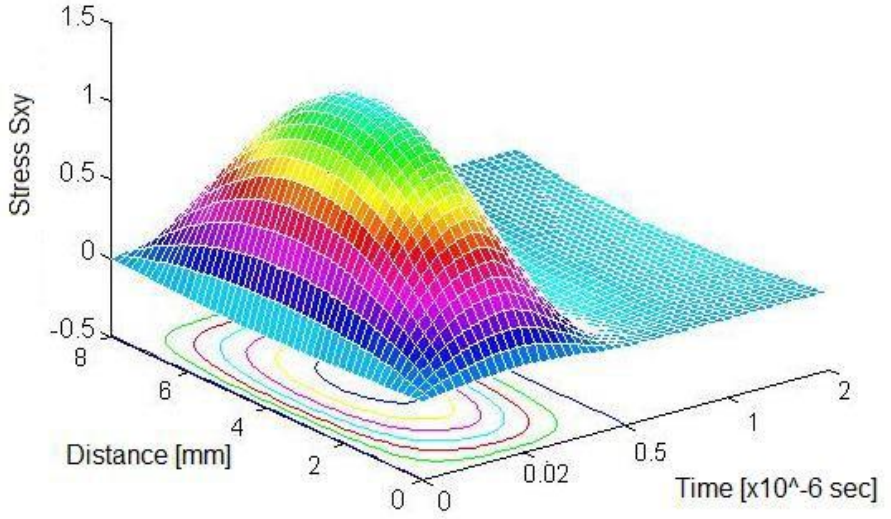

Figure VI.2.8. In-plane elastic stress field within sample 1.

In **Figure VI.2.9** and **Figure VI.2.10** is being plotted the displacement fields recorded in the epicenter direction at time arrival corresponding to the incidence at the laser source side, respectively at the detection side.

These resemble the experimentally recorded signals especially at the incidence since again the negative spike can be underlined.

Since thermal strain exists along with elastic ones due to both transient and inherent nature of the laser source, in **Figure VI.2.11** is represented the count plots of these fields along epicenter direction in sample 1.

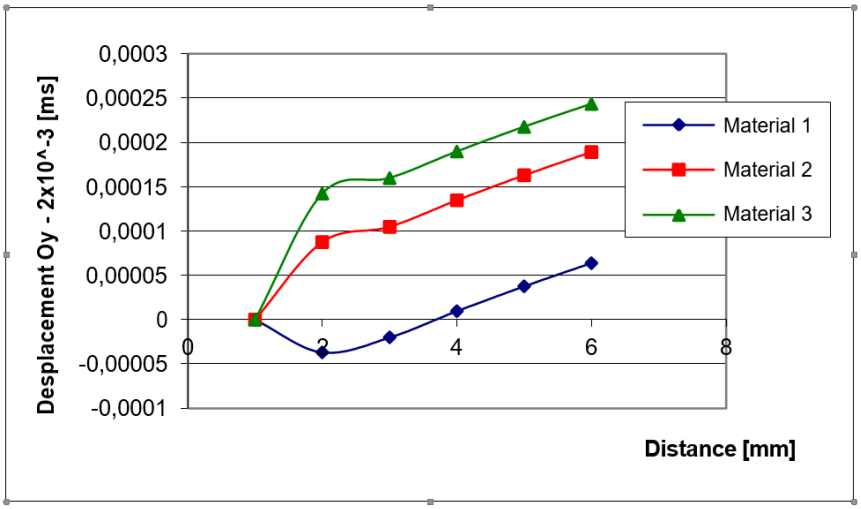

Figure VI.2.9. Displacement field in epicenter direction recorded at 2 microsec.

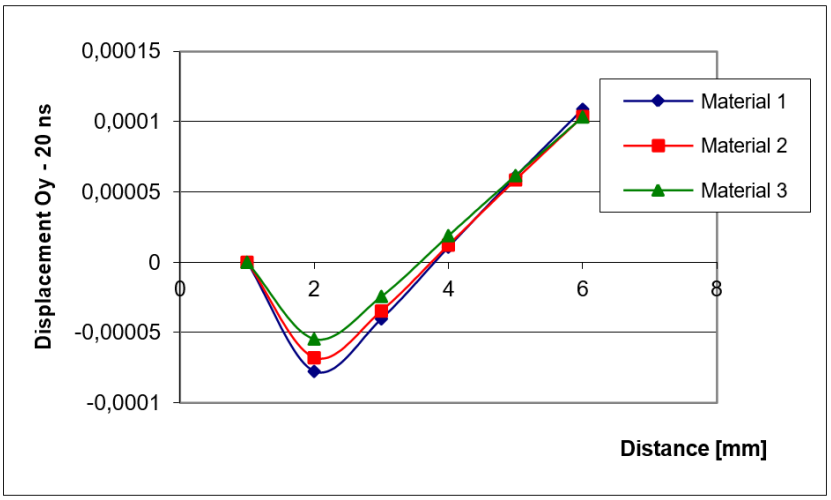

Figure VI.2.10. Displacement field in epicenter direction recorded at 20 nanosec.

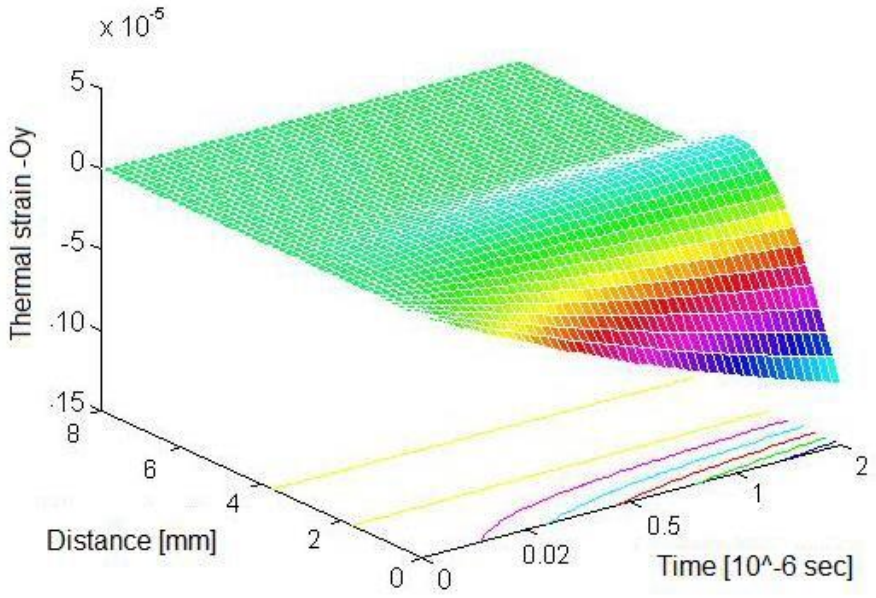

Figure VI.2.11. Thermal strain field within sample 1 along epicenter direction.

Noteworthy is the variation of the strain field that has the same trend in all composite samples. This is very high nearby the surface and turns to diminishing on the receiver side. The same hold in the experimental side for high- amplitude incidence pulses of laser source.

Furthermore, as the pulses depart from the incidence side, a relaxation process occurs. This can be sized in the strain field variation, irrespective of elastic or thermal ones.

Regarding all simulation results, the specimen shape does not influence the stress/strain field in epicenter direction. Contrary, in practice this gives rise to other types of waves had should be further identified and quantified.

VI.2.5. Conclusions.

The issue of laser generated ultrasound still captures researchers' attention due to its feasibility in enabling material properties' recovery from experimental recorded displacement fields.

A circular approach has been deployed herein to enable comparison between related experimentally signals and FEM simulated stress/strain or displacement variations.

On the other hand, optimized numerical recovery procedures of properties in isotropic/anisotropic materials are well developed and successfully used by several research groups. In this case, one particular developed is used for particle epoxy reinforced composites elastic coefficients' recovery proven different volume fraction of constitutive.

Despite the advent of FEM deployment on solving thermal transient propagation like the herein approached subject, a closer attention should be pay on capturing the entire coupled effects due to the loading conditions (i.e. temporal range, distribution, incidence to surface, etc.).

In relation with above, it's noteworthy for mention the breakdown in encompassing the overall effects generated by wave propagation, longitudinally and transversally. This can be related to the shortage in computer resources and abilities in running incrementally time/space distributed loading conditions.

JOURNAL OF OPTOELECTRONICS AND ADVANCED MATERIALS Vol. 17, No. 7-8, July – August 2015, p. 1032 - 1037

Particle reinforced composites' elastic properties retrieval by aid of laser generated ultrasound waves

D. LUCA MOTOC[a*], S. FERRANDIZ BOU[b], A. POP[c]
[a]*Department of Materials Science, Transilvania University, 500036 Brasov, Romania*
[b]*Department of Mechanical and Materials Engineering, Polytechnic University of Valencia, Spain*
[c]*Department of Mechatronics, University of Oradea, 410087 Oradea, Romania*

The paper aims to present a comparative analysis on numerical approaches carried on particle reinforced polymer composites viscoelastic properties' recovery procedure deployed to assist a laser generated ultrasound experimental configuration. A laser ultrasound technique was used to record the displacement fields within the composite specimens. A numerical procedure developed with Laser Group from University of Bordeaux is assisting the elastic coefficients' recovery process from the recorded signal. Corresponding theoretical displacements and stress/strain fields were simulated by finite-element method and further compared to the experimental signals. Agreement between the experimentally recorded signals and theoretical predictions is being found.

(Received April 9, 2015; accepted June 24, 2015)

Keywords: Polymer composites, Elastic properties, Laser ultrasound, Ablation mode

VI.3. Thermal properties comparison of hybrid CF/FF and BF/FF cyanate ester based composites.

VI.3.1. Introduction.

Green composites and natural fibers industry surpassed the limits for threshold attributes on their developed products after decades of focused research work, being on the verge of leveraging their performance attributes, including affordability, wide-range commercial applications and environmental concerns. The smart combination between natural reinforcements and/or biopolymers, initially intended to address the light-weight and low-cost issues, inherited globally the individual material properties of their constitutive, especially on thermal and acoustic insulation, or enabled synergetic effects in terms of mechanical and dynamical properties while combined as hybrid composite architectures [228-230]. Thermal degradation and fire retardant properties of natural reinforcement polymer based composites captured the researchers' attention over the last decade, mostly due to environmental concerns and safety issues. Alvarez [231], Manfredi [232], Lazko [233], Bar [234] or Kollia [235] and co-authors reported on the changes of aimed material properties for a couple of reinforcements embedded within synthetic resins such as vinyl ester, unsaturated polyester or cyanate ester, in or without surface conditioning by aid of flame retardant agents. Their findings enabled insights into the overall material behavior while establishing new routes for further developments and performance enhancements.

Literature survey allows a comprehensive insight into the world of extensive works on various combinations of materials from renewable resources, more or less environmental friendly and/or fully biodegradable under controlled conditions. Critical

reviews covering the encountered challenges, individual material selection criteria, compatibility, effective properties, manufacturing and processing techniques, economic and environmental impact as well as their ability to meet social and materials need worldwide were kindly provided by several groups of researchers [236-240]. They argued on natural materials' potential benefits despite their inherent hydrophilic nature that prior requires physically or chemically conditioning to improve the fiber/matrix adhesion to limit the penalties of the resulting composite material performances.

In addition, since through hybridization improvements on the combination's effective properties were mostly achieved by individual material selection, both fibers and matrix, by smart reinforcement layering or intimately connecting, predictability about the preferences on the composite architectures adopted by different researcher teams and lately by various industry players worldwide can be easily identified [241-245].

The green polymer based composites developed hitherto used natural fibers acquired from cellulose/lignocelluloses sources (e.g. jute, flax, hemp, ramie, sisal, wood, etc.) embedded mainly within unsaturated polyester resins and epoxies. Attempt on getting an answer to the question regarding the superiority of natural reinforcements over glass fibers from an environmental perspective was given both by Joshi [246] and Wambua [9] and their co-authors using some previous studies based on life cycle assessments (LCA) and several drivers to debate on the tackled issue.

Recently, were reported studies on resins developed from renewable resources (e.g. linseed oil, soybean oil, etc.) as polymer matrices for natural reinforcements which all shown good mechanical, thermo-physical or dynamical properties in comparison with their counterparts [247-249]. In the paper of Mosiewicki et al. [250] was summarized the main vegetable oils based composite architectures, covering macro, micro- and nano-scale range on the reinforcement dimension and examples in special applications as coatings, adhesives, foams and shape memory materials. Furthermore, the paper of Lligadas et al. [251] enables the reader to get acquitting with a different perspective on bio-based materials tailored as posing certain material properties, focusing on their biomedical application potential. Further insights on the issue were given by Fombuena

et al. with their comprehensive study regarding the mechanical and thermal properties of various protein fillers embedded within an epoxidized soybean oil (ESBO) novel resin combination cured by aid of nadic methyl anhydride [252]. The study revealed enhancement on the properties under the focus with filler weight fraction increase.

Flax and hemp fibers classified as favorites among the preferences while selecting the reinforcements for this composite class. A recent paper of Pil et al. attempted to provide a large spectrum of facts and data while arguing positively the question used as title regarding the fascination of designers for these types of natural materials [253].

They succeeded to capture the substantial spectrum of applications deploying these materials due to their intrinsic property of having a high vibration damping capacity in addition to the excellent mechanical properties and lower environmental impact compared with the glass and carbon reinforced composites.

In addition, the nature and individual features of the polymer matrix strongly influence mechanical and temperature-dependent properties, like storage modulus or damping factor. Subsequently, matrix-material selection must be tackled as sharing the same importance in the composite design. For example, epoxy resin was preferred in the early stages of advanced composite development and has maintained its position, even following extensive research into new blend formulas to transcend the drawbacks encountered with respect to transition temperature, moisture control, toxicity, polymer viscosity, etc. [254, 255] Next, epoxy resin was used to enhance the individual processing properties of other polymer resins through novel blend synthesis. Special attention was given to the synthesis with cyanate ester thermosetting resin. The latter is particularly preferred for its material performance (e.g. high strength, low dielectric constant and dissipation factor, radar transparency, flame retardant, etc.) in high-temperature environments. Moreover, used as a matrix material for carbon fibers, reinforced composites satisfy the low-weight structural material requirements in the aerospace industry. In addition, cyanate ester resin is acknowledged for its recyclable potential under chemical attack or for its self-healing capacity while enhanced with epoxy resin filled micro-capsules, allowing the reuse of reinforcements in remanufacturing processes

[256, 257]. To the author's knowledge, no systematic study has been carried out on the effect of different stacking sequences and the content of natural reinforcements, especially flax fibers, in combination with carbon fibers or basalt fibers, as hybrid architectures. Further, there are no reports available on natural-fiber reinforced cyanate ester based prepregs/laminates.

The present paper explores the feasibility of tailoring hybrid architectures based on flax in combination either with carbon or basalt fibers prepregs. The synergetic effect due to hybridization will be emphasized individually on different stacking sequences by deploying a novel resin system made by cyanate ester and epoxy resins followed by a couple of important material properties' investigation. Debate on effective thermo-physical properties (e.g. thermal expansion and thermal conductivity) and thermal decomposition within selected temperature range of herein samples focuses on the perspective of deploying basalt fibers as potential replacements of carbon reinforcements in applications driven by economic issues [258].

VI.3.2. Experimental procedure.

VI.3.2.1. Material selection and resin blend formulation.

Commercial available plain weave 1/1 flax (n. FF), carbon-fiber (n. CF) and basalt fiber (n. BF) fabrics were selected as reinforcements. The novel resin blend was formulated by intimately mixing dicyanate ester pre-polymer (n. CE - 75% vol.) with methyl ethyl ketone (MEK) solution and further stirring with diglycidyl ether of bisphenol F (n. DGEBF) epoxy resin under a 70:30 (vol.%) ratio in the presence of a bisphenol A hardener. Individual reinforcement properties and resin components are summarized in **Table VI.3.1** and **Table VI.3.2**, respectively.

Table VI.3.1. Material data of the present reinforcements.

Property	**Carbon fiber (n. CF) (KDK 8003)**	**Basalt fiber (n. BF)**	**Flax fiber (n. FF)**
Fabric area weight (g/m^2)	200 ± 10	475 ± 10	175 ± 10
Fabric thickness (mm)	0.30 ± 0.05	0.35 ± 0.05	0.40 ± 0.05
Commercial tradename	SIGRATEX®	-	-
Supplier	SGL Technologies GmbH	DBF Deustsche Basalt Faser GmbH	Leinenweberei Hoffmann GmbH
Thermal expansion (mstrain/^{o}C)*	0.2	3.5	30
Thermal conductivity (W/m ^{o}C)*	80	0.038	0.3

* CES EduPack 2016 (Granta Design Limited)

Table VI.3.2. Individual physical properties of polymer system.

Property	**Cyanate ester resin (Primaset™ BA 230 S)**	**DGEBF epoxy resin (Epikote™ 862)**
Glass transition temperature (^{o}C)	320 (by DMA)	270 (by DSC)
Viscosity @ 25 ^{o}C (mPa s)	450 ± 100	740 ± 150
Density @ 20 ^{o}C (g/cm^3)		1.18 ± 0.02
Curing agent	Bisphenol A	
Supplier	Lonza	Momentive

VI.3.2.2. Sample preparation.

The hybrid composite laminates (dimensions: 310 mm x 310 mm) were produced by stacking individually nine either solely FF and/or combined with CF or BF for the hybrid prepreg sheets. The prepregs were manufactured in situ after having previously an optimized formula of the novel polymer blend. ISO 15034:1999 standardized procedures were used to determine the resin flow while ISO 15040:1999 was used to evaluate the gel time. A temperature-controlled oven was used to compress (i.e. at 50 kN) and fully cure the composite plates at constant temperature of 180 °C, for one hour. The overall fiber loading fluctuated as shown in Table 3 and an average of 5 % of resin flow was measured, after lamination, for all hybrid composite plates. Solely FF and hybrid FF/CF or FF/BF composite laminates, posing high-quality surfaces, were obtained. Sample thickness ranged from 2.5 to 3 mm depending on the stacking sequence.

With respect to the stacking sequence, in the case of the hybrid architectures, the higher strength material (i.e. CF, BF) was layered as the outermost, exterior and exterior/middle layers. Flax fibers were layered in between due to their lower material performance. **Table VI.3.3** lists the stacking layering codes used to further address the hybrid composite architectures, and their individual and total volume fraction within the final laminate.

Table VI.3.3. Details on hybrid composites stacking sequences, assigned codes and volume fractions.

Stacking sequence	Laminate codes	Reinforcements volume fraction (vol%)		Total fiber loading (vol%)
		nf	sf	
□□□□□□□□□	9FF	45	-	45
■□□□□□□□■	BF/7FF/BF	21	14	35
■□□□■□□□■	BF/3FF/BF/3FF/BF	13	17	30
■□□□□□□□■	CF/7FF/CF	18	17	35
■□□□■□□□■	CF/3FF/CF/3FF/CF	19	11	30

VI.3.2.3. Material characterization.

Dilatometry (DIL) and laser flash analysis (LFA)

Expansion in composites where monitored by aid of a push rod dilatometer DIL 402 PC (Netzsch GmbH, D), in controlled atmosphere, within 25 °C – 250 °C temperature range and a 4 K min-1 heating rate, in accordance with ASTM E228:2011 standard procedures. Two successive scans were performed to remove thermal history and to retrieve the aimed thermo-physical property - linear coefficient of thermal expansion (CTE). Thermal conductivities of specimens were retrieved by aid of LFA 447 NanoFlash™ device (Netzsch GmbH, D), within 25 °C – 150 °C temperature range according with the ISO 22007-4:2008 standard procedures. Samples were covered back and forth with a thin layer of graphite to enhance their emission/absorption properties. The density at room temperature was obtained by the buoyancy flotation method. Thermal conductivity data corresponds to the mean value of the recorded values out of 5 single shots on each point considered.

Thermogravimetric analysis (TGA)

Thermogravimetric analysis on specimens was performed by aid of a STA 449 F3 Jupiter® (Netzsch GmbH, D) at a heating rate of 10 K min^{-1}, in N^2 atmosphere at a 20 mL min^{-1} flow rate, in accordance with ISO 11358-1:2014. Dynamic mode was deployed in the heating step within the selected 25 °C – 850 °C temperature range. Alumina crucible was used for each individual specimen excerpt. The weight loss was recorded in response to temperature increases.

Scanning electron microscopy (SEM)

Specimens' morphology was examined by aid scanning electron microscopy (SEM) on an EVO MA 25 (Zeiss, D) at room temperature, deploying different magnification modes - 500x and 2.0 K x, respectively. The prevailing images, after sputtering the samples with a gold thin layer, were closely investigated to qualitatively characterize the fiber–matrix interfaces.

VI.3.3. Micromechanical approaches – RoM/iRoM and RoHM/iRoHM.

Effective thermal properties of individual laminate (i.e. FF, BF or CF) and correspondingly tailored composite architectures were predicted deploying rules of mixtures and inverse mixtures (RoM/iRoM) as well as rules of hybrid mixtures and inverse hybrid mixtures (RoHM) respectively, as delivered in **Table VI.3.4**. In the expressions of addressed thermal properties the following hold for the fiber loadings - V_{nf} and V_{sf}, either natural or synthetic, while Vt is the total reinforcement volume fraction.

Table VI.3.4. RoM and RoHM expressions of thermo-physical properties.

Thermal property	RoM/iRoM		RoHM/iRoHM
	natural fiber based composites	synthetic fiber reinforced composites	
Linear coefficient of thermal expansion	$\alpha_{nfc} = \alpha_{nf} V_{nf} + \alpha_m (1 - V_{nf})$	$\alpha_{sfc} = \alpha_{sf} V_{sf} + \alpha_m (1 - V_{sf})$	$\alpha_c = \alpha_{nfc} V_{cnf} + \alpha_{csf} V_{sfc}$ *
Thermal conductivity	$\frac{1}{k_{nfc}} = \frac{V_{nf}}{k_{nf}} + \frac{(1 - V_{nf})}{k_m}$	$\frac{1}{k_{sfc}} = \frac{V_{sf}}{k_{sf}} + \frac{(1 - V_{sf})}{k_m}$	$\frac{1}{k_c} = \frac{V_{cnf}}{k_{nfc}} + \frac{V_{sfc}}{k_{csf}}$ *

* $V_{cnf} = \frac{V_{nf}}{V_t}$, $V_{csf} = \frac{V_{sf}}{V_t}$, $V_t = V_{nf} + V_{sf}$

Deviation from the reference (i.e. 9FF architecture) of the experimental values reveals the hybrid effects, which can be ranked as positive or negative according to Marom et al. [259]. These hybrid effects highlight the influence of stacking sequences and synthetic reinforcement's nature upon addressed thermal properties being indicators for the synergetic behavior of the combinations. On the other hand, since the retrieved thermal conductivity values represent through thickness measurements, RoM and RoHM must be replaced with their correspondingly inverse expressions accounting for the applied external load and fibers' orientation. This series model provides the lowest values of the composites' equivalent thermal conductivity [260, 261]. Nonetheless, more appropriate micromechanical approaches may be deployed to account for the reinforcement characteristics (i.e. anisotropy, orientation, waviness, etc.) but are thought to surpass the purpose of herein contribution and debate.

VI.3.4. Results and discussion.

VI.3.4.1. Effect of structure on the effective thermal properties.

SEM images from **Figure VI.3.1**, (a) and (b) were collected for the FF specimens and the highest number of layers of BF reinforcements in the hybrid composite samples to reveal the synergetic effects on their morphology. Images clearly evidence the weak adhesion between the CE&DGEBF resin and BF fibers due to the high sensitivity of CE resin to - OH groups and other volatiles present in the untreated fibers. Moreover, different types of interactions can be outlined in these composites function of fiber types. These are interactions between the fiber bundles and interactions between the cells of natural fiber. The latter is of particular importance because it can cause interfibrillar failure and uncoiling of the helical fibrils, and thus diffuse matrix cracking in practical applications [262]. In addition, **Figure VI.3.1(b)** reveals both fiber/matrix adhesion and the beauty of the fiber orientation. The latter can be considered to be in favor of BF while the replacements of CF with these are becoming an issue.

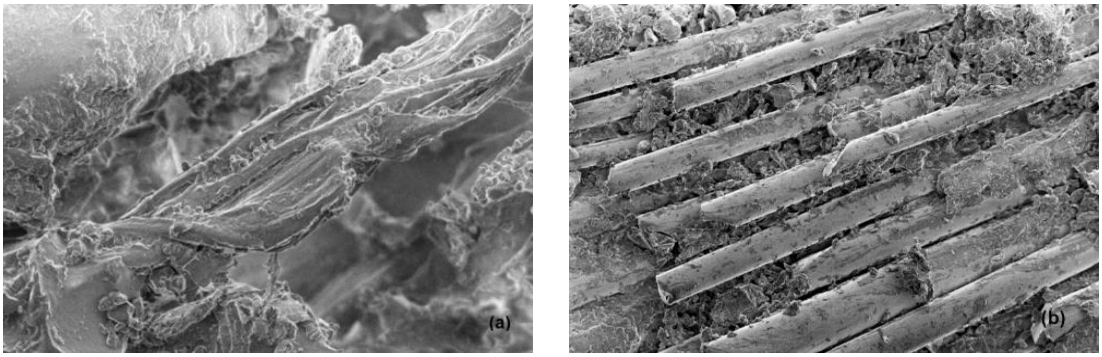

Figure VI.3.1. SEM images of the side views for (a) 9FF and (b) BF/3FF/BF/3FF/BF composites.

VI.3.4.2. Effect of hybridization on the expansion behavior

Thermal strain fields with FF and either CF/FF or BF/FF reinforced novel cyanate ester based composites experience the same tendency over the temperature range (**Figure VI.3.2**), such as a linear increase before a peak value, followed by a similar decrease toward the final value. Furthermore, physical alpha curves (**Figure VI.3.3**)

reveal approximately linear variation with temperature increases, exception the behavior shown between 100 to 150 °C associated with an abrupt decrease. This behavior can be regarded mainly to the hydrophilic nature of FF fibers, namely the aforementioned -OH groups and other volatiles that react with the resin as the temperature increase. Novel CE&DGEBF resin has a complicated structure and prone to be highly sensitive to the moisture. Thermal history cannot be accounted with the responsible mechanisms to the overall expansion behavior since the second runs were reported.

The increase in the rigid phase content with the hybrid architectures influences the amplitude of recorded data such there is a direct connection irrespective of the reinforcement deployed, CF or BF. On the other hand, the CF hybrid composites, either symmetrical or unsymmetrical stacked, reveal an opposite behavior to their BF counterparts, especially on the alpha curves variation as the temperature increases. This overall lowering effect can be assigned to the extremely low or negative thermal expansion of CF with temperature increases as widely acknowledged or shown by herein authors into a previous contribution [263]. Moreover, the higher the CF content the more pronounced is the decrease on the overall linear coefficient of thermal expansion values, especially within 150 °C to 250 °C temperature range.

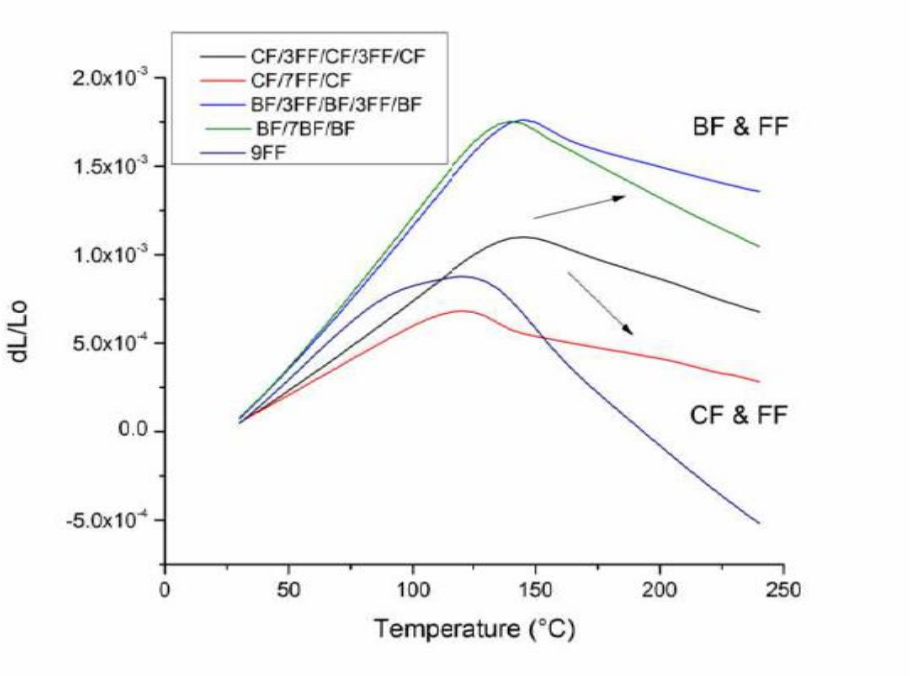

Figure VI.3.2. Thermal strain within various stacking sequences of CF and BF reinforced composites.

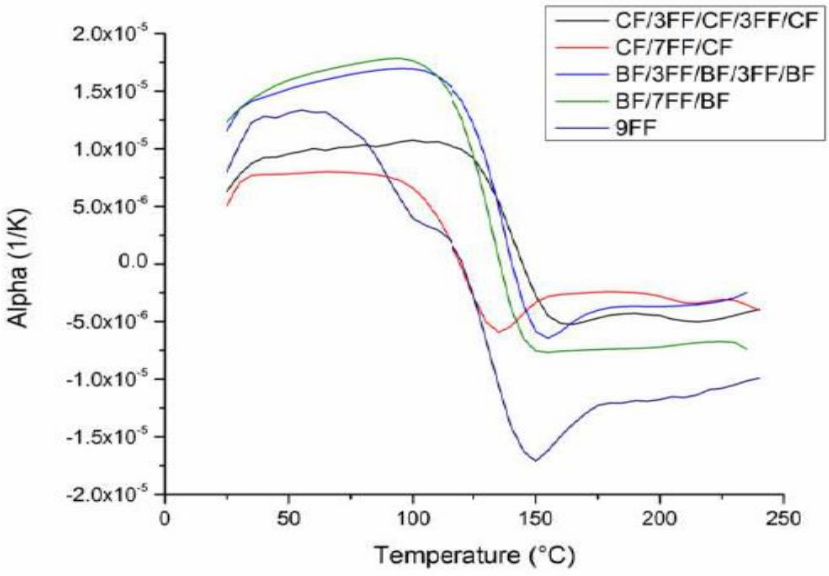

Figure VI.3.3. Technical alpha at different temperatures from DIL measurements.

A theoretical predicted vs. experimentally retrieved values' (see values listed in **Table VI.3.5**) comparison, in terms of relative error (see **Figure VI.3.4**, square symbol), reveal high discrepancies up to 95% in case of 9FF architecture and approximately 60% to 92% for the hybrid combinations, irrespective of the synthetic reinforcement. These values have to be viewed in accordance to their significance as long as the theoretically values belong to the upper limit predicted by micromechanical expressions within literature [261].

Table VI.3.5. Experimental CTE values, curve peaks and associated temperatures.

Laminate codes	**Reinforcements volume fraction (vol%)**		
	CTE (x10^{-6} K)	**CTE$_{max}$ (x10^{-6} K)**	**Temperature (°C)**
9FF	2.346	0.8904	121.9
BF/7FF/BF	4.794	1.7543	140.3
BF/3FF/BF/3FF/BF	6.245	1.7622	145.2
CF/7FF/CF	1.236	0.6821	120.7
CF/3FF/CF/3FF/CF	3.102	1.1155	144.1

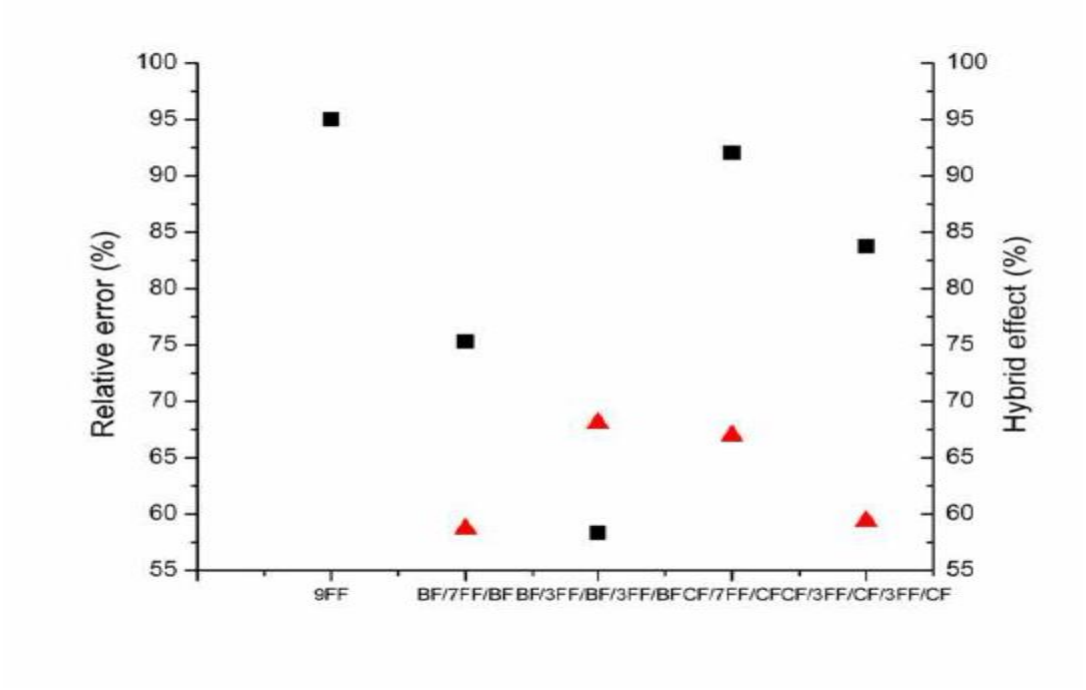

Figure VI.3.4. Hybrid effects and relative errors on CTE values with herein composites.

With respect to the hybrid effects, accounting for the relative differences between the experimentally retrieved values from either CF/FF or BF/FF combinations and 9FF reference specimen (see **Figure VI.3.4**, triangle symbol), positive departures were recorded in all cases. Thereof, irrespective of the stacking sequence, the presence of synthetic fibers (i.e. CF or BF) within the composite architecture enables a synergetic behavior at the overall assembly level from a thermal expansion perspective.

VI.3.4.3. Effect of hybridization on the thermal conductivity.

Figure VI.3.5 depicts the thermal conductivity curves of the analyzed polymer composite specimens, between 0.116 and 0.299 W $m^{-1}K^{-1}$ within selected temperature range. As it can be seen, thermal conductivity values of the hybrid composites, irrespective of the synthetic reinforcement, are in the same order of magnitude and can be ranked as thermal insulators despite the presence of a thermal conductivity phase. Moreover, a slight difference on thermal conductivity values retrieved from the CF and BF hybrid architectures is present within temperature range.

In particular, it seems that BF reinforced hybrid composite specimens are exhibiting enhanced thermal conductivities compared both with the reference and CF architectures. Indeed, sudden changes in thermal conductivity between 75 °C and 125 °C with BF hybrid architectures can be observed in the above graphical representation. These changes can be related both to the glass transitions and synergetic behavior while combined with FF reinforcements, being consistent with the thermal expansion behavior of the similar architectures.

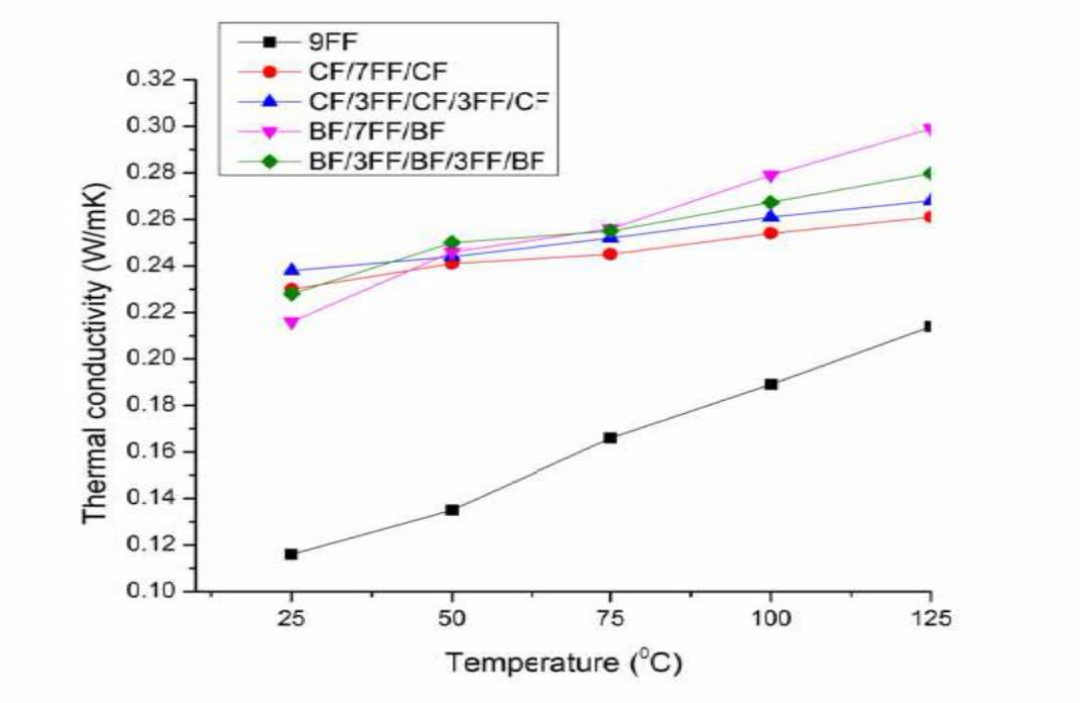

Figure VI.3.5. Thermal conductivity variations at different temperature values from LFA measurements.

Supplementary, due to the relatively small values of the through-thickness thermal conductivities, heat dissipations from panels made from these materials are limited, restricting thus their potential applications. Indirectly, the heat dissipation issue can be tackled based on the hybrid effect reflecting the synergy due to sequencing and individual reinforcement selection compared with the reference. The results are presented in **Figure VI.3.6** and seem to be more pronounced for CF hybrid specimens accounting the thermal conductivities values recorded at room temperatures. A conductivity enhancement factor (n. TCEF, in %), defined as the relative error between the retrieved hybrid composite architectures and matrix thermal conductivities at 25 °C, can be used further to debate on the heat dissipation within the specimens (see **Figure VI.3.6**). The values vary from 15% up to 38% showing an increasing tendency in terms of efficiency due to hybridization and deployment of more synthetic layers within the composites.

On the other hand, the relative error values unveil relatively small differences among the predicted and experimentally retrieved values on FF and CF/FF hybrid architectures (between 45% up to 60%) in comparison with the BF reinforced architectures (up to 200%). The latter should be assigned to the individual thermal conductivity values of BF fabrics reported with literature [264].

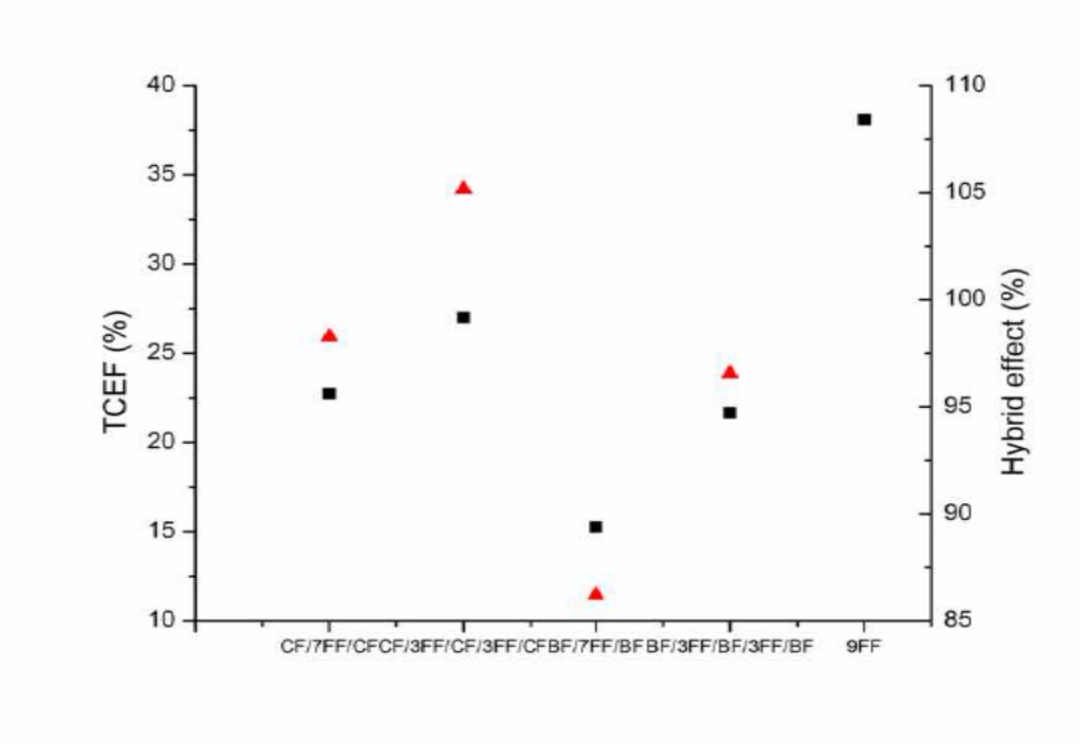

Figure VI.3.6. Hybrid effects on thermal conductivity and TCEF values comparison with herein composites.

VI.3.4.4. Thermal decomposition of hybrid composites.

In order to provide an extended perspective on other temperature related properties on herein hybrid CF and BF reinforced composites, a systematical study was carried out by means of thermogravimetric analysis (TGA) under controlled nitrogen atmosphere. Weight losses vs. temperature together with their derivatives are being delivered in **Figure VI.3.7** and **Figure VI.3.8**. Additionally, relative mass losses and residues as well as peak values from both curves were extracted and listed in **Table VI.3.6** to aid thermal degradation characterization in inert atmosphere (i.e. pyrolysis).

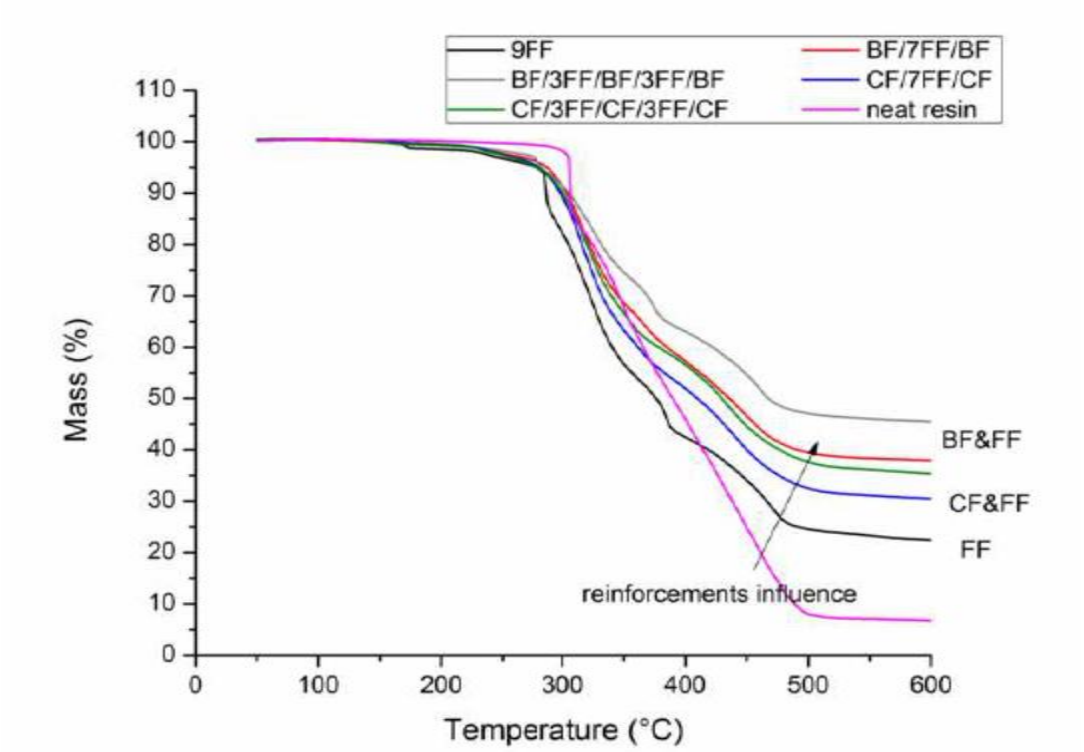

Figure VI.3.7. TGA mass loss-temperature profiles of FF and CF/BF reinforced hybrid composite architectures.

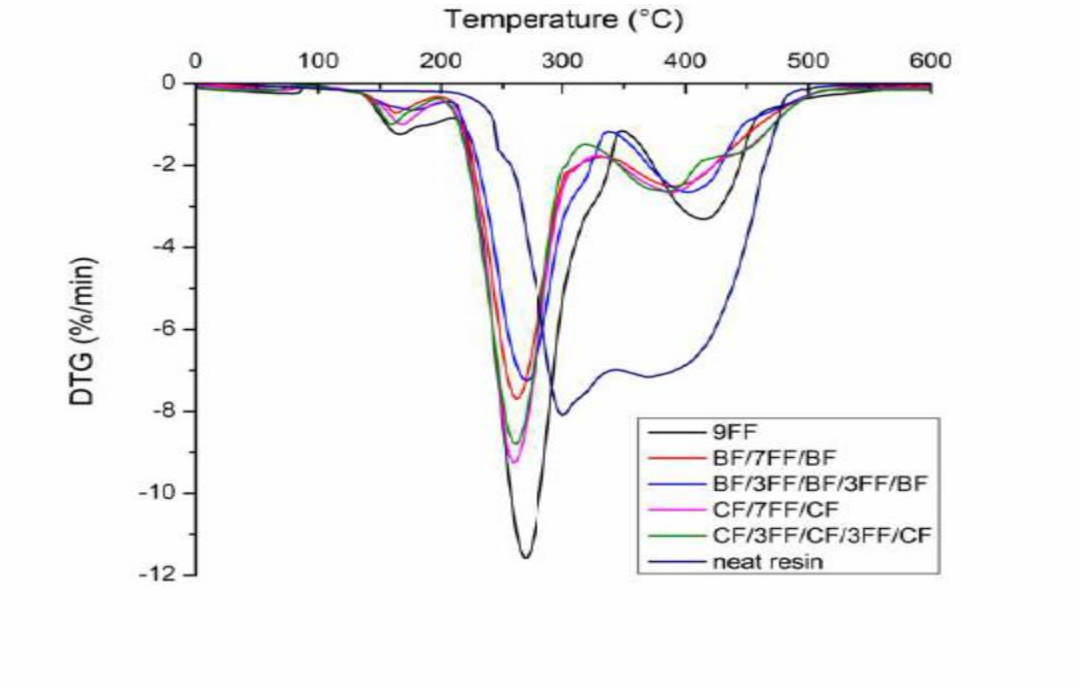

Figure VI.3.8. DTG profiles of FF and CF/BF reinforced hybrid composite architectures.

As it can be seen, both neat CE&DGEBF resin and either FF or CF/BF hybrid reinforced composites revealed two peaks in the DTG curves. With a single exception, the unsymmetrical CF stacked layers composite, in all fiber reinforced specimens, the first DTG peaks can be identified around 320 °C and further attributed to the decomposition of the primary and secondary walls of flax fibers, especially to cellulose micro fibrils [236, 265]. With the exception, there was encountered a shift toward 365 °C that can be attributed to the shielding effect caused by the presence of CF fibers. TGA curves are shifted to lowering temperatures showing a decrease in thermal stability of all hybrid composites. This could be the result of degradation of both natural/synthetic fibers and fibers/matrix interfacial bonding. Furthermore, the stacking layer number and reinforcement type seems to influence the magnitude of the decomposition peaks, too. Thus, from the plotting can be identified a decreasing tendency of the first peaks with the addition of synthetic reinforcements, both CF and BF, with smaller values for the latter architectures.

Moreover, the TG/DTG curves of the novel formula of neat polymer resin reveal a beginning of thermal decomposition near 350 °C that will be present further in the decomposition process of the natural/synthetic reinforced composites in their second peaks.

The less pronounced deflections within 100 °C up to 200 °C temperature range encountered in the DTG curves can be regarded to decomposition of hemicelluloses micro fibrils from the composition of flax fibers, whereas the lignin component of the flax fibers is decomposing near 400 °C [236]. The latter cannot be separated from decomposition of the polymer resin that further holds within 350 °C and 450 °C temperature range, revealing a second shoulder around the same temperature point. This temperature range corresponds to a 50% weight loss for all composite excerpts and more pronounced shifts to lowering temperatures in the second peaks recorded with hybrid specimens can be seen comparatively with the pure resin system. These shifts can be regarded to a char layer formation from the CF or BF layers that decompose with temperature increases. This char layer inhibits the heat and mass transfer from the inner layers of flax fibers and/or synthetic fibers and the melting resin toward the surface, thus affecting the thermal stability of correspondingly composites.

Finally, comments on residues may further aid the thermal decomposition processes analysis of herein composite architectures. Correspondingly values listed in **Table VI.3.6** highlights the amount of char assumed mainly from synthetic fibers that were not decomposed near 850 °C, the temperature end considered for the experimental recordings. Thus, at this temperature value, it seems that BF reinforced hybrid excerpts are decomposing slower compared with their counterparts, the shielding effect due to the presence of the former synthetic reinforcement being increasingly pronounced.

Table VI.3.6. Thermogravimetric parameters and degradation temperatures at different levels of TG weight loss.

Laminate codes	Onset (°C)	Temperatures at different weight loss (°C)				1st DTG peak (°C)	2nd DTG peak (°C)	Residue(%)
		5%	25%	50%	75%			
9FF	276.2	277.7	314.2	376.3	491.6	323.8	-	19.55
BF/7FF/BF	289.0	-	331.5	435.8	-	318.0	-	35.67
BF/3FF/BF/3FF/BF	281.9	282.2	348.2	467.6	-	324.4	434.9	41.46
CF/7FF/CF	289.3	280.2	323.4	410.0	-	315.7	423.3	29.94
CF/3FF/CF/3FF/CF	333.2	-	350.1	372.6	-	367.6	641.8	30.06
CE&DGEBF resin	378.4	-	398.2	420.8	618.9	347.5	410.0	0.05

VI.3.5. Conclusions.

The paper aimed to develop, investigate and debate the overall temperature related behavior of differently stacked sequences of synthetic- (i.e. CF/BF) and natural- (i.e. FF) fiber-reinforced laminates. The novel thermosetting cyanate ester formula proved to fulfill adhesion criterion and easiness during handling while deployed as the matrix for the laminates, spawning high-quality surface samples. The synergetic effects, due to individual synthetic or natural reinforcements and various stacking sequences were debated accounting on the effective thermo-physical properties (i.e. thermal expansion, thermal conductivity) and thermal decomposition processes.

Thus, from the previous findings, improvements in the coefficients of thermal expansion and thermal conductivity values can be noticed for all hybrid composite architectures herein, irrespective of the constitutive stacking sequence and reinforcement material compared with the reference (9FF). Furthermore, CF reinforced hybrids revealed poor performances both in thermal expansion and thermal conductivity values in comparison with BF reinforced hybrids for the same stacking sequence. These effects are not necessarily negative in terms of overall thermo-physical properties and should be assigned to the transversal anisotropy particular about the CF reinforcements.

Positive and negative hybrid effects were accounted for while comparing the predicted values with the experimental data. As expected, and consistent with reported values within the literature, the RoM based predictions reveal the highest values since they represent the upper bounds on the CTE values. On the other hand, RoHM predicted values are closer to the experimental data, and thus a better predictor model for the hybrid composite architectures.

Inverse RoM and RoHM formula were accounted in the effective thermal conductivity predictions proven the experimental setup enabling through thickness measurements. Comparisons revealed the anisotropic behavior particular about the CF reinforcements that are impeding heat dissipation from these panels and thereby their overall performances.

Furthermore, if cost issues become stringent with respect to the individual material selection of the hybrid composite constituents with the aim of similar thermo-physical effective properties, decision making can focus on the less expensive reinforcements herein, namely basalt fibers, which have proven to be highly competitive and less anisotropic along all directions.

The conclusions from this study can be thought to apply to a broad range of lignocellulosic reinforcements (e.g. kenaf, ramie, hemp, coir, jute, etc.) by stacking similarly in combination to carbon or basalt fibers or accounted for other hybrid composite architectures.

Thermal properties comparison of hybrid CF/FF and BF/FF cyanate ester based composites

D. Luca Motoc[1], S. Ferrandiz Bou[2], R. Balart[2]

[1]*Department of Automotive and Transport Engineering, Transilvania University of Brasov, 50017 Eroilor Av., Romania*

[2]*Department of Mechanical and Materials Engineering, Polytechnic University of Valencia, Plaza Ferrandiz-Carbonell, s/n, Alcoy (Alicante), Spain*

D. Luca Motoc (corresponding author)

Phone: (+) 40 742 585238

Email: danaluca@unitbv.ro or danalucamotoc@yahoo.com

Abstract: Thermo-physical properties of hybrid synthetic/natural reinforcements represent a challenging issue for material designers since several factors have to be accounted in terms of stacking sequence, fibre/matrix interface and individual material properties of constitutive. In this study, a novel cyanate ester resin formula was developed and deployed as a matrix for similar architectures of various stacking sequences of carbon (CF) or basalt fibres (BF) in combination with flax fibers (FF). Coefficients of linear thermal expansion (CTE) and thermal conductivities were debated in terms of CF or BF stacking sequences and volume fraction accounting for the reinforcements' anisotropy behavior with selected temperature range. Further comparison aided by rules of hybrid mixtures (RoHM/iRoHM) enabled a perspective on combinations' synergy, highlighting the insulating character of tailored composites.
Thermo-gravimetric analysis (TGA) supplemented the insights into the temperature dependent properties through information on the decomposition temperatures of constitutive and peaks shift compared to the reference (solely FF) in the DTG curves that can be regarded to the shielding effects caused by synthetic reinforcements (CF or BF).

.

Chapter VII

Chapter VII. Conclusions on the original work.

VII.1. Global conclusions.

Tailoring hybrid polymer composite materials process is a multidisciplinary endeavor that overlaps with various branches of engineering, material science, applied mathematics and chemical physics. In some cases, the boundaries set with these disciplines are due to particular methods, models and results that can be applied to study hybrid composite materials and vice versa.

The ability to tailor hybrid polymer composites with a unique spectrum of properties rests fundamentally on the ability to relate the effective properties to the microstructure, one of the essential aims of this habilitation thesis. Furthermore, the availability of predictable material properties shortens the manufacturing cost associated with structural components in *mechanical engineering applications* (e.g. aircraft, space vehicles, automobiles, insulation, heat exchangers, recreational products, micro electromechanical systems, etc.) as primary aimed by developers.

The reader has to account that the content of herein work was already published and indexed in worldwide data bases. Similar research activities were carried in relation to above, and those stated in the following section of the next chapter. The results should be sought as part of an ongoing publishing activity in co-authored peer-review journals.

VII.1.1. Mechanical properties of hybrid polymer composites.

- Elastic properties of hybrid polymer combinations are highly influenced both by the volume fraction of constitutive and material type (i.e. synthetic, natural) in addition to their stacking sequence, layer number and fiber orientation.
- Positive hybrid effects were obtained in all cases against the predicted values using *rules of the hybrid mixtures* (RoHM) model irrespective of the reinforcement type.
- The higher the particle volume fraction of the filler the smaller the differences between the retrieved elastic moduli in case of ceramic fillers, while using

metallic reinforcements this reverses. In addition, differences between the elastic moduli from tensile and flexure tests account approximately for 35% and 45% while embedding the metallic constitutive in 5% and 10% volume fractions, respectively.

- Environmentally hybrid polymer composite conditioning (e.g. low temperatures, temperature range, water immersion, etc.) further impacts the experimentally retrieved elastic property in some extends, thus revealing information on materials' sustainability.
- Differences between the effective elastic properties of environmentally conditioned and unconditioned hybrid particle-fiber polymer composites are higher if specimens were prior subjected to range temperature in comparison with those undergoing low temperatures (i.e. approximately 6 to 8% versus values < 4%).
- In the light of above, these differences should not be sought negatively or highly impacting the hybrid composite behavior while used as material in structural components. Moreover, prior environmentally conditioned hybrid composite specimens are experiencing longer stress-strain dependence until the first signs of delamination appear opposite to the applied load, irrespective of the reinforcement type.
- Carbon fiber reveals its effectiveness while embedded as reinforcement irrespective of the stacking layer sequences. This can be sized on the elastic properties that improve while the reinforcement content increases.
- The effective mechanical properties of these hybrid composites are being also influenced by the capacity of stress transferring between the fibre-matrix interfaces and fibres' different breakage mechanisms.
- It was shown that hybrid composites' strength is strongly influenced by reinforcements/matrix interface because depend on effective stress between constitutive and matrix.
- Conversely, the effective stiffness of hybrid composite architectures depends significantly on constitutive loading and not on reinforcements/matrix adhesion, since these have higher individual elastic properties comparatively with polymer matrix.

- A critical evaluation of experimentally retrieved data and available predicted values was provided in order to enable information gathering on strengthening and stiffening mechanisms in these tailored hybrid particle-fibre and fibre-fibre polymer composites.

VII.1.2. Dynamic mechanical properties of hybrid polymer composites.

- The effect of hybridization on the dynamic mechanical properties was approached for commercial epoxy and novel epoxy blends polymer composites.
- Generally, in all cases the storage and loss modulus revealed the same tendencies, namely a decrease as the temperature increases, which is associated with the softening of the unsaturated polyester or epoxy matrices at higher temperatures.
- A single frequency value (i.e. 1 Hz) was used for the dynamically applied load upon all hybrid composite specimens while preserving the same temperature range, from 25 °C to 250 °C.
- The resin systems (i.e. unsaturated polyester and epoxy resins) match well with the reinforcements revealing the absence of additional relaxation peaks in the experimentally retrieved curves.
- The storage moduli of *particle-fiber* hybrid polymer composites are experiencing an increase with increasing of the particle content that can be regarded as the reinforcement effect imparted by the constitutive that are more rigid than the polymer matrix.
- On the other hand, the loss modulus curves are being distributed over a wider range. Since these are indicative of the dissipated energy, the negative shift as the ceramic filler content increases and broadening of the loss modulus peak can be attributed to the relaxation processes within the hybrid composite.
- Damping factors used further to characterize the hybrid composite specimens, reveal the same negative shift recorded around glass transition temperature

value as the particle content phase increases revealing thus an increase in the mobility of polymer molecules on the particle/fiber/matrix interfaces.

- Cole-Cole diagrams plotted to indicate the extent of departure from the ideal shape with the content increase reveal the heterogeneity of the hybrid polymer composites as well as the relatively good reinforcements/matrix interface.
- Micromechanical predictions made using *linear rules of hybrid mixture* (RoHM) and *inverse rules of hybrid mixture* (iRoHM) reveal differences while comparing with the experimental retrieved values.
- In addition, positive hybrid effects were revealed by all composite specimens, irrespective of the particle filler content.
- Likewise, the dynamic mechanical characteristics of *fiber-fiber hybrid* polymer composites experience the same tendencies on their storage and loss moduli variation as the temperature increase.
- In relation to above, the transversal isotropy number and number of stacking layers particular about the carbon-fiber reinforcement phase are strongly influencing both effective storage and loss moduli.
- The storage modulus of the hybrid composite specimens experiences a strong decrease as the number of the UD carbon-fiber ply-ups increases and transversally disposed with respect to the general reference system.
- On the other hand, the loss modulus reveals small differences and the same wide-range distribution over the temperature range as the number of carbon-fiber layer increases and longitudinally disposed with respect to the general reference system.
- Furthermore, the positive shifts on the damping factor recorded for all hybrid composite specimens reveal the effectiveness of both fibers (i.e. GF and CF) as reinforcements irrespective of their stacking sequence, layer number and orientation
- Individually tackled Cole-Cole plots, for both longitudinal and transversal disposed carbon-fibers, reveal the heterogeneity of the hybrid fiber-fiber composite specimens and suitable indicators on the relatively good fibers/matrix interfaces.

- All the experimental findings reveal the effectiveness of the carbon-fiber as reinforcement in various polymer composites architectures as well as its behavior while disposed differently with respect to the loading direction.

VII.1.3. Thermo-physical changes of hybrid polymer composites.

- Generally, thermal stress and instantaneous linear coefficient of thermal expansion of herein tailored polymer composites are strongly affected by the same identified influencing factors as above, namely constitutive individual properties and reinforcement parameters (i.e. shape, orientation, concentration, etc.).
- In addition, both thermal properties experience an increase as temperature increases up to glass transition temperature, and successive runs have to be applied to remove thermal history from the manufacturing steps.
- In tailored *particle-fiber* hybrid polymer composites both thermal strain fields developed within specimens and instantaneous CTE variation with temperature reveal a decrease if particle filler concentration's increases irrespective of their material type.
- Theoretical predictions on effective CTE reveal the same decreasing tendency as the particle content increases and relatively large differences when compared with the experimentally retrieved values.
- The environmental conditioning steps considered prior property estimation reveal discrepancies on recorded thermal strain fields and instantaneous CTE variation with temperature for hybrid architectures while particle content increases. These differences can be seen in all records irrespective of the environmental conditioning regime applied.
- In addition, these should be regarded to the polymer matrix degradation nearby the composite's surface due to environmental conditioning induced micro-cracks, water removal and not to structural changes within the hybrid architecture.

- Moreover, these differences are less significant if hybrid composite specimens undergo a low-temperature program comparatively with temperature range or hygroscopic environmental conditioning.
- In tailored *fiber-fiber* hybrid polymer composites a supplementary influencing factor has to be accounted, namely fibers' orientation along to the measuring head direction.
- Like above, both thermal strain fields and instantaneous CTE are experiencing differences as temperature increases due to both constitutive concentration and orientation.
- The increase of UD carbon-fiber layers number and accounting their transversal isotropy as orientation with the measuring head changes, a lowering in both thermal strain and instantaneous CTE values can be easily highlighting.
- The findings are consistent with the other references with literature that classified this type of material as 'negatively' behaving. The later signify that this type of material highly contributes to the lowering of the property under consideration.
- Instantaneous CTE curves enable supplementary property retrieval, namely glass transition temperature on the curve peak. This parameter is particular important while testing a novel polymer matrix and a tailored hybrid composite architecture. Unfortunately, huge discrepancies were found to apply for this temperature value (e.g. 30 °C) comparatively with DMA or DSC measurements. Consequently, the later measurement test runs are favored.
- The *particle-particle* tailored hybrid polymer composites accounted the same influencing factors as previously, namely constitutive shape, distribution and concentration.
- The thermal properties were highly influenced by aforementioned, and the same overall thermal property lowering effect was gathered as the concentration of the carbon particle reinforcement increased.
- The numerous spikes in the CTE curve, irrespective of the carbon particles' concentration, can be regarded both to the temperature step set to record the experimental values as well as to the reinforcement/matrix interfaces that undergo changes as temperature increases.

- Furthermore, the instantaneous CTE variation with temperature range enables to retrieve supplementary information on the polymer matrix, namely those on glass temperature.
- In addition, the positive shift encountered with the carbon particle concentration increases reveals the prevalence of relaxation phenomenon at the reinforcements/matrix interface.
- As previously underlined, glass temperature transition value differs from that foreseen through DSC measurements (see polymer's technical sheet from the company's supplier). The latter measurement type is favored in literature.
- Theoretical predicted vs. experimentally retrieved CTE values shown small discrepancies if the double inclusion method was accounted comparatively with the well-known *Mori-Tanaka* model.
- In relation to above, these differences should be sought from the necessity to account other influencing factors, including their distribution and agglomeration within the polymer matrix.

VII.1.4. Electrical properties of hybrid polymer composites.

- These types of measurements were carried out solely on *particle-particle* polymer composites and envisaged the influences particular about the constitutive combination, individual geometry and distribution-related specificities.
- From experimental retrieved values, one should acknowledge that electrical conductivity of herein tailored hybrid polymer combinations' ranks within semiconductor range (i.e. 10^{-2} to 10^{2} $\Omega \cdot m$) and increases with the increase of current density. The latter can be regarded to electro-thermal effects within the composite structure.
- In addition, effective electrical resistivity of herein hybrid polymer specimens experiences an abrupt decrease with the increase on the metallic particle volume fraction and increase of the current density applied upon these.
- Differences between the experimentally retrieved and predicted values of effective electrical conductivities (e.g. *Milton* and *Hashin-Shtrikman* bounds) should be sought to relay on the reinforcements' distribution and agglomeration within the hybrid composite structure that highly contributed to particle-particle interfaces enabling the conductive paths.

Chapter VIII

Chapter VIII. Future research lines.

VIII.1. Directions of scientific research.

VIII.1.1. Beyond the 'state-of-the-art' of physical and mechanical properties of hybrid composites.

In light of the above review, the major contribution that is foreseen by author concerns with the fostering of novel hybrid woven out of solely synthetic/natural fibres or combinations of their (e.g. inter, intra- or comingled) followed by emerging tailored architectures to address the performance criteria and optimization designs settings.

More specifically, further emerging deployment mutually agree on:

- Avoidance of the variability in natural fibre properties related to the location and time of harvest, processing conditions as well as their sensitivity to temperature, moisture and UV radiation.
- Avoidance of the problems caused by the hydrophilic nature in case of cellulose/lignocelluloses fibres that greatly influence their mechanical properties.
- Necessity of additional modifications like in case of cellulose/lignocelluloses fibres whose surface properties need supplementary improvements (e.g. physical or chemical methods) to guarantee the compatibility between fibres and matrix material.
- Problems caused by the physical properties regarding to the fibre dimensions, defects, strength and structure encountered in case of natural fibres.

The 'state-of-the-art' with hybrid polymer based composites mechanical properties, gathered findings generated and related shortcomings on the: fibre/matrix materials' compatibility, reinforcement structure and chemical composition or manufacturing techniques are foreseen to allow a smooth transition to other types of hybrids. In this regard, innovation and creativity are desirable to surmount shortages of skills and fill-in gap with missing information.

VIII.1.2. Beyond the 'state-of-the-art' of dynamical mechanical properties of hybrid composites.

With regard to related contributions depicted within habilitation thesis and other surveys on deployment of DMA technique will foreseen:

- Attempts for experimental research and data processing with aim of further comparison between the retrieved data from various DMA configurations (e.g. 3-point bending, penetration, double cantilever method, and single cantilever method) and hybrid polymer based composite architectures.
- Retrieved data processing (e.g. Cole-Cole plots, energy of activation, estimation of kinetic parameters, etc.) to size the contribution of the main influencing factors upon the dynamical behaviour and impact resistance of the constitutive over the temperature range settings.
- Drafting novel micromechanical based theoretical models to encompass the hybrid effect within the composite combinations to predict the temperature-dependent related properties.
- Mutually reinforcing theoretical predictions and experimentally retrieved values systemic approach to further assess the overall performance of the hybrid composite architecture under the focus.

VIII.1.3. Beyond the 'state-of-the-art' of thermal properties of hybrid composites

At a glance, Chapter 1 can be summarized as underpinning the recent contributions on thermal properties and temperature-related behaviour in hybrid polymer based composites, irrespective of reinforcement specificities. Consequently, these can be regarded to the natural trend in the materials' design and performance assignments by improving their structural functionality. Furthermore, from manufacturing processing point of view, knowledge on issue enables great thermal formability of these types of materials.

In the light of above, following the acknowledgement on 'state-of the-art' around the issue can be targeted new challenges, including:

- Monitoring and quantifying the thermal properties' changes of hybrid polymer based composites while subjected to thermal aging, thermal cycling or extreme thermal cycling conditions, both on in-situ or real manufacturing/working conditions.
- Evaluation of kinetic parameters and degradation mechanism of hybrid polymer based composites under various temperature ranges using different thermal analysis methods (e.g. DSC, DMA, TGA) followed by further correlation with predicted data from several theoretical predictions developed and reported in literature.
- Assessment of thermal properties in hybrid polymer based composites subjected to extreme environmental loading conditions (e.g. cryogenic, elevated and high temperatures).
- Development of newly theory models related to dynamic properties to enable a better approach on distribution functions, both temperature and frequency related, toward a more realistic characterization of hybrid composites.

VIII.1.4. Beyond the 'state-of-the-art' of electrical properties of hybrid composites.

Since dielectric spectroscopy of polymer based composite materials fail to capture researchers' interest due to several reasons, including the testing equipments acquisition high rate, a strong industrial interest on dielectric and electric properties of these materials can be identified. The latter can be regarded to the growing use of these materials in electronic devices, optoelectronic switches, printed board circuitry and microwave subassemblies for radar, fuel cell, etc.

Following this industry interest and acknowledging the information gaps within the scientific literature with respect to the issue, concerns should be addressed with respect to the:

- Dielectric behaviour of polymer matrices, including in-situ real time monitoring of kinetics and rheology of cure within a wide range of frequencies (i.e. 10^{-5} to 10^{11} Hz), temperature range (i.e. extreme low to very high) and correlation with other types of measurements.
- Dielectric properties' changes encountered for different hybrid polymer based composites architectures function of reinforcements' concentration, geometry, distribution, other prior specimen's conditioning, etc.
- Monitoring of relaxation phenomena and related parameters over the time and function of applied frequency, to enable information and knowledge gathering on the issue.

VIII.1.5. Beyond the 'state-of-the-art' of all effective material properties of hybrid composites.

In addition, underpinning the advancements both in hybrid composites and related effective material properties, combinations of various efficient, cost-effective and environmentally friendly reinforcement materials that can be tailored in place of/along with fewer environmentally-friendly materials can be tackled. The hybridization process needs further attention both in terms of experimental research and theoretical approaches. Inter alia, multi-scale theoretical models are required to be developed to tackle the contributions of the constitutive. Nevertheless, particular concerns are given to:

- Setting a multi-scale modelling framework for prediction of the effective material properties (e.g. mechanical, thermal, dynamical, electrical, etc.) in case of the hybrid polymer based composite structures.
- Encompassing in the multi-scale models the non-linear behaviour due to the matrix material and sizing the influence of the fillers' length (e.g. short, continuous) on the effective properties of the hybrid polymer based composites developed.

- Development of theoretical models for temperature-dependent effective material properties' prediction at different states encountered during thermal conditioning (e.g. glassy, leathery, rubbery and decomposed).
- Considering coupled-analysis issues and dependencies for time shortening from the process and next, material design steps to be ready for manufacturing structure design levels.

Multi-scale engineering or *continuum modelling* of materials can be considered as further research directions proven the missing information available and weak understanding about the issue. In addition, semi-empirical models can be further developed to encompass the already identified influencing factors upon the effective retrieved material properties.

References.

1. Bunsell, A.R. and B. Harris, *Hybrid carbon and glass fibre composites.* Composites, 1974. **5**(4): p. 157-164.

2. Summerscales, J. and D. Short, *Carbon fibre and glass fibre hybrid reinforced plastics.* Composites, 1978. **9**(3): p. 157-166.

3. Short, D. and J. Summerscales, *Hybrids – a review: Part 2. Physical properties.* Composites, 1980. **11**(1): p. 33-38.

4. Ashby, M.F. and Y.J.M. Bréchet, *Designing hybrid materials.* Acta Materialia, 2003. **51**(19): p. 5801-5821.

5. Ashby, M.F., *Chapter 11 - Designing Hybrid Materials*, in *Materials Selection in Mechanical Design (Fourth Edition)*, M.F. Ashby, Editor. 2011, Butterworth-Heinemann: Oxford. p. 299-340.

6. Pegoretti, A., et al., *Intraply and interply hybrid composites based on E-glass and poly(vinyl alcohol) woven fabrics: tensile and impact properties.* Polymer International, 2004. **53**(9): p. 1290-1297.

7. Fukunaga, H., T.-W. Chou, and H. Fukuda, *Strength of Intermingled Hybrid Composites.* Journal of Reinforced Plastics and Composites, 1984. **3**(2): p. 145-160.

8. Kretsis, G., *A review of the tensile, compressive, flexural and shear properties of hybrid fibre-reinforced plastics.* Composites, 1987. **18**(1): p. 13-23.

9. Wambua, P., J. Ivens, and I. Verpoest, *Natural fibres: can they replace glass in fibre reinforced plastics?* Composites Science and Technology, 2003. **63**(9): p. 1259-1264.

10. Faruk, O., et al., *Biocomposites reinforced with natural fibers: 2000–2010.* Progress in Polymer Science, 2012. **37**(11): p. 1552-1596.

11. La Mantia, F.P. and M. Morreale, *Green composites: A brief review.* Composites Part A: Applied Science and Manufacturing, 2011. **42**(6): p. 579-588.

12. Marom, G., et al., *Hybrid effects in composites: conditions for positive or negative effects versus rule-of-mixtures behaviour.* Journal of Materials Science, 1978. **13**(7): p. 1419-1426.

13. Swolfs, Y., L. Gorbatikh, and I. Verpoest, *Fibre hybridisation in polymer composites: A review.* Composites Part A: Applied Science and Manufacturing, 2014. **67**: p. 181-200.

14. Torquato, S., *Random heterogeneous materials : microstructure and macroscopic properties*. 2002, New York, NY [u.a.]: Springer.

15. Biron, M., *7 - Future Prospects for Thermosets and Composites*, in *Thermosets and Composites (Second Edition)*, M. Biron, Editor. 2014, William Andrew Publishing: Oxford. p. 475-501.

16. Ahmad, F., et al., *Hybrid Composites for Engineering Application*, in *Composite Technologies for 2020*, L. Ye, Y.W. Mai, and Z. Su, Editors. 2004, Woodhead Publishing. p. 545-550.

17. Fiore, V., G. Di Bella, and A. Valenza, *Glass–basalt/epoxy hybrid composites for marine applications.* Materials & Design, 2011. **32**(4): p. 2091-2099.

18. Lau, D., *Hybrid fiber-reinforced polymer (FRP) composites for structural applications*, in *Developments in Fiber-Reinforced Polymer (FRP) Composites for Civil Engineering*, N. Uddin, Editor. 2013, Woodhead Publishing. p. 205-225.

19. Sathishkumar, T., J. Naveen, and S. Satheeshkumar, *Hybrid fiber reinforced polymer composites – a review.* Journal of Reinforced Plastics and Composites, 2014. **33**(5): p. 454-471.

20. Lehmhus, D., et al., *Taking a downward turn on the weight spiral – Lightweight materials in transport applications.* Materials & Design, 2015. **66, Part B**(0): p. 385-389.

21. Wang, M. and N. Pan, *Predictions of effective physical properties of complex multiphase materials.* Materials Science and Engineering: R: Reports, 2008. **63**(1): p. 1-30.

22. Jawaid, M. and H.P.S. Abdul Khalil, *Cellulosic/synthetic fibre reinforced polymer hybrid composites: A review.* Carbohydrate Polymers, 2011. **86**(1): p. 1-18.

23. Ashori, A. and S. Sheshmani, *Hybrid composites made from recycled materials: Moisture absorption and thickness swelling behavior.* Bioresource Technology, 2010. **101**(12): p. 4717-4720.

24. Curtu, I., Motoc Luca D., *Micromecanica materialelor compozite*. 2009, Editura Universităţii Transilvania din Braşov, ISBN 978-973-598-469-4.

25. Berryman, J.G., *Hybrid effective medium approximations for random elastic composites.* Mechanics of Materials, 2014. **70**(0): p. 115-135.

26. Garboczi, E.J. and J.G. Berryman, *Elastic moduli of a material containing composite inclusions: effective medium theory and finite element computations.* Mechanics of Materials, 2001. **33**(8): p. 455-470.

27. Berryman, J.G. and P.A. Berge, *Critique of two explicit schemes for estimating elastic properties of multiphase composites.* Mechanics of Materials, 1996. **22**(2): p. 149-164.

28. Nemat-Nasser, S.H., M., *Micromechanics: overall properties of heterogeneous materials*. 1999: North-Holland. 786.

29. Hu, G.K. and G.J. Weng, *The connections between the double-inclusion model and the Ponte Castaneda–Willis, Mori–Tanaka, and Kuster–Toksoz models.* Mechanics of Materials, 2000. **32**(8): p. 495-503.

30. Schjødt-Thomsen, J. and R. Pyrz, *The Mori–Tanaka stiffness tensor: diagonal symmetry, complex fibre orientations and non-dilute volume fractions.* Mechanics of Materials, 2001. **33**(10): p. 531-544.

31. Tan, H., et al., *The Mori–Tanaka method for composite materials with nonlinear interface debonding.* International Journal of Plasticity, 2005. **21**(10): p. 1890-1918.

32. Böhm, H.J. and S. Nogales, *Mori–Tanaka models for the thermal conductivity of composites with interfacial resistance and particle size distributions.* Composites Science and Technology, 2008. **68**(5): p. 1181-1187.

33. Mercier, S. and A. Molinari, *Homogenization of elastic–viscoplastic heterogeneous materials: Self-consistent and Mori-Tanaka schemes.* International Journal of Plasticity, 2009. **25**(6): p. 1024-1048.

34. Peng, X., et al., *Evaluation of mechanical properties of particulate composites with a combined self-consistent and Mori–Tanaka approach.* Mechanics of Materials, 2009. **41**(12): p. 1288-1297.

35. Lu, P., *Further studies on Mori–Tanaka models for thermal expansion coefficients of composites.* Polymer, 2013. **54**(6): p. 1691-1699.

36. Liu, L. and Z. Huang, *A Note on mori-tanaka's method.* Acta Mechanica Solida Sinica, 2014. **27**(3): p. 234-244.

37. Dong, X.N., et al., *A generalized self-consistent estimate for the effective elastic moduli of fiber-reinforced composite materials with multiple transversely isotropic inclusions.* International Journal of Mechanical Sciences, 2005. **47**(6): p. 922-940.

38. Kanaun, S.K. and D. Jeulin, *Elastic properties of hybrid composites by the effective field approach.* Journal of the Mechanics and Physics of Solids, 2001. **49**(10): p. 2339-2367.

39. Aboudi, J.A.S.M.B., B. A. , *Micromechanics of composite materials: A generalized multiscale analysis approach.* 2012, Butterworh-Heinemann. 1032.

40. Gibson, R.F., *A review of recent research on mechanics of multifunctional composite materials and structures.* Composite Structures, 2010. **92**(12): p. 2793-2810.

41. Lee, D.J., et al., *Analysis of effective elastic modulus for multiphased hybrid composites.* Composites Science and Technology, 2012. **72**(2): p. 278-283.

42. Lee, D.J., et al., *Statistical modeling of effective elastic modulus for multiphased hybrid composites.* Polymer Testing, 2015. **41**(0): p. 99-105.

43. Teodorescu, H., et al., *Some averaging methods in the micromechanics of composite materials with periodic structure*. ACMOS '08: Proceedings of the 10th Wseas International Conference on Automatic Control, Modelling and Simulation, ed. M. Demiralp, et al. 2008. 210-214.

44. Fu, S.-Y., G. Xu, and Y.-W. Mai, *On the elastic modulus of hybrid particle/short-fiber/polymer composites.* Composites Part B: Engineering, 2002. **33**(4): p. 291-299.

45. Dong, C. and I.J. Davies, *Flexural strength of bidirectional hybrid epoxy composites reinforced by E glass and T700S carbon fibres.* Composites Part B: Engineering, 2015. **72**(0): p. 65-71.

46. Mishnaevsky Jr, L. and G. Dai, *Hybrid carbon/glass fiber composites: Micromechanical analysis of structure–damage resistance relationships.* Computational Materials Science, 2014. **81**(0): p. 630-640.

47. Dong, C., Sudarisman, and I. Davies, *Flexural Properties of E Glass and TR50S Carbon Fiber Reinforced Epoxy Hybrid Composites.* Journal of Materials Engineering and Performance, 2013. **22**(1): p. 41-49.

48. Benveniste, Y., *Revisiting the generalized self-consistent scheme in composites: Clarification of some aspects and a new formulation.* Journal of the Mechanics and Physics of Solids, 2008. **56**(10): p. 2984-3002.

49. Hashin, Z. and S. Shtrikman, *A variational approach to the theory of the elastic behaviour of multiphase materials.* Journal of the Mechanics and Physics of Solids, 1963. **11**(2): p. 127-140.

50. Carlos Afonso, J. and G. Ranalli, *Elastic properties of three-phase composites: analytical model based on the modified shear-lag model and the method of cells.* Composites Science and Technology, 2005. **65**(7–8): p. 1264-1275.

51. Christensen, R.M., *A critical evaluation for a class of micro-mechanics models.* Journal of the Mechanics and Physics of Solids, 1990. **38**(3): p. 379-404.

52. Mori, T. and K. Tanaka, *Average stress in matrix and average elastic energy of materials with misfitting inclusions.* Acta Metallurgica, 1973. **21**(5): p. 571-574.

53. Chiang, M.Y.M., et al., *Prediction and three-dimensional Monte-Carlo simulation for tensile properties of unidirectional hybrid composites.* Composites Science and Technology, 2005. **65**(11–12): p. 1719-1727.

54. Lua, J., *Thermal–mechanical cell model for unbalanced plain weave woven fabric composites.* Composites Part A: Applied Science and Manufacturing, 2007. **38**(3): p. 1019-1037.

55. Teodorescu-Draghicescu, H., et al., *On the elastic constants of a fibre-reinforced composite laminate*. Proceedings of the 2nd WSEAS International Conference on Engineering Mechanics, Structures and Engineering Geology, ed. N.E. Mastorakis, O. Martin, and X.J. Zheng. 2009. 155-158.

56. Wu, Z., *Three-dimensional exact modeling of geometric and mechanical properties of woven composites.* Acta Mechanica Solida Sinica, 2009. **22**(5): p. 479-486.

57. Amico, S.C., C.C. Angrizani, and M.L. Drummond, *Influence of the Stacking Sequence on the Mechanical Properties of Glass/Sisal Hybrid Composites.* Journal of Reinforced Plastics and Composites, 2010. **29**(2): p. 179-189.

58. Ary Subagia, I.D.G., et al., *Effect of stacking sequence on the flexural properties of hybrid composites reinforced with carbon and basalt fibers.* Composites Part B: Engineering, 2014. **58**(0): p. 251-258.

59. Reis, P.N.B., et al., *Flexural behaviour of hybrid laminated composites.* Composites Part A: Applied Science and Manufacturing, 2007. **38**(6): p. 1612-1620.

60. Yahaya, R., et al., *Effect of layering sequence and chemical treatment on the mechanical properties of woven kenaf–aramid hybrid laminated composites.* Materials & Design, 2015. **67**(0): p. 173-179.

61. Manders, P.W. and M.G. Bader, *The strength of hybrid glass/carbon fibre composites.* Journal of Materials Science, 1981. **16**(8): p. 2233-2245.

62. Selmy, A.I., et al., *In-plane shear properties of unidirectional glass fiber (U)/random glass fiber (R)/epoxy hybrid and non-hybrid composites.* Composites Part B: Engineering, 2012. **43**(2): p. 431-438.

63. Valença, S.L., et al., *Evaluation of the mechanical behavior of epoxy composite reinforced with Kevlar plain fabric and glass/Kevlar hybrid fabric.* Composites Part B: Engineering, 2015. **70**(0): p. 1-8.

64. Dutra, R.C.L., et al., *Hybrid composites based on polypropylene and carbon fiber and epoxy matrix.* Polymer, 2000. **41**(10): p. 3841-3849.

65. Czigány, T., *Special manufacturing and characteristics of basalt fiber reinforced hybrid polypropylene composites: Mechanical properties and acoustic emission study.* Composites Science and Technology, 2006. **66**(16): p. 3210-3220.

66. Chen, W., et al., *Basalt fiber–epoxy laminates with functionalized multi-walled carbon nanotubes.* Composites Part A: Applied Science and Manufacturing, 2009. **40**(8): p. 1082-1089.

67. Carmisciano, S., et al., *Basalt woven fiber reinforced vinylester composites: Flexural and electrical properties.* Materials & Design, 2011. **32**(1): p. 337-342.

68. Priya, S.P. and S.K. Rai, *Mechanical Performance of Biofiber/Glass-reinforced Epoxy Hybrid Composites.* Journal of Industrial Textiles, 2006. **35**(3): p. 217-226.

69. Dhakal, H.N., et al., *Development of flax/carbon fibre hybrid composites for enhanced properties.* Carbohydrate Polymers, 2013. **96**(1): p. 1-8.

70. Almeida Júnior, J.H.S., et al., *Study of hybrid intralaminate curaua/glass composites.* Materials & Design, 2012. **42**(0): p. 111-117.

71. Almeida Jr, J.H.S., et al., *Hybridization effect on the mechanical properties of curaua/glass fiber composites.* Composites Part B: Engineering, 2013. **55**(0): p. 492-497.

72. Mansor, M.R., et al., *Hybrid natural and glass fibers reinforced polymer composites material selection using Analytical Hierarchy Process for automotive brake lever design.* Materials & Design, 2013. **51**(0): p. 484-492.

73. Romanzini, D., et al., *Influence of fiber content on the mechanical and dynamic mechanical properties of glass/ramie polymer composites.* Materials & Design, 2013. **47**(0): p. 9-15.

74. Alavudeen, A., et al., *Mechanical properties of banana/kenaf fiber-reinforced hybrid polyester composites: Effect of woven fabric and random orientation.* Materials & Design, 2015. **66, Part A**(0): p. 246-257.

75. Boopalan, M., M. Niranjanaa, and M.J. Umapathy, *Study on the mechanical properties and thermal properties of jute and banana fiber reinforced epoxy hybrid composites.* Composites Part B: Engineering, 2013. **51**(0): p. 54-57.

76. Li, W., et al., *On improvement of mechanical and thermo-mechanical properties of glass fabric/epoxy composites by incorporating CNT–Al2O3 hybrids.* Composites Science and Technology, 2014. **103**(0): p. 36-43.

77. Lin, G.-m., et al., *Hybrid effect of nanoparticles with carbon fibers on the mechanical and wear properties of polymer composites.* Composites Part B: Engineering, 2012. **43**(1): p. 44-49.

78. Rahmanian, S., et al., *Mechanical characterization of epoxy composite with multiscale reinforcements: Carbon nanotubes and short carbon fibers.* Materials & Design, 2014. **60**(0): p. 34-40.

79. Qin, W., et al., *Mechanical and electrical properties of carbon fiber composites with incorporation of graphene nanoplatelets at the fiber–matrix interphase.* Composites Part B: Engineering, 2015. **69**(0): p. 335-341.

80. Gamze Karsli, N., S. Yesil, and A. Aytac, *Effect of hybrid carbon nanotube/short glass fiber reinforcement on the properties of polypropylene composites.* Composites Part B: Engineering, 2014. **63**(0): p. 154-160.

81. Boualem, N. and Z. Sereir, *Accelerated aging of unidirectional hybrid composites under the long-term elevated temperature and moisture concentration.* Theoretical and Applied Fracture Mechanics, 2011. **55**(1): p. 68-75.

82. Burks, B. and M. Kumosa, *The effects of atmospheric aging on a hybrid polymer matrix composite.* Composites Science and Technology, 2012. **72**(15): p. 1803-1811.

83. Tsai, Y.I., et al., *Influence of hygrothermal environment on thermal and mechanical properties of carbon fiber/fiberglass hybrid composites.* Composites Science and Technology, 2009. **69**(3–4): p. 432-437.

84. Barjasteh, E., et al., *Thermal aging of fiberglass/carbon-fiber hybrid composites.* Composites Part A: Applied Science and Manufacturing, 2009. **40**(12): p. 2038-2045.

85. Barjasteh, E. and S.R. Nutt, *Moisture absorption of unidirectional hybrid composites.* Composites Part A: Applied Science and Manufacturing, 2012. **43**(1): p. 158-164.

86. Menard, K.P., *Dynamic Mechanical Analysis: A Practical Introduction*. 2008, CRC Press. p. 240.

87. Deng, S., M. Hou, and L. Ye, *Temperature-dependent elastic moduli of epoxies measured by DMA and their correlations to mechanical testing data.* Polymer Testing, 2007. **26**(6): p. 803-813.

88. Ornaghi, H.L., et al., *Mechanical and dynamic mechanical analysis of hybrid composites molded by resin transfer molding.* Journal of Applied Polymer Science, 2010. **118**(2): p. 887-896.

89. Mohanty, S., S.K. Verma, and S.K. Nayak, *Dynamic mechanical and thermal properties of MAPE treated jute/HDPE composites.* Composites Science and Technology, 2006. **66**(3–4): p. 538-547.

90. Romanzini, D., et al., *Preparation and characterization of ramie-glass fiber reinforced polymer matrix hybrid composites.* Materials Research, 2012. **15**: p. 415-420.

91. Faguaga, E., et al., *Effect of water absorption on the dynamic mechanical properties of composites used for windmill blades.* Materials & Design, 2012. **36**(0): p. 609-616.

92. Bai, Y., T. Vallée, and T. Keller, *Modeling of thermal responses for FRP composites under elevated and high temperatures.* Composites Science and Technology, 2008. **68**(1): p. 47-56.

93. Idicula, M., et al., *Dynamic mechanical analysis of randomly oriented intimately mixed short banana/sisal hybrid fibre reinforced polyester composites.* Composites Science and Technology, 2005. **65**(7–8): p. 1077-1087.

94. Mahieux, C.A. and K.L. Reifsnider, *Property modeling across transition temperatures in polymers: a robust stiffness–temperature model.* Polymer, 2001. **42**(7): p. 3281-3291.

95. Mahieux, C.A. and K.L. Reifsnider, *Property modeling across transition temperatures in polymers: application to thermoplastic systems.* Journal of Materials Science, 2002. **37**(5): p. 911-920.

96. Springer, G.S., *Model for Predicting the Mechanical Properties of Composites at Elevated Temperatures.* Journal of Reinforced Plastics and Composites, 1984. **3**(1): p. 85-95.

97. Gu, P. and R.J. Asaro, *Structural buckling of polymer matrix composites due to reduced stiffness from fire damage.* Composite Structures, 2005. **69**(1): p. 65-75.

98. Lee-Sullivan, P. and D. Dykeman, *Guidelines for performing storage modulus measurements using the TA Instruments DMA 2980 three-point bend mode: I. Amplitude effects1.* Polymer Testing, 2000. **19**(2): p. 155-164.

99. Shao, Q. and P. Lee-Sullivan, *Guidelines for performing storage modulus measurements using the TA Instruments DMA 2980 three-point bend mode II. Contact stresses and machine compliance.* Polymer Testing, 2000. **19**(3): p. 239-250.

100. Díez-Pascual, A.M., M. Naffakh, and M.A. Gómez-Fatou, *Mechanical and electrical properties of novel poly(ether ether ketone)/carbon nanotube/inorganic fullerene-like WS2 hybrid nanocomposites: Experimental measurements and theoretical predictions.* Materials Chemistry and Physics, 2011. **130**(1–2): p. 126-133.

101. Tan, J., T. Kitano, and T. Hatakeyama, *Crystallization of carbon fibre reinforced polypropylene.* Journal of Materials Science, 1990. **25**(7): p. 3380-3384.

102. Kelly, A., et al., *Controlling thermal expansion to obtain negative expansivity using laminated composites.* Composites Science and Technology, 2005. **65**(1): p. 47-59.

103. Kelly, A., R.J. Stearn, and L.N. McCartney, *Composite materials of controlled thermal expansion.* Composites Science and Technology, 2006. **66**(2): p. 154-159.

104. Jefferson, G., T.A. Parthasarathy, and R.J. Kerans, *Tailorable thermal expansion hybrid structures.* International Journal of Solids and Structures, 2009. **46**(11–12): p. 2372-2387.

105. Zhao, L.Z., et al., *Thermal expansion of a novel hybrid SiC foam–SiC particles–Al composites.* Composites Science and Technology, 2007. **67**(15–16): p. 3404-3408.

106. Hatta, H., T. Takei, and M. Taya, *Effects of dispersed microvoids on thermal expansion behavior of composite materials.* Materials Science and Engineering: A, 2000. **285**(1–2): p. 99-110.

107. Pradere, C. and C. Sauder, *Transverse and longitudinal coefficient of thermal expansion of carbon fibers at high temperatures (300–2500 K).* Carbon, 2008. **46**(14): p. 1874-1884.

108. Gabr, M.H., et al., *Mechanical and thermal properties of carbon fiber/polypropylene composite filled with nano-clay.* Composites Part B: Engineering, 2015. **69**(0): p. 94-100.

109. Sauder, C., J. Lamon, and R. Pailler, *Thermomechanical properties of carbon fibres at high temperatures (up to 2000 °C).* Composites Science and Technology, 2002. **62**(4): p. 499-504.

110. Praveen, R.S., et al., *Hybridization of carbon–glass epoxy composites: An approach to achieve low coefficient of thermal expansion at cryogenic temperatures.* Cryogenics, 2011. **51**(2): p. 95-104.

111. Esposito, M., et al., *Fiber Bragg Grating sensors to measure the coefficient of thermal expansion of polymers at cryogenic temperatures.* Sensors and Actuators A: Physical, 2013. **189**(0): p. 195-203.

112. Tezvergil, A., L.V.J. Lassila, and P.K. Vallittu, *The effect of fiber orientation on the thermal expansion coefficients of fiber-reinforced composites.* Dental Materials, 2003. **19**(6): p. 471-477.

113. Dzenis, Y.A., *Thermal expansion of a composite with a hybrid granular-fibrous filler.* Mechanics of Composite Materials, 1989. **25**(2): p. 173-182.

114. Camacho, C.W., et al., *Stiffness and thermal expansion predictions for hybrid short fiber composites.* Polymer Composites, 1990. **11**(4): p. 229-239.

115. Jang, J.-S., et al., *Experimental and analytical investigation of mechanical damping and CTE of both SiO2 particle and carbon nanofiber reinforced hybrid epoxy composites.* Composites Part A: Applied Science and Manufacturing, 2011. **42**(1): p. 98-103.

116. Jin, F.-L. and S.-J. Park, *Thermal properties of epoxy resin/filler hybrid composites.* Polymer Degradation and Stability, 2012. **97**(11): p. 2148-2153.

117. Papanicolaou, G.C., A.S. Bouboulas, and N.K. Anifantis, *Thermal expansivities in fibrous composites incorporating hybrid interphase regions.* Composite Structures, 2009. **88**(4): p. 542-547.

118. Price, C.D., et al., *Modelling the elastic and thermoelastic properties of short fibre composites with anisotropic phases.* Composites Science and Technology, 2006. **66**(1): p. 69-79.

119. Tsukamoto, H., *A mean-field micromechanical approach to design of multiphase composite laminates.* Materials Science and Engineering: A, 2011. **528**(7–8): p. 3232-3242.

120. Nayak, S.K., S. Mohanty, and S.K. Samal, *Influence of short bamboo/glass fiber on the thermal, dynamic mechanical and rheological properties of polypropylene hybrid composites.* Materials Science and Engineering: A, 2009. **523**(1–2): p. 32-38.

121. Alsina, O.L.S., et al., *Thermal properties of hybrid lignocellulosic fabric-reinforced polyester matrix composites.* Polymer Testing, 2005. **24**(1): p. 81-85.

122. Han, Z. and A. Fina, *Thermal conductivity of carbon nanotubes and their polymer nanocomposites: A review.* Progress in Polymer Science, 2011. **36**(7): p. 914-944.

123. Mallik, S., et al., *Investigation of thermal management materials for automotive electronic control units.* Applied Thermal Engineering, 2011. **31**(2–3): p. 355-362.

124. Otiaba, K.C., et al., *Thermal interface materials for automotive electronic control unit: Trends, technology and R&D challenges.* Microelectronics Reliability, 2011. **51**(12): p. 2031-2043.

125. Lee, G.-W., et al., *Enhanced thermal conductivity of polymer composites filled with hybrid filler.* Composites Part A: Applied Science and Manufacturing, 2006. **37**(5): p. 727-734.

126. Sevostianov, I., *On the thermal expansion of composite materials and cross-property connection between thermal expansion and thermal conductivity.* Mechanics of Materials, 2012. **45**(0): p. 20-33.

127. Sevostianov, I., *Dependence of the Effective Thermal Pressure Coefficient of a Particulate Composite on Particles Size.* International Journal of Fracture, 2007. **145**(4): p. 333-340.

128. Takei, T., H. Hatta, and M. Taya, *Thermal expansion behavior of particulate-filled composites II: Multi-reinforcing phases (hybrid composites).* Materials Science and Engineering: A, 1991. **131**(1): p. 145-152.

129. Dunn, M.L., et al., *Thermal Conductivity of Hybrid Short Fiber Composites.* Journal of Composite Materials, 1993. **27**(15): p. 1493-1519.

130. Bigg, D.M., *Thermal conductivity of heterophase polymer compositions*, in *Thermal and Electrical Conductivity of Polymer Materials*. 1995, Springer Berlin Heidelberg. p. 1-30.

131. Choi, S. and J. Kim, *Thermal conductivity of epoxy composites with a binary-particle system of aluminum oxide and aluminum nitride fillers.* Composites Part B: Engineering, 2013. **51**(0): p. 140-147.

132. Teng, C.-C., et al., *Synergetic effect of thermal conductive properties of epoxy composites containing functionalized multi-walled carbon nanotubes and aluminum nitride.* Composites Part B: Engineering, 2012. **43**(2): p. 265-271.

133. Zhou, T., et al., *Improved thermal conductivity of epoxy composites using a hybrid multi-walled carbon nanotube/micro-SiC filler.* Carbon, 2010. **48**(4): p. 1171-1176.

134. Zhou, S., et al., *Experiments and modeling of thermal conductivity of flake graphite/polymer composites affected by adding carbon-based nano-fillers.* Carbon, 2013. **57**(0): p. 452-459.

135. Kandare, E., et al., *Improving the through-thickness thermal and electrical conductivity of carbon fibre/epoxy laminates by exploiting synergy between graphene and silver nano-inclusions.* Composites Part A: Applied Science and Manufacturing, 2015. **69**(0): p. 72-82.

136. Pak, S.Y., et al., *Synergistic improvement of thermal conductivity of thermoplastic composites with mixed boron nitride and multi-walled carbon nanotube fillers.* Carbon, 2012. **50**(13): p. 4830-4838.

137. Ranjeth Kumar Reddy, T., T. Subba Rao, and R. Padma Suvarna, *Studies on thermal characteristics of cow dung powder filled glass–polyester hybrid composites.* Composites Part B: Engineering, 2014. **56**(0): p. 670-672.

138. Chen, L., et al., *Modeling and analysis of synergistic effect in thermal conductivity enhancement of polymer composites with hybrid filler.* International Journal of Heat and Mass Transfer, 2015. **81**(0): p. 457-464.

139. Goyal, V. and A.A. Balandin, *Thermal properties of the hybrid graphene-metal nano-micro-composites: Applications in thermal interface materials.* Applied Physics Letters, 2012. **100**(7): p. 073113.

140. Schuster, J., et al., *Thermal conductivities of three-dimensionally woven fabric composites.* Composites Science and Technology, 2008. **68**(9): p. 2085-2091.

141. Krach, A. and S.G. Advani, *Influence of Void Shape, Void Volume and Matrix Anisotropy on Effective Thermal Conductivity of a Three-Phase Composite.* Journal of Composite Materials, 1996. **30**(8): p. 933-946.

142. Kulkarni, M.R. and R.P. Brady, *A model of global thermal conductivity in laminated carbon/carbon composites.* Composites Science and Technology, 1997. **57**(3): p. 277-285.

143. Thomann, U.I., M. Sauter, and P. Ermanni, *A combined impregnation and heat transfer model for stamp forming of unconsolidated commingled yarn preforms.* Composites Science and Technology, 2004. **64**(10–11): p. 1637-1651.

144. Turias, I.J., J.M. Gutiérrez, and P.L. Galindo, *Modelling the effective thermal conductivity of an unidirectional composite by the use of artificial neural networks.* Composites Science and Technology, 2005. **65**(3–4): p. 609-619.

145. Newnham, R.E., D.P. Skinner, and L.E. Cross, *Connectivity and piezoelectric-pyroelectric composites.* Materials Research Bulletin, 1978. **13**(5): p. 525-536.

146. Taya, M., *Electronic Composites. Modeling, Characterization, Processing, and MEMS Applications*. 2008: Cambridge University Press.

147. Kim, W.J., M. Taya, and M.N. Nguyen, *Electrical and thermal conductivities of a silver flake/thermosetting polymer matrix composite.* Mechanics of Materials, 2009. **41**(10): p. 1116-1124.

148. El Hasnaoui, M., et al., *Modelling of dielectric relaxation processes of epoxy-resin filled with carbon black particles.* Physica B: Condensed Matter, 2014. **433**(0): p. 62-66.

149. Novák, I., I. Krupa, and I. Janigová, *Hybrid electro-conductive composites with improved toughness, filled by carbon black.* Carbon, 2005. **43**(4): p. 841-848.

150. Shen, L., et al., *The combined effects of carbon black and carbon fiber on the electrical properties of composites based on polyethylene or polyethylene/polypropylene blend.* Polymer Testing, 2011. **30**(4): p. 442-448.

151. Jin, J., et al., *Enhancing the electrical conductivity of polymer composites.* European Polymer Journal, 2013. **49**(5): p. 1066-1072.

152. Othman, R.N., I.A. Kinloch, and A.N. Wilkinson, *Synthesis and characterisation of silica–carbon nanotube hybrid microparticles and their effect on the electrical properties of poly(vinyl alcohol) composites.* Carbon, 2013. **60**(0): p. 461-470.

153. Puértolas, J.A. and S.M. Kurtz, *Evaluation of carbon nanotubes and graphene as reinforcements for UHMWPE-based composites in arthroplastic applications: A review.* Journal of the Mechanical Behavior of Biomedical Materials, 2014. **39**(0): p. 129-145.

154. Wichmann, M.H.G., et al., *Glass-fibre-reinforced composites with enhanced mechanical and electrical properties – Benefits and limitations of a nanoparticle modified matrix.* Engineering Fracture Mechanics, 2006. **73**(16): p. 2346-2359.

155. Lonjon, A., et al., *Electrical conductivity improvement of aeronautical carbon fiber reinforced polyepoxy composites by insertion of carbon nanotubes.* Journal of Non-Crystalline Solids, 2012. **358**(15): p. 1859-1862.

156. Yamamoto, N., R. Guzman de Villoria, and B.L. Wardle, *Electrical and thermal property enhancement of fiber-reinforced polymer laminate composites through controlled implementation of multi-walled carbon nanotubes.* Composites Science and Technology, 2012. **72**(16): p. 2009-2015.

157. George, G., et al., *Dielectric behaviour of PP/jute yarn commingled composites: Effect of fibre content, chemical treatments, temperature and moisture.* Composites Part A: Applied Science and Manufacturing, 2013. **47**(0): p. 12-21.

158. Yang, C.Q., Z.S. Wu, and H. Huang, *Electrical properties of different types of carbon fiber reinforced plastics (CFRPs) and hybrid CFRPs.* Carbon, 2007. **45**(15): p. 3027-3035.

159. Yao, L., et al., *Modeling and experimental verification of dielectric constants for three-dimensional woven composites.* Composites Science and Technology, 2008. **68**(7–8): p. 1794-1799.

160. Zhan, M., R.P. Wool, and J.Q. Xiao, *Electrical properties of chicken feather fiber reinforced epoxy composites.* Composites Part A: Applied Science and Manufacturing, 2011. **42**(3): p. 229-233.

161. Thomassin, J.-M., et al., *Polymer/carbon based composites as electromagnetic interference (EMI) shielding materials.* Materials Science and Engineering: R: Reports, 2013. **74**(7): p. 211-232.

162. Al-Saleh, M.H. and W.H. Saadeh, *Hybrids of conductive polymer nanocomposites.* Materials & Design, 2013. **52**(0): p. 1071-1076.

163. Zheming, G., et al., *Electrical properties and morphology of highly conductive composites based on polypropylene and hybrid fillers.* Journal of Industrial and Engineering Chemistry, 2010. **16**(1): p. 10-14.

164. da Silva, A.B., et al., *Synergic effect in electrical conductivity using a combination of two fillers in PVDF hybrids composites.* European Polymer Journal, 2013. **49**(10): p. 3318-3327.

165. Yang, S.-Y., et al., *Synergetic effects of graphene platelets and carbon nanotubes on the mechanical and thermal properties of epoxy composites.* Carbon, 2011. **49**(3): p. 793-803.

166. Yu, C.-R., et al., *Electrical and dielectric properties of polypropylene nanocomposites based on carbon nanotubes and barium titanate nanoparticles.* Composites Science and Technology, 2011. **71**(15): p. 1706-1712.

167. Salinier, A., et al., *Electrical, rheological and mechanical characterization of multiscale composite materials based on poly(etherimide)/short glass fibers/multiwalled carbon nanotubes.* Composite Structures, 2013. **102**(0): p. 81-89.

168. Motaghi, A., A. Hrymak, and G.H. Motlagh, *Electrical conductivity and percolation threshold of hybrid carbon/polymer composites.* Journal of Applied Polymer Science, 2014: p. n/a-n/a.

169. Yan, J., et al., *Elastic and electrically conductive carbon nanotubes/chitosan composites with lamellar structure.* Composites Part A: Applied Science and Manufacturing, 2014. **67**(0): p. 1-7.

170. Yan, J. and Y.G. Jeong, *Synergistic effect of hybrid carbon fillers on electric heating behavior of flexible polydimethylsiloxane-based composite films.* Composites Science and Technology, 2015. **106**(0): p. 134-140.

171. Jayamani, E., et al., *Comparative Study of Dielectric Properties of Hybrid Natural Fiber Composites.* Procedia Engineering, 2014. **97**(0): p. 536-544.

172. *ASTM D3171-15, Standard Test Methods for Constituent Content of Composite Materials*. 2015: ASTM International.

173. Samper, M.D., et al., *Properties of composite laminates based on basalt fibers with epoxidized vegetable oils.* Materials & Design, 2015. **72**: p. 9-15.

174. Samper, M.D., et al., *New environmentally friendly composite laminates with epoxidized linseed oil (ELO) and slate fiber fabrics.* Composites Part B: Engineering, 2015. **71**: p. 203-209.

175. *ASTM D3039 / D3039M-14, Standard Test Method for Tensile Properties of Polymer Matrix Composite Materials*. 2014, ASTM International.

176. *ASTM D7264 / D7264M-15, Standard Test Method for Flexural Properties of Polymer Matrix Composite Materials*. 2015, ASTM International.

177. Özturk, S., *The effect of fibre content on the mechanical properties of hemp and basalt fibre reinforced phenol formaldehyde composites.* Journal of Materials Science, 2005. **40**(17): p. 4585-4592.

178. *ISO 6721-1:2011Plastics - Determination of dynamic mechanical properties - Part 1: General principles*. 2011.

179. Motoc Luca, D., S. Ferrandiz Bou, and R. Balart Gimeno, *Effects of fibre orientation and content on the mechanical, dynamic mechanical and thermal expansion properties of multi-layered glass/carbon fibre-reinforced polymer composites.* Journal of Composite Materials, 2014.

180. Karad, S.K., D. Attwood, and F.R. Jones, *Moisture absorption by cyanate ester modified epoxy resin matrices. Part V: effect of resin structure.* Composites Part A: Applied Science and Manufacturing, 2005. **36**(6): p. 764-771.

181. *ASTM D4065-12, Standard Practice for Plastics: Dynamic Mechanical Properties: Determination and Report of Procedures*. 2001, ASTM International.

182. G. Szebenyi, T.C., B. Magyar, J. Karger-Kocsis, *3D printing-assisted interphase engineering of polymer composites: Concept and feasibility.* eXPRESS Polymer Letter, 2017. **11**(7): p. 525-530.

183. *ASTM E473-14, Standard Terminology Relating to Thermal Analysis and Rheology*. 2014, ASTM International.

184. *ASTM E831-14, Standard Test Method for Linear Thermal Expansion of Solid Materials by Thermomechanical Analysis*. 2014.

185. *ASTM D696-08, Standard Test Method for Coefficient of Linear Thermal Expansion of Plastics Between -30°C and 30°C With a Vitreous Silica Dilatometer*. 2008, ASTM International.

186. *ISO 11403-2, Plastics - Acquisition and presentation of comparable multipoint data - Part 2: Thermal and processing properties*. 2012.

187. *ASTM D570-98(2010)e1, Standard Test Method for Water Absorption of Plastics*. 2010, ASTM International.

188. *ASTM D5229 / D5229M-14, Standard Test Method for Moisture Absorption Properties and Equilibrium Conditioning of Polymer Matrix Composite Materials*. 2014, ASTM International.

189. Bismarck, A., et al., *Surface characterization of flax, hemp and cellulose fibers; Surface properties and the water uptake behavior.* Polymer Composites, 2002. **23**(5): p. 872-894.

190. Fu, S.Y., et al., *Hybrid effects on tensile properties of hybrid short-glass-fiber-and short-carbon-fiber-reinforced polypropylene composites.* Journal of Materials Science, 2001. **36**(5): p. 1243-1251.

191. Grozdanov, A. and G. Bogoeva-Gaceva, *Carbon Fibers/Polyamide 6 Composites Based on Hybrid Yarns.* Journal of Thermoplastic Composite Materials, 2010. **23**(1): p. 99-110.

192. Miyagawa, H., et al., *Comparison of experimental and theoretical transverse elastic modulus of carbon fibers.* Carbon, 2006. **44**(10): p. 2002-2008.

193. Stevanovic, M. and D.P. Sekulic, *Macromechanical characteristics deduced from three-point flexure tests on unidirectional carbon/epoxy composites.* Mechanics of Composite Materials, 2003. **39**(5): p. 387-392.

194. Valenza, A., V. Fiore, and G. Di Bella, *Effect of UD Carbon on the Specific Mechanical Properties of Glass Mat Composites for Marine Applications.* Journal of Composite Materials, 2010. **44**(11): p. 1351-1364.

195. Mujika, F., *On the difference between flexural moduli obtained by three-point and four-point bending tests.* Polymer Testing, 2006. **25**(2): p. 214-220.

196. Cao, S.H., Z.S. Wu, and X. Wang, *Tensile Properties of CFRP and Hybrid FRP Composites at Elevated Temperatures.* Journal of Composite Materials, 2009. **43**(4): p. 315-330.

197. Menard, H.P., *Dynamic mechanical analysis: a practical introduction.* 2nd ed. Boca Raton, USA: CRC Press, 2008, p. 123.

198. Dubouloz-Monnet, F., P. Mele, and N.D. Alberola, *Glass fibre aggregates: consequences on the dynamic mechanical properties of polypropylene matrix composites.* Composites Science and Technology, 2005. **65**(3-4): p. 437-443.

199. Kishi, H., et al., *Damping properties of thermoplastic-elastomer interleaved carbon fiber-reinforced epoxy composites.* Composites Science and Technology, 2004. **64**(16): p. 2517-2523.

200. Taniguchi, N., et al., *Dynamic tensile properties of carbon fiber composite based on thermoplastic epoxy resin loaded in matrix-dominant directions.* Composites Science and Technology, 2009. **69**(2): p. 207-213.

201. Bosze, E.J., et al., *High-temperature strength and storage modulus in unidirectional hybrid composites.* Composites Science and Technology, 2006. **66**(13): p. 1963-1969.

202. Pothan, L.A., et al., *Dynamic Mechanical and Dielectric Behavior of Banana-Glass Hybrid Fiber Reinforced Polyester Composites.* Journal of Reinforced Plastics and Composites, 2010. **29**(8): p. 1131-1145.

203. Pothan, L.A., et al., *The static and dynamic mechanical properties of banana and glass fiber woven fabric-reinforced polyester composite.* Journal of Composite Materials, 2005. **39**(11): p. 1007-1025.

204. Jakubinek, M.B., C.A. Whitman, and M.A. White, *Negative thermal expansion materials.* Journal of Thermal Analysis and Calorimetry, 2010. **99**(1): p. 165-172.

205. Ito, T., T. Suganuma, and K. Wakashima, *Glass fiber/polypropylene composite laminates with negative coefficients of thermal expansion.* Journal of Materials Science Letters, 1999. **18**(17): p. 1363-1365.

206. Kia, H.G., *Thermal expansion of sheet molding compound materials.* Journal of Composite Materials, 2008. **42**(7): p. 681-695.

207. Pardini, L.C. and M.L. Gregori, *Modeling elastic and thermal properties of 2.5D carbon finer and carbon/SiC hybrid matrix composites by homogenization method.* Journal of Aerospace Technology and Management, 2010. **2**: p. 183-194.

208. Chimenti, D.E., *Review of air-coupled ultrasonic materials characterization.* Ultrasonics, 2014. **54**(7): p. 1804-1816.

209. Hosten, B., *STIFFNESS MATRIX INVARIANTS TO VALIDATE THE CHARACTERIZATION OF COMPOSITE-MATERIALS WITH ULTRASONIC METHODS.* Ultrasonics, 1992. **30**(6): p. 365-371.

210. Hosten, B. and M. Castaings, *Comments on the ultrasonic estimation of the viscoelastic properties of anisotropic materials.* Composites Part a-Applied Science and Manufacturing, 2008. **39**(6): p. 1054-1058.

211. Karabutov, A.A., A.A. Karabutov, and O.A. Sapozhnikov, *Determination of the elastic properties of layered materials using laser excitation of ultrasound.* Physics of Wave Phenomena, 2010. **18**(4): p. 297-302.

212. Karabutov, A.A., et al., *Laser ultrasonic investigation of the elastic properties of unidirectional graphite-epoxy composites.* Mechanics of Composite Materials, 1998. **34**(6): p. 575-582.

213. Karabutov, A.A., I.M. Pelivanov, and N.B. Podymova, *Nondestructive evaluation of graphite-epoxy composites by the laser ultrasonic method.* Mechanics of Composite Materials, 2000. **36**(6): p. 497-500.

214. Audoin, B., *Non-destructive evaluation of composite materials with ultrasonic waves generated and detected by lasers.* Ultrasonics, 2002. **40**(1-8): p. 735-740.

215. Guilbaud, S. and B. Audoin, *Characterization of temperature-induced stiffness changes in a C-PMR15 composite material by means of laser generated and detected ultrasound.* Composites Science and Technology, 2001. **61**(3): p. 433-438.

216. Pan, Y., et al., *Identification of laser-generated ultrasounds in the response of the cylinder over time and space.* Ultrasonics, 2006. **44**: p. E1249-E1253.

217. Kozhushko, V.V. and P. Hess, *Laser-induced focused ultrasound for nondestructive testing and evaluation.* Journal of Applied Physics, 2008. **103**(12): p. 9.

218. Seiner, H. and M. Landa, *Sensitivity analysis of an inverse procedure for determination of elastic coefficients for strong anisotropy.* Ultrasonics, 2005. **43**(4): p. 253-263.

219. Chatellier, J.Y. and M. Touratier, *A NEW METHOD FOR DETERMINING ACOUSTOELASTIC CONSTANTS AND PLANE STRESSES IN TEXTURED THIN PLATES.* Journal of the Acoustical Society of America, 1988. **83**(1): p. 109-117.

220. Kalkis, V., M. Kalnins, and Y. Zitsans, *Application of the ultrasonic method for the control of thermosetting polymer materials.* Mechanics of Composite Materials, 1997. **33**(3): p. 282-292.

221. Li, Z.Q., et al., *Determination of the elastic constants of metal-matrix composites by a laser ultrasound technique.* Composites Science and Technology, 2001. **61**(10): p. 1457-1463.

222. Wang, J.J., et al., *Numerical simulation of laser-generated ultrasound in non-metallic material by the finite element method.* Optics and Laser Technology, 2007. **39**(4): p. 806-813.

223. Yuan, L., et al., *Laser-induced ultrasonic waves in steels with gradient changes of elastic property.* Optics and Laser Technology, 2008. **40**(2): p. 325-329.

224. Motoc Luca, D., *Contribution to the study of stress state and physical properties of materials using nondestructive testing methods.* PhD Thesis, 2002.

225. Audoin, B. and C. Bescond, *Measurement by LASER-generated ultrasound of four stiffness coefficients of an anisotropic material at elevated temperatures.* Journal of Nondestructive Evaluation, 1997. **16**(2): p. 91-100.

226. Aussel, J.D. and J.P. Monchalin, *PRECISION LASER-ULTRASONIC VELOCITY-MEASUREMENT AND ELASTIC-CONSTANT DETERMINATION.* Ultrasonics, 1989. **27**(3): p. 165-177.

227. Deschamps, M. and C. Bescond, *NUMERICAL-METHOD TO RECOVER THE ELASTIC-CONSTANTS FROM ULTRASOUND GROUP VELOCITIES.* Ultrasonics, 1995. **33**(3): p. 205-211.

228. Assarar, M., et al., *Evaluation of the damping of hybrid carbon-flax reinforced composites.* Composite Structures, 2015. **132**: p. 148-154.

229. Duc, F., et al., *Damping of thermoset and thermoplastic flax fibre composites.* Composites Part a-Applied Science and Manufacturing, 2014. **64**: p. 115-123.

230. Saba, N., et al., *A review on dynamic mechanical properties of natural fibre reinforced polymer composites.* Construction and Building Materials, 2016. **106**: p. 149-159.

231. Alvarez, V., E. Rodriguez, and A. Vazquez, *Thermal degradation and decomposition of jute/vinylester composites.* Journal of Thermal Analysis and Calorimetry, 2006. **85**(2): p. 383-389.

232. Manfredi, L.B., et al., *Thermal degradation and fire resistance of unsaturated polyester, modified acrylic resins and their composites with natural fibres.* Polymer Degradation and Stability, 2006. **91**(2): p. 255-261.

233. Lazko, J., et al., *Flame retardant treatments of insulating agro-materials from flax short fibres.* Polymer Degradation and Stability, 2013. **98**(5): p. 1043-1051.

234. Bar, M., R. Alagirusamy, and A. Das, *Flame Retardant Polymer Composites.* Fibers and Polymers, 2015. **16**(4): p. 705-717.

235. Kollia, E., et al., *Degradation behavior of glass fiber reinforced cyanate ester composites under hydrothermal ageing.* Polymer Degradation and Stability, 2015. **121**: p. 200-207.

236. Azwa, Z.N., et al., *A review on the degradability of polymeric composites based on natural fibres.* Materials & Design, 2013. **47**: p. 424-442.

237. Cheung, H.Y., et al., *Natural fibre-reinforced composites for bioengineering and environmental engineering applications.* Composites Part B-Engineering, 2009. **40**(7): p. 655-663.

238. Dittenber, D.B. and H.V.S. GangaRao, *Critical review of recent publications on use of natural composites in infrastructure.* Composites Part a-Applied Science and Manufacturing, 2012. **43**(8): p. 1419-1429.

239. Faruk, O., et al., *Biocomposites reinforced with natural fibers: 2000-2010.* Progress in Polymer Science, 2012. **37**(11): p. 1552-1596.

240. Jawaid, M. and H. Khalil, *Cellulosic/synthetic fibre reinforced polymer hybrid composites: A review.* Carbohydrate Polymers, 2011. **86**(1): p. 1-18.

241. Jawaid, M., H. Khalil, and O.S. Alattas, *Woven hybrid biocomposites: Dynamic mechanical and thermal properties.* Composites Part a-Applied Science and Manufacturing, 2012. **43**(2): p. 288-293.

242. LeGault, M., *Natural fiber composites: market share, one part at the time.* Composites World, 2016: p. 68-75.

243. Praveen, R.S., et al., *Hybridization of carbon-glass epoxy composites: An approach to achieve low coefficient of thermal expansion at cryogenic temperatures.* Cryogenics, 2011. **51**(2): p. 95-104.

244. Rojo, E., et al., *Effect of fiber loading on the properties of treated cellulose fiber-reinforced phenolic composites.* Composites Part B-Engineering, 2015. **68**: p. 185-192.

245. Swolfs, Y., L. Gorbatikh, and I. Verpoest, *Fibre hybridisation in polymer composites: A review.* Composites Part a-Applied Science and Manufacturing, 2014. **67**: p. 181-200.

246. Joshi, S.V., et al., *Are natural fiber composites environmentally superior to glass fiber reinforced composites?* Composites Part a-Applied Science and Manufacturing, 2004. **35**(3): p. 371-376.

247. Alam, M., et al., *Vegetable oil based eco-friendly coating materials: A review article.* Arabian Journal of Chemistry, 2014. **7**(4): p. 469-479.

248. Bakare, F.O., et al., *Thermomechanical properties of bio-based composites made from a lactic acid thermoset resin and flax and flax/basalt fibre reinforcements.* Composites Part a-Applied Science and Manufacturing, 2016. **83**: p. 176-184.

249. Bertomeu, D., et al., *Use of eco-friendly epoxy resins from renewable resources as potential substitutes of petrochemical epoxy resins for ambient cured composites with flax reinforcements.* Polymer Composites, 2012. **33**(5): p. 683-692.

250. Mosiewicki, M.A. and M.I. Aranguren, *A short review on novel biocomposites based on plant oil precursors.* European Polymer Journal, 2013. **49**(6): p. 1243-1256.

251. Lligadas, G., et al., *Renewable polymeric materials from vegetable oils: a perspective.* Materials Today, 2013. **16**(9): p. 337-343.

252. Fombuena, V., et al., *Study of the Properties of Thermoset Materials Derived from Epoxidized Soybean Oil and Protein Fillers.* Journal of the American Oil Chemists Society, 2013. **90**(3): p. 449-457.

253. Pil, L., et al., *Why are designers fascinated by flax and hemp fibre composites?* Composites Part a-Applied Science and Manufacturing, 2016. **83**: p. 193-205.

254. Mallarino, S., J.F. Chailan, and J.L. Vernet, *Glass fibre sizing effect on dynamic mechanical properties of cyanate ester composites - I. Single frequency investigations.* European Polymer Journal, 2005. **41**(8): p. 1804-1811.

255. Wooster, T.J., et al., *Thermal, mechanical, and conductivity properties of cyanate ester composites.* Composites Part a-Applied Science and Manufacturing, 2004. **35**(1): p. 75-82.

256. Sothje, D., C. Dreyer, and M. Bauer, *Advanced possibilities in thermoset recycling.* The 3rd International Conference on Thermosets, Berlin (Germany), 2013.

257. Yuan, L., et al., *A cyanate ester/microcapsule system with low cure temperature and self-healing capacity.* Composites Science and Technology, 2013. **87**: p. 111-117.

258. Czigany, T., *Special manufacturing and characteristics of basalt fiber reinforced hybrid polypropylene composites: Mechanical properties and acoustic emission study.* Composites Science and Technology, 2006. **66**(16): p. 3210-3220.

259. Marom, G., et al., *HYBRID EFFECTS IN COMPOSITES - CONDITIONS FOR POSITIVE OR NEGATIVE EFFECTS VERSUS RULE-OF-MIXTURES BEHAVIOR.* Journal of Materials Science, 1978. **13**(7): p. 1419-1426.

260. Cherki, A.B., et al., *Experimental thermal properties characterization of insulating cork-gypsum composite.* Construction and Building Materials, 2014. **54**: p. 202-209.

261. Torquato, S., *Random heterogeneous materials : microstructure and macroscopic properties.* New York, NY Springer, 2002.

262. Bismarck, A., et al., *Surface characterization of flax, hemp and cellulose fibers; Surface properties and the water uptake behavior.* Polymer Composites, 2002. **23**(5): p. 872-894.

263. Motoc, D.L., S.F. Bou, and R.B. Gimeno, *Effects of fibre orientation and content on the mechanical, dynamic mechanical and thermal expansion properties of multi-layered glass/carbon fibre-reinforced polymer composites.* Journal of Composite Materials, 2015. **49**(10): p. 1211-1221.

264. EduPack, C., *Granta Design.* 2013.

265. Monteiro, S.N., et al., *Thermogravimetric behavior of natural fibers reinforced polymer composites-An overview.* Materials Science and Engineering a-Structural Materials Properties Microstructure and Processing, 2012. **557**: p. 17-28.